NASA CONTRACTOR REPORT

NASA CR-679

INFLUENCE OF UPSTREAM FLOW DISCONTINUITIES ON THE ACOUSTIC POWER RADIATED BY A MODEL AIR JET

by Colin G. Gordon and Gideon Maidanik

Prepared by
BOLT BERANEK AND NEWMAN, INC.
Cambridge, Mass.
for Langley Research Center

NATIONAL AERONAUTICS AND SPACE ADMINISTRATION • WASHINGTON, D. C. • JANUARY 1967

NASA CR-679

INFLUENCE OF UPSTREAM FLOW DISCONTINUITIES ON THE ACOUSTIC POWER RADIATED BY A MODEL AIR JET

By Colin G. Gordon and Gideon Maidanik

Prepared under Contract No. NAS 1-4974 by
BOLT BERANEK AND NEWMAN, INC.
Cambridge, Mass.

for Langley Research Center

NATIONAL AERONAUTICS AND SPACE ADMINISTRATION

For sale by the Clearinghouse for Federal Scientific and Technical Information
Springfield, Virginia 22151 – Price $3.00

TABLE OF CONTENTS

TABLE OF CONTENTS (Continued)

TABLE OF CONTENTS (Continued)

LIST OF ILLUSTRATIONS

INFLUENCE OF UPSTREAM FLOW DISCONTINUITIES ON THE ACOUSTIC POWER RADIATED BY A MODEL AIR JET

By: Colin G. Gordon and Gideon Maidanik

Assisted by: Clayton H. Allen, Sheila E. Widnall, Eugene Ring, and John E. Ffowcs Williams

ABSTRACT

This report presents the results of an experimental study of the sound-radiation changes produced by inserting a flow spoiler into a model air jet, a short distance upstream from the exit plane of the jet pipe. In this work, we have concentrated on accurate measurements of the total and spectral sound power radiated by such a system. The work is restricted to the broad-band sound radiation at subsonic flow velocities. Spoiler-generated noise is shown to be dipole in character. It displays a dependence upon the sixth-power-of-flow velocity as compared with the eighth-power law of the free-jet quadrupole sources. Being fundamentally more efficient, it dominates the total noise radiation from the typical model jet system over most of the velocity range. The results of measurements on a large variety of flow spoilers have shown that the total and spectral power may be described empirically in terms of easily measured parameters of the geometry and air flow. This empirical formulism correlates well with a semitheoretical model of dipole noise. It is felt that a formulation of this sort may have wide application to the prediction of surface-induced sounds in both real and model systems. Some of the results, however, show significant deviation from a well-behaved dipole model. It is postulated that in-pipe quadrupole sources are active under certain, as yet undefined, conditions. A tentative formulation shows

how such secondary sources may fit into a prediction scheme. This study is directed towards obtaining a better understanding of the noise associated with the high bypass-ratio fan-jet engine.

INTRODUCTION

The classical theory of aerodynamic noise generation as first presented by Lighthill (ref. 1) describes the mechanism whereby the free turbulence, produced in the mixing region of the jet exhaust, radiates sound. It is shown that the sources of noise are equivalent to acoustic quadrupoles and that the noise generated will increase in intensity according to the eighth power of the exhaust velocity. This theoretical observation is well-confirmed experimentally for both real and model jet flows, at least for conditions where the upstream flow is clean and the exit velocity is in the high subsonic range. It has been experimentally observed, however, that under conditions of rough (turbulent) flow the eighth power law gives way to a lower exponent of velocity. Specific examples are contained in the work of Mawardi and Dyer (ref. 2), for real turbojet engines, and Lassiter and Hubbard (ref. 3), Fitzpatrick and Lee (ref. 4), and Ffowcs Williams and Gordon (ref. 5), on model air-jet systems.

By themselves, these observations imply that as the speed of the jet exhaust is reduced — for example, as a design parameter of the modern fan-jet engine or, alternatively, under low-throttle conditions for the conventional jet engine — the noise level may not be reduced to the extent predicted on the basis of a quadrupole-dominated source system. The picture is further darkened by the fact that the modern fan-jet engine must also cause a sizeable increase in the exhaust turbulence levels on account of the air-propelling machinery. Thus if in-pipe turbulence is a parameter in the lowering of the velocity exponent, this might cause a further increase in the radiated noise from such a system.

The implication from these observations is that under the conditions of high turbulence and low exhaust velocity a fundamentally different source of noise dominates the sound field. Two fundamental mechanisms having a lower exponent of velocity than the eighth are available from the current aerodynamic noise theory. Surface sources as predicted by Curle's (ref. 6) extension of Lighthill's arguments would look like acoustic dipoles and would increase in intensity with the sixth power of a typical flow velocity. Such sources are induced by the reaction of the turbulent pipe (or wake) flow on solid surfaces. Since the exit lip of the jet pipe is one possible location for such dipolelike sources, it has been termed "lip noise." Support struts and other such surface discontinuities must also play a role in this dipole mechanism.

Yet a further source of noise suggests itself if any unsteady mass flow occurs as a result of the exhaust plane turbulence, or of rough burning in the engine combustion chambers. Such a source would radiate like an acoustic monopole and might be related to the fourth power of jet velocity.

The three mechanisms of equivalent quadrupole, dipole, and monopole radiation are illustrated diagrammatically in Fig. 1, as they might apply to the jet engine. It is apparent that, as the flow velocity is reduced, control of the radiated noise must pass from the quadrupole to either the dipole or monopolelike mechanisms.

At this stage, a word of caution is appropriate to these discussions. Present theoretical knowledge of aerodynamic noise is based on the assumption that the sources are immersed in an infinite acoustic medium, and there is theoretical evidence to suggest that when these sources are confined within a pipe their behavior may change in quite a fundamental way (see Appendix A).

Nevertheless, as we shall see later, it is observed experimentally that sources having the appropriate velocity exponents do exist within the pipe environment and are identifiable with conventional source mechanisms. Thus, to some extent at least, the diagrammatic description of Fig. 1 is justified. It is suggested here that, in fact, the energy generated by the in-pipe sources occurs at sufficiently high frequencies that their radiation efficiency is not significantly different from that in the free-space environment.

The purpose of the program described in this report is to study the noise radiation from a model jet system as the level and scale of the turbulence within the pipe is changed. Although the study was originally formulated on the basis of noise-generating mechanisms being located essentially at the exit plane of the jet pipe, the experiments have shown that, in fact, neither the exit plane nor the turbulence flowing across it are of fundamental importance in this respect. Neither has there been found any significant evidence of monopolelike radiation during these studies. This is perhaps not surprising in view of the almost incompressible nature of subsonic air flow. Any fluctuation in the exhaust would require a compensating inlet fluctuation. This does not mean, however, that in the practical situation such sources are not to be found. The measurements of Mawardi and Dyer (ref. 2), and others, strongly suggest that monopole sources are indeed present. It seems reasonable to suppose that, in the real engine, rough burning could produce the necessary perturbations of volume flow. In the model experiment, no such perturbations of the air supply were available and some further experimentation along these lines is recommended for future work.

The present study, therefore, is entirely related to the mechanisms of surface (dipole) and volume (quadrupole) noise generation in a jet pipe environment. More specifically, the study has considered only the broad-band aspects of this noise. As far as possible, any discrete-frequency instabilities such as might occur through stable vortex shedding or through mechanical resonance of the spoiler-pipe configuration have been eliminated from the study. Such discrete-tone behavior is perhaps relevant to the real structure and to the pure-tone components of compressor and turbine noise. Some experimental observations on such discrete-frequency behavior are made later in this report.

Surface-noise generation within a model jet-pipe system is immediately relevant to the fan-noise problem, to lip noise, and noise associated with flow around diffusers, diffuser support straps, flow straighteners, and so on. Important applications of the present work are also foreseen in the field of duct- and diffuser-generated noise in high-velocity air-handling systems.

The surface forces generated within the jet pipe radiate sound which thereafter propagates along the pipe as an acoustic wave and radiates into free space. The acoustics of the pipe, therefore, must be a parameter in this problem, particularly as they affect the radiation impedance of the exit plane and the amplitude of the sound waves incident on the exit plane.

A further parameter to be considered is the turbulence level which existed in the pipe prior to the insertion of the flow spoiler. A spoiler inserted in smooth low turbulence or laminar flow will generate surface noise associated with the production of a turbulent wake behind the spoiler. The same spoiler inserted in a highly turbulent flow will radiate much more strongly since additional, and often much larger, surface forces will be generated on the body by the impinging turbulence.

The observation — that a surface generates more noise from "someone elses turbulence" than from its own — was perhaps first made by G. I. Taylor (ref. 7) who observed that when a toasting fork is waved through the air it generates significantly more noise when the plane of the prongs lies in the direction of motion than it does when the plane of the prongs lies perpendicular to the motion. We advocate this observation as a principle of paramount importance whenever surfaces are immersed in an existing turbulent flow. The reason is clearly that whereas it is generally difficult for a surface to generate, in its immediate environment, turbulence of its own scale — necessary for generating significant force fluctuations — such large scale turbulence may well be generated by upstream obstructions.

The experiments described in this report have covered a wide range of flow configurations applied to a low-turbulence pipe system. The studies have included strip spoilers placed across the flow, having different widths and placed at different angles of attack. Ring spoilers around the internal periphery of the pipe have also been studied as have sudden changes in pipe section. The effect of varying the distance between the spoiler and the exit plane has been examined also. Throughout the studies, the experimentation has concentrated on accurate measurements of the total radiated sound power and the frequency spectrum of this power. A very high level of accuracy has been achieved in this respect. Data resulting from the study, in addition to the total power and spectra measurements, also include details of the radiation directivity patterns.

Throughout the experimentation, it has been observed that the radiated power in most instances correlates well with the sixth power of typical flow velocity and it is deduced, therefore, that the power is dominated by dipolelike sources associ-

ated with unsteady surface forces produced by the turbulence. It has also been determined that, in the main, these sources are located on or close to the experimental flow spoiler and that, in the generalized problem at least, "lip noise" plays no significant role.

It is found that over a wide range of geometries, the total power radiation from a "spoiled" pipe, as illustrated in Fig. 2, is described by the relation

$$P_A \sim \rho_\ell U_\ell^3 D^2 M_\ell^3 \quad , \tag{1}$$

where U_ℓ is the local (constricted) velocity in the vicinity of the spoiler and M_ℓ is the normalized velocity U_ℓ/c_a. D is the pipe diameter, c_a is the velocity of sound, and ρ_ℓ is the local air density. The latter is approximately equal to the downstream atmospheric density ρ_a. The constant of proportionality for Eq. (1) has been found experimentally to be about 3×10^{-5}.

Equation (1) has been derived, in fact, by correlation between the sound power and the measured pressure drop across the spoiler. It is possible to estimate the constriction velocity U_ℓ on the basis of a Bernoulli equation, provided that the upstream total head p_o is measured sufficiently close to the obstruction and that potential flow is assumed to exist down to the constriction point. The dynamic head at the constriction is therefore given by

$$\frac{1}{2} \rho_\ell U_\ell^2 + p_\ell = \frac{1}{2} \rho_1 U_1^2 + p_1 = p_o \quad .$$

If atmospheric pressure is assumed to penetrate upstream to the region of maximum constriction velocity, then $\rho_\ell = \rho_a$ and Eq. (1) may be rewritten as

$$P_A = k\,(p_o - p_a)^3\, D^2/\rho_a{}^2 c_a{}^3 \quad , \tag{2}$$

where k has a value of about 2.5×10^{-4}. This formulation gives the acoustic power in terms of easily measureable properties of the total flow. It is consistent with the notion that the sound is of aerodynamic origin and seems to correlate well with the data.

The formulation of the power radiated from the spoiled pipe does not explicitly include any details of the flow spoiler. In fact, this information is implicit within the pressure drop, and the dimensions of the spoiler appear only in determining the form of the frequency spectrum.

It is interesting now to dompare Eq. (1) which describes dipole radiation, with the equation that describes the quadrupole radiation from the free-jet region. The latter is given by

$$P_A = k' \rho_a U_a{}^3 D^2 M_a{}^5 \quad , \tag{3}$$

where D, ρ_a, and c_a are as defined earlier; U_a is the exit plane velocity; and $M_a = U_a/c_a$. The value of k' indicated by our experiments is of the order 10^{-4}. This agrees well with the value found by Fitzpatrick and Lee (ref. 4), and later confirmed by several other experimental surveys (for example, see Lighthill (ref. 8).

A comparison of Eqs. (1) and (3) show how the dipolelike sound must become dominant at the low exhaust speeds, and, for small constriction ratios where U_ℓ and M_ℓ approximate to U_a and

M_a, the coefficients of these formulas are such that the change-over occurs at a value of $M_a \approx 0.6$.

We have studied a large variety of spoilers of fundamentally different geometries and have observed a good correlation of the data on the basis of these extremely simple formulas. This is a striking result which we feel is of general relevance and may be applied to good effect in various diverse fields of duct-generated aerodynamic noise. We illustrate this point with two examples. The first, taken from information supplied by Langley Research Center, describes an environmental noise facility in which piped high-pressure air is blown through a 15 in. diameter pipe forming a series of right-angle turns to produce a random-noise source. Although most of the operational range of this equipment lies in the above critical pressure regime, for which our "subsonic" formulation cannot apply, there is some data within the subsonic region to which our analysis is pertinent. It is observed (from the data supplied by Langley) that the total radiated sound increases approximately with the third power of the operating pressure in the low-pressure range. This is consistent with surface-noise generation for subsonic flow. The application of Eq. (2) for a value of $(p_o - p_a)$ of 10 in. of mercury gives an estimated total power radiation of 144 dB (re 10^{-12} Watts). On the basis of the quoted reverberation time of the test cell (about 2 sec) and the quoted sound-pressure level in the reverberant field (137 dB re 0.0002 μbar), the actual power generated under an operating pressure of 10 in. Hg is 146 dB (re 10^{-12} Watts). The agreement is acceptable.

Our second example comes from the opposite end of the scale — low-velocity flow through an air-conditioning diffuser. The form of the diffuser is an initially round section making a constant area transition to an exhaust slot. The purpose of the diffuser is to inject comparatively high-velocity air from the

side walls of an auditorium to carry into the center area. Tests conducted by the manufacturers showed about 50 dB (re 10^{-12} Watts) of sound generated in the middle frequency range at the planned operating pressure. It is apparent from an examination of this unit that this part of the noise spectrum is associated with a reinforcing ring on the inside periphery of the diffuser. The application of Eq. (2) at the quoted operating pressure predicts a radiated power level of 55 dB (re 10^{-12} Watts). Again, the agreement is satisfactory.

This universal prediction of the dipole radiation field is, in fact, the main result of this report. It is stressed, even though there exist theoretical arguments to predict that its form might vary as the source is immersed more deeply within the pipe. There are also experimental configurations and flow conditions that show some deviation from a dipolelike behavior. These are most interesting, particularly since their frequency spectra show evidence of quadrupolelike characteristics at high frequencies and high flow velocities. We have obtained very striking normalizations of these data which suggest an intense quadrupolelike activity within the jet pipe under particular, as yet undefined, conditions. It is suggested that this phenomenon may be related to the interaction of a spoiler with a particular scale of impinging flow turbulence.

The two theoretical approaches relevant to a study of in-pipe sources are presented, respectively, in Section I and Appendix A of this report. The first approach develops a semi-phenomenological theory which describes aerodynamic sources in general and which is particularly directed towards providing a means for interpreting the experimental results. The second and more fundamental approach, which is currently incomplete, considers one-dimensional acoustic waves of turbulence origin pro-

pagating down the pipe. This second approach suggests dependence on flow parameters radically different from the free-field case. Our experimental observations to date, however, show no evidence of such a change and so this theory is as yet unsubstantiated.

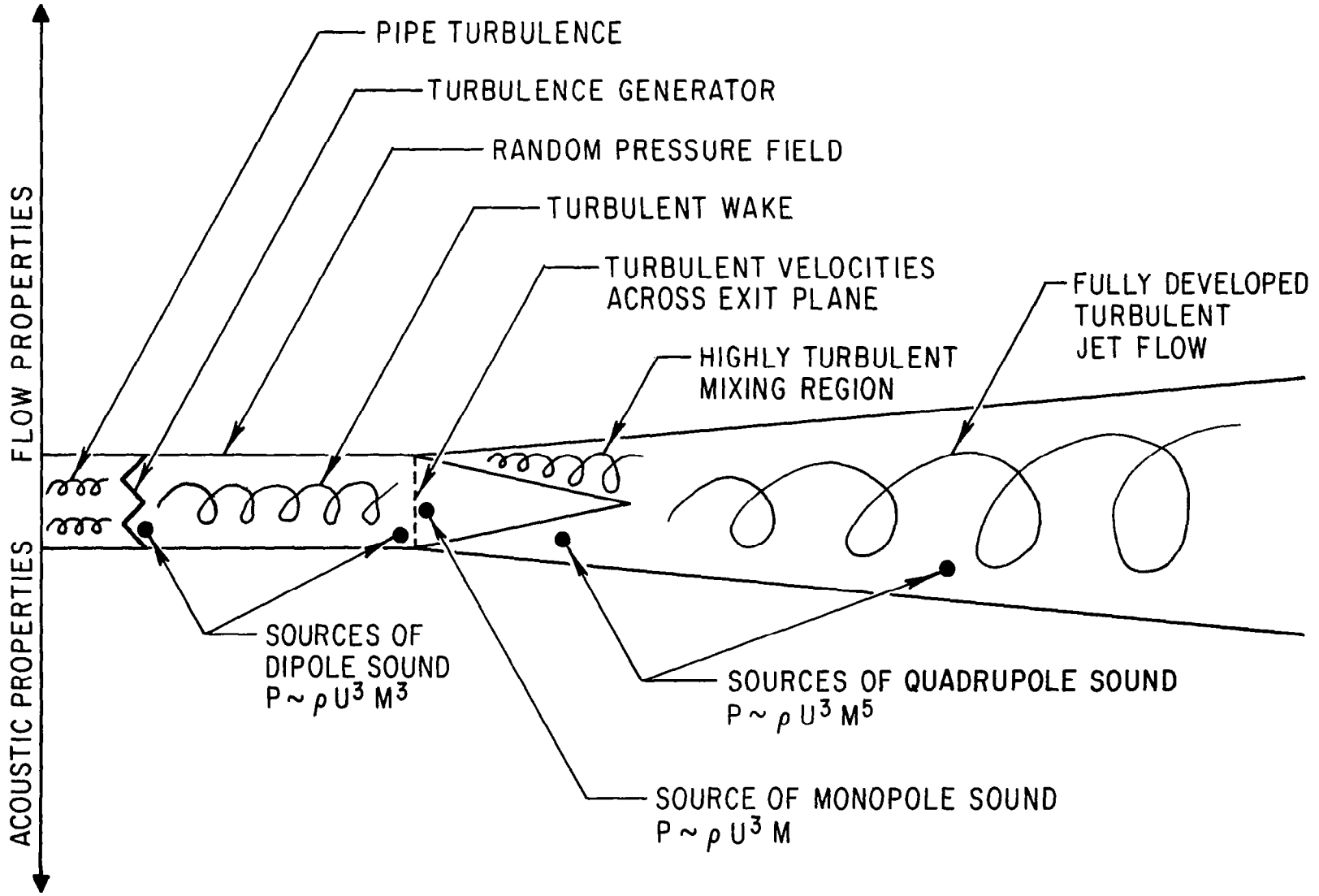

FIG. 1 SCHEMATIC ILLUSTRATION OF THE NOISE PRODUCED BY JET TURBULENCE

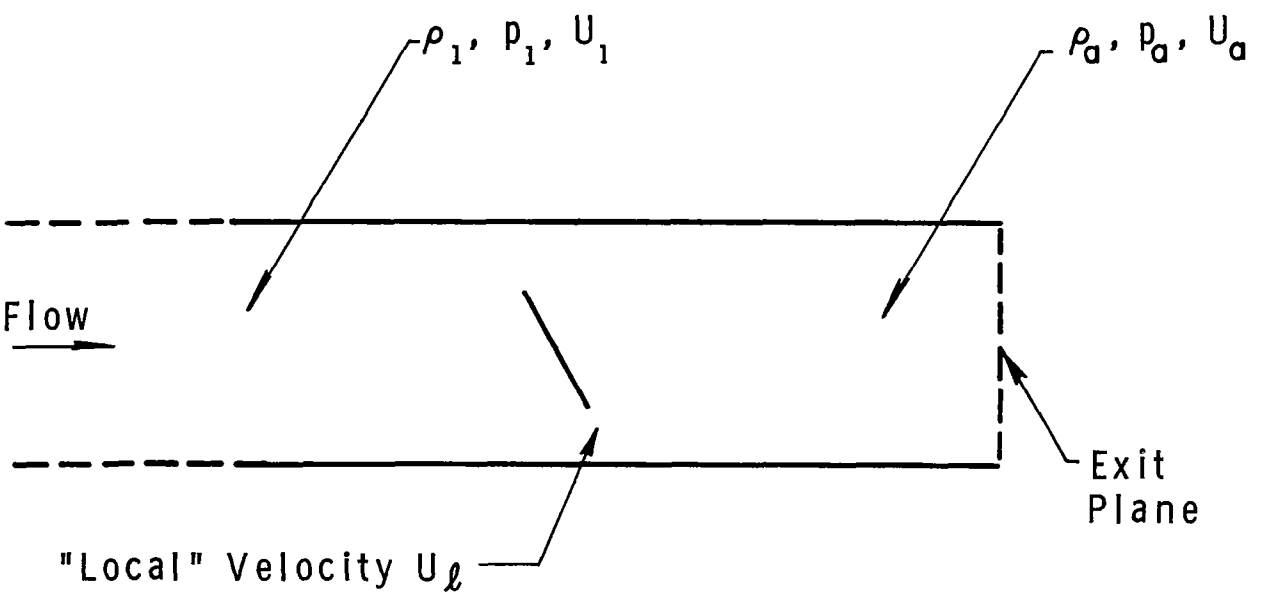

FIG.2 SCHEMATIC OF STRIP SPOILER IN PIPE

I. AERODYNAMIC SOUND SOURCES

In this chapter, we discuss some theoretical aspects of sound radiation by aerodynamically induced sources. It is not the purpose of this discussion to derive a rigorous theory of aerodynamic noise but rather to derive, by heuristic arguments, expressions for the power radiated by aerodynamically produced sound sources that will enable us to present the experimental data in a coherent and meaningful manner.

We start by considering the problem of sound generation by acoustic sources, and we argue that these can be specified in terms of mass injection per unit volume per unit time and in terms of forces per unit volume acting on the fluid in which the sources are immersed. We then derive the expression for the radiated power in terms of the source strengths, and we define these source strengths for monopole, dipole, and quadrupole sources. We argue that aerodynamically produced sources can be specified in terms of uncorrelated dipole sources and uncorrelated quadrupole sources. We derive the expression for the radiated power spectra of these sources in terms of the frequency, convective-velocity distribution, the mean convective velocity, and the spatial dimensionality of the sources. We define the Strouhal number and show that the radiated power spectra are most conveniently expressed in terms of proportionate frequency bands (e.g., octave bands). Finally, we obtain the normalized form of the radiated power spectra and the total radiated power that is most suited for the presentation of the experimental data.

1.1 The Wave Equation and Acoustic Sources

In this section, we derive the acoustic wave equation and examine its general solution in terms of acoustic sources. The behavior of a dynamical system can be described in terms of conservation equations, i.e., mass, momentum, etc. It is usual to deduce the aerodynamic sound sources by manipulating the equations of conservation of mass and momentum so as to derive the linear acoustic wave equation possessing source terms (refs. 1, 9-11). These terms are then classified according to their multiplicity: monopole, dipole, quadrupole, etc. In casting the problem in terms of the conservation equations, two avenues are open to us. The first consists of subjecting the solution of the wave equation to the physical boundary conditions, and the second consists of replacing the boundary conditions by a system of mass and momentum sources. Of course both approaches must lead to identical solutions; however, it is, at times, more convenient to interpret the problem in terms of the one rather than the other approach. Moreover, one may cast the problem in terms of a mixture of both approaches, where only certain physical boundaries are replaced by a system of mass and momentum sources. To accommodate both approaches, or a mixture thereof, we state the appropriate equations of conservations as follows:

$$\frac{\partial \rho}{\partial t} + \nabla \cdot (\rho \underset{\sim}{u}) = \overline{Q} \quad , \tag{4}$$

and

$$\frac{\partial (\rho \underset{\sim}{u})}{\partial t} + \nabla \cdot [\rho (\underset{\sim}{u};\underset{\sim}{u}) + \underset{\approx}{p}] = \overline{\underset{\sim}{F}} \quad . \tag{5}$$

Here, $\overline{Q}\ (\underset{\sim}{x},t)$ is the mass per unit volume per unit time, which is introduced externally at position $\underset{\sim}{x}$ at time t into the fluid; $\overline{\underset{\sim}{F}}\ (\underset{\sim}{x},t)$ is the total effective external force per unit volume acting on the fluid at position $\underset{\sim}{x}$ at time t. The quantity $(\underset{\sim}{u};\underset{\sim}{u})$ is the velocity-vector tensor and $\underset{\approx}{p}$ is the pressure tensor. Finally, ρ is the fluid density.

Injected mass is deficient in local momentum, unless it is injected at a point that moves at the local velocity. Accordingly, the injection of mass at a rate Q necessarily disturbs the momentum equilibrium by an amount $Q\underset{\sim}{u}$. The total effective external force is therefore the sum of $\underset{\sim}{f}$, the externally applied force, and $Q\underset{\sim}{u}$. Similar comments will apply equally to the internal energy introduced by the injected mass. Since the fluctuations considered here are essentially isotropic, we do not need to consider the energy equation.

Operating on Eq. (4) by $\partial/\partial t$ and on Eq. (5) by ∇, one readily obtains

$$\left(\frac{\partial^2}{\partial t^2} - c_a^2\nabla^2\right)\rho = \left[\frac{\partial \overline{Q}}{\partial t} - \nabla\cdot\overline{\underset{\sim}{F}} + \nabla;\ \nabla:\ \left[\rho(\underset{\sim}{u};\underset{\sim}{u}) + (\underset{\approx}{p} - \underset{\approx}{I}c_a^2\rho)\right]\right]$$

$$= S \quad , \tag{6}$$

where c_a is the speed of sound in the fluid at rest. The quantity $\underset{\approx}{I}$ is the unit tensor (idemfactor).

The general acoustic radiation solution of Eq. (6) is (ref. 12)

$$(\rho-\rho_a)\ (\underset{\sim}{x},t) = \frac{1}{4\pi c_a^2}\int_o^{t^+} dt_o \int_{V_o} d\underset{\sim}{x}_o\ G(\underset{\sim}{x},t\,|\,\underset{\sim}{x}_o,t_o)S(\underset{\sim}{x}_o,t_o)$$

$$+ \frac{1}{4\pi} \int_{o}^{t^+} dt_o \int_{\underset{\sim}{A}_o} d\underset{\sim}{A}_o \left[G \operatorname{grad}_o \rho - (\rho - \rho_a) \operatorname{grad}_o G \right]$$

$$- \frac{1}{4\pi c_a^2} \int_{V_o} d\underset{\sim}{x}_o \left[\left(\frac{\partial G}{\partial t_o} \right)_{t_o=0} (\rho - \rho_a) - G_{t_o=0} \left(\frac{\partial \rho}{\partial t_o} \right)_{t_o=0} \right] , \tag{7}$$

where $G(\underset{\sim}{x}, t \,|\, \underset{\sim}{x}_o, t_o)$ is the Green's function defined by

$$\left(\frac{\partial^2}{\partial t^2} - c_a^2 \nabla^2 \right)_o G = - \delta(\underset{\sim}{x} - \underset{\sim}{x}_o) \, \delta(t - t_o) \quad , \tag{8}$$

and G satisfied the appropriate homogeneous boundary conditions. The parameters subscripted by zero refer to the source region, and the unsubscripted parameters refer to the point of observation. The ambient density is ρ_a. The second term on the righthand side of Eq. (7) represents the effect of the spatial boundary conditions, and the third term involves the initial conditions (the temporal boundary conditions). If S is to contain all boundaries, the last two terms on the righthand side of Eq. (7) are absent. These terms are written such that they are embodied in the first term as sources. The last term, in particular, plays a role only in transient problems; it vanishes when steady-state conditions have been reached.

The derivation of the wave equation via Eqs. (4) and (5) makes clear that the type of sources with which we are dealing

are those that can be specified in terms of quantities equivalent to those of the sources $\overline{Q}$ and $\underset{\sim}{\overline{F}}$ — that is, in terms of mass injection per unit volume per unit time and in terms of forces per unit volume. In general then, we consider $S(\underset{\sim}{x}_o, t_o)$ to contain all sources, including boundaries such that Eq. (7) consists of the first term on the right-hand side only. This transformation is sufficient to render the irradiated space free and the Green's function for the problem becomes (ref. 12)

$$G(\underset{\sim}{x}, t \,|\, \underset{\sim}{x}_o, t_o) = \delta\left(\frac{|\underset{\sim}{x}-\underset{\sim}{x}_o|}{c_a} - t + t_o\right) \Big/ |\underset{\sim}{x} - \underset{\sim}{x}_o| \quad , \qquad (9)$$

where δ is the Dirac delta function. All sources are then radiating into free space.

1.2 Classification of the Acoustic Sources and Their Nature

In this section, we classify the acoustic sources according to the nature of their farfield radiative properties. We define their strengths and state the expressions for the power that they radiate.

In free space, externally injected mass generates an acoustic far field that is equivalently that of a monopole of strength $\frac{\partial Q}{\partial t}$. Similarly, a force generates an acoustic far field that is equivalently that of a dipole of strength $\nabla \cdot \underset{\sim}{F} = \frac{1}{c_a} \nabla \left[|\underset{\sim}{x}-\underset{\sim}{x}_o| \cdot \frac{\partial \underset{\sim}{F}}{\partial t} \right]$ The acoustic power radiated to the far field by a single source is defined as

$$\text{Power radiated by a single source} \sim |\text{source strength}|^2 / \rho_a c_a . \qquad (10)$$

Should we have known that all the sources are uncorrelated, we could have readily deduced the acoustic power radiated to the far field simply by adding their individual powers as given in Eq. (10). However, in practice, one usually encounters situations where some correlation between the fundamental sources (the Q sources and the $\underset{\sim}{F}$ sources) exists and the problem is thereby greatly increased in complexity. There are, nevertheless, situations where the problem is tractable. These situations are those for which the spatial correlation of the sources is confined to a small region and the nature of the correlation can be uniquely interpreted on physical grounds. Then one may consider the sources as being uncorrelated, but at the expense of defining sources of higher multiplicity than the fundamental monopole and dipole sources.

To make the point clear, let us consider an example. We assume that a system does not possess means for supporting individual forces, for there are no mechanisms to provide the necessary "action and reaction" balance. We conclude that if forces are, nevertheless, generated in the fluid they must be produced in pairs such that the forces in each pair have their magnitudes equal but their phases opposite. Pairs of this kind constitute sources that are equivalently quadrupole and higher poles. One may argue that when such pairs are generated by purely aerodynamic processes, the production of poles of higher order than the quadrupole is a less likely process than that of quadrupole production. In this way, one may assume that in this example the dominant sources are quadrupoles. The quadrupole source strength is given in terms of the constituent forces:

$$\text{Quadrupole strength} \equiv \left[\nabla\left(\left|\underset{\sim}{x}-\underset{\sim}{x}_o\right|\right) \cdot \underset{\sim}{\eta}\right]\left[\left|\underset{\sim}{x}-\underset{\sim}{x}_o\right| \cdot \frac{\partial^2 \underset{\sim}{F}}{c_a^2 \partial t^2}\right] , \quad (11)$$

where $\underset{\sim}{\eta}$ is a vector of magnitude equal to the separation between the two constituent forces in a direction along a line joining the centers of action of the two forces.

It can be shown that the last source term on the right-hand side of Eq. (6) is essentially a quadrupole source of the type given in Eq. (11). It is interesting to note that this source term arises, and is the only one to arise, in the absence of physical surfaces, whenever the velocity field is unsteady. The power radiated by a single quadrupole source is given by Eqs. (10) and (11).

1.3 The Power Spectrum of Radiation by Aerodynamically Produced Sources

In this section, we derive a suitable form for the aerodynamically produced sources and state the expression for the power spectrum radiated by these sources. In this expression, we consider the power radiated by several distinct mechanisms as each produces its own aerodynamic sources.

It is an experimental observation that turbulent velocities, which are closely related to the acoustic sources, have relatively small spatial correlation. This indicates that sources are uncorrelated in accordance with the requirement that we imposed on the acoustic sources above. We may thus consider the radiation of a single source and evaluate the power radiated by an ensemble of sources by simply adding the power radiated by the individual sources.

We shall adopt the procedure discussed in the previous section to derive a semiphenomenological expression for the power radiated by aerodynamically produced sources. For this

purpose, it is necessary to decipher the functional form of the Q and $\underset{\sim}{F}$ sources. Since Q is a rate of mass addition, it is proportional to ρuA, while $\underset{\sim}{F}$, being a force, is proportional to dynamical forces $\rho u^2 A_F$, where A and A_F are areas to be associated with these sources.

In the final analysis, our interest lies in the power spectrum and the total power radiated by the distribution of sources. Since the latter power is derivable from the former, we consider in some detail the power spectrum of an aerodynamically generated acoustic radiation. We observe first that the frequency components of the Q and $\underset{\sim}{F}$ sources, are determined by the spectral components of $\underset{\sim}{u}$. Thus, a single frequency component of u generates two frequencies in $\underset{\sim}{F}$, one at double the frequency of the other. When the spectral components are differentiated with respect to time, the result is that the components are multiplied by a factor $i\omega$ ($2i\omega$ in the case of a component at double the angular frequency). It is natural to assume that the amplitude of the fluctuating velocity $\underset{\sim}{u}$ is proportional to the amplitude of the convective velocity $\underset{\sim}{U}$ when the sources arise in the absence of externally induced fluctuations. We limit our consideration to such situations.

We are not able to develop an exact formulation for the radiated sound, and shall have to rely on dimensional analysis for a formulation that can be useful in organizing the experimental results. Making use of Eqs. (10) and (11) and noting again that production of higher-order poles than quadrupole is not likely to occur in abundance, we obtain for the power spectrum

$$\omega\tilde{P}(\omega) = \left\{\frac{\omega^2 U^4}{c_a^3} A_F^2 \rho_a + \frac{\omega^4 U^4}{c_a^5} \eta^2 A_F'^2 \rho_a\right\} \beta(\omega) \quad , \qquad (12)$$

where the first term on the right-hand side arises from dipole sources and the second from quadrupole sources. The spectrum $\beta(\omega)$ is assumed to be the same for both monopole and dipole sources. The surface area associated with the dipole source is A_F, and $\eta A_F'$ is the volume associated with the quadrupole source.

There may be present more than one boundary or region of turbulence that leads to the production of dipole and/or quadrupole sources. In such cases $\tilde{P}(\omega)$ is a summation over all such boundaries and regions.

1.4 The Radiated Power Spectrum in Terms of the Strouhal Number

In unsteady flow, the frequency must vary in proportion to U/δ, and the constant of proportionality is the Strouhal number S_t.

$$(\omega/2\pi) \simeq \frac{S_t U}{\delta} \quad , \qquad (13)$$

where δ is a typical linear spatial dimension of the sources. Replacing ω in Eq. (12) by S_t yields

$$\omega\,\tilde{P}(\omega) \simeq \left(\rho_a S_t^2 U^6/\delta^2 c_a^3\right)\left[A_F^2 + \frac{S_t^2 U^2 \eta^2}{c_a^2 \delta^2} A_F'^2\right] \beta'(S_t) \quad , \qquad (14)$$

where β' is the source spectrum as a function of the Strouhal number.

Equation (14) is the central result of our argument. It provides us with a format for the interpretation of the experimental results.

1.5 Effects of Pipe Enclosure on the Sound Radiation

The general form of the expression for radiated power given in Eq. (14) is appropriate for multipole sources in free space. Much of the work reported here, however, concerns sources that are enclosed by a rigid pipe. It is necessary, therefore, to inquire about the effect that this enclosure may have on the radiated sound.

The point can perhaps best be exemplified by considering the monopole source of sound in an infinitely long pipe as shown in Fig. 3(a). Suppose that the pipe has a cross-sectional area A_p. Then, at low frequencies where the acoustic wavelength $\lambda_a >> (A_p)^{1/2}$, the radiated power from the source is just

$$\Pi_{rad} = \overline{u^2} \cdot \left(\frac{A}{A_p}\right)^2 \cdot \frac{1}{2} \rho c A_p \sim U^2 \quad , \tag{15}$$

assuming that $u \sim U$. If the major frequency content of Q, therefore, is in this low-frequency regime, one finds that the radiated sound varies as U^2.

If the same source is radiating at a high frequency, such that $\lambda_a << A_p^{1/2}$, then the walls of the pipe will have less influence on the radiation and the radiated power will approach the infinite-space value:

$$\Pi_{rad} = \frac{\omega^2 \rho}{4\pi c} A^2 \overline{u^2} \sim S_t^2 U^4 \ . \tag{16}$$

Thus, the pipe enclosure will cause a change in the velocity dependence of monopole radiation, depending on the dominant frequencies in the source. Clearly, intermediate power laws of velocity are possible if the dominant frequencies are intermediate between these extremes.

It is possible to draw similar conclusions for higher-order sources. For example, in Fig. 3(b), two dipoles are shown: one oriented with its axis normal to the pipe axis, and the other with its axis parallel to the pipe axis. In the former case, there will be no radiation from the dipole when $\lambda_a \gg A_p^{1/2}$, since this configuration cannot excite the plane-wave mode of the pipe (the only propagating mode at these frequencies). The radiation from such a dipole is then less than its free-space value.

The dipole with its axis parallel to the pipe axis will likely have its radiation increased from the infinite space value in an amount depending on the cross-sectional geometry of the pipe. When the cross section is rectangular, this can be studied by the method of images, as is done in Appendix A. If the cross section corresponds to a coordinate line of one of the spaces in which the two-dimensional Helmholtz equation is separable, then an eigenfunction expansion can be used to evaluate these effects (ref. 13).

Fortunately, in the experiments reported here, the frequencies are sufficiently high so that free space radiation efficiencies are likely to be appropriate. They are also broad band so that we can average over pipe resonances. In this case, the fact that the pipe is finite does not affect the radiation laws.

1.6 Spoilers as Sound Generators

The introduction of spoilers (passive physical surfaces) in the flow in the pipe introduces a mechanism for the production of dipole sources in accordance with our earlier discussion. It is, therefore, natural to assume that the first term on the right-hand side of Eq. (14) represents an important contribution to the radiated power. It may be argued that, although the spoiler introduces a wake region where quadrupole sources could form, the higher efficiency of the dipole sources should lead to dominance of dipole radiation. However, the spectral analysis of the radiated power, which Eq. (14) represents, shows that at the higher frequencies (or higher Strouhal numbers) the radiation may be dominated by quadrupole radiation. Moreover, in addition to the particular spoiler under consideration, there may exist other spoilers or other mechanisms that induce sources, e.g., the exit flow, the discontinuity at the edge of the pipe, etc. In such cases, the radiated power is given by summing the respective radiated powers. One may argue in some specific situation that a particular mechanism may be dominant (e.g., a particular spoiler) in over-all radiated power. Again, however, on a spectral basis, the particular mechanisms may show dominance in a particular range of the spectrum and allow another to dominate in a different range.

1.7 Interpretative Procedures and the Normalization of the Radiated Power

The major purpose of the analysis discussed above is to examine the minimum number of components that are necessary to

interpret the data in a coherent and well-defined manner. It is, therefore, expedient to make simplifying assumptions regarding the radiation which is consistent with the above formalism and examine their validity by the experimental data. Any conclusions that may be drawn from such a procedure are in the nature of inferences rather than a bonafide proof of the theoretical arguments.

First, we note that it is convenient to write $\tilde{P}(\omega)\omega$, $\beta'(S_t)$, and S_t in terms of proportionate bands (e.g., octave bands). Provided the spectrum $\tilde{P}(\omega)$ and $\beta'(S_t)$ are fairly smooth, we may set

$$S_t^2 \beta'(S_t) \simeq k\bar{\beta}\ (\bar{S}_t) \quad ,$$

and

$$P(\omega)\omega \simeq kP_B(\bar{\omega}) \quad , \tag{17}$$

where $\bar{\omega}$ and $\bar{S}_t$ are, to all purposes, the center points of the respective bands, and k is a constant.

Second, we assume that the dipolelike sources contribute dominantly to the radiated power and that a single mechanism dominates all others. For this situation, we obtain from Eq. (14)

$$P_B(\bar{\omega}) \simeq (\rho_a\ U^6/\delta^2 c_a^{\,2})\ A_F^{\,2}\ \bar{\beta}\ (\bar{S}_t) \quad . \tag{18}$$

In pipe flows with a spoiler inserted in the pipe, it is rather difficult to ascertain the mean velocity U that is as-

sociated with the dipole source production. It is reasonable to relate this velocity to the maximum velocity attainable in the pipe, for this velocity must occur in the vicinity of the spoiler. Thus, if the stagnation pressure on the upstream side of the spoiler is denoted by p_o and on the downstream side the pressure is denoted by p_a (usually atmospheric), then we may set

$$(p_o - p_a) \simeq \frac{1}{2} \rho_a U^2 \quad . \tag{19}$$

Both p_o and p_a are rather simple quantities to measure experimentally. From Eqs. (18) and (19) we then have

$$\frac{P_B(\omega)}{(p_o - p_a)^3 (A_F^2/\rho_a^2 c_a^3 \delta^2)} \simeq \overline{\beta} \quad (\overline{S}_t) \quad , \tag{20}$$

$$\frac{P_{tot}}{(p_o - p_a)^3 (A_F^2/\rho_a^2 c_a^3 \delta^2)} \simeq \overline{\beta}_{tot} \quad \text{(a constant)} \quad . \tag{21}$$

Thus, if our assumption is reasonable, the experimental data of the power band spectra, normalized as indicated by Eq. (20), should be a function of the band Strouhal number $\overline{S}_t$ only. Similarly, the total power normalized by the same function should prove to be constant. [Eq. (21) is essentially that derived by Yudin (ref. 14).] Extensive experimental data (presented in subsequent chapters) normalized in this way bear out, to a certain extent, the contention of the assumptions. Some deviation from Eqs. (20) and (21) is found, however. Of particular interest are those deviations that appear at the higher Strouhal numbers in the case of the power band

spectra and at the higher mean convective velocities [higher values of (p_o-p_a)] in the case of the total power. [It is of interest to note that Yudin (ref. 14) examined the validity of Eq. (21) in the range of lower mean convective velocities than has been reached in the present experimental work.] However, we have seen that Eq. (21) is incomplete and should be modified to account for the quadrupoles. This is readily done by inclusion of both terms in Eq. (14), giving

$$\frac{P_B(\bar{\omega})}{(p_o-p_a)^3\ (A_F^2/\rho_a^2 c_a^3 \delta^2)\left[1 + (\frac{\bar{\omega}}{\omega_c})^2\right]} \simeq \bar{\beta}\ (\bar{S}_t) \qquad (22)$$

and

$$\frac{P_{tot}}{(p_o-p_a)^3\ (A_F^2/\rho_a^2 c_a^3 \delta^2)\left[1 + \frac{(p_o-p_a)}{p_c}\right]} \simeq \bar{\beta}_{tot}\ , \qquad (23)$$

respectively, where ω_c and p_c are a constant frequency and pressure, respectively, which may be functions of the dimension of the spoiler and/or the pipe.

As we shall see in subsequent chapters, these last two equations are in good accord with experimental findings. Indeed, the equations derived here by a heuristic treatment can be rigorously established from Lighthill's theory, and the agreement is confirmation of the relevance of that theory to the present experiment.

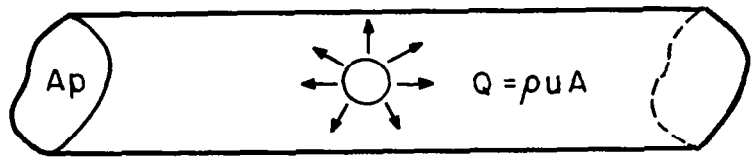

a) SIMPLE SOURCE MODEL

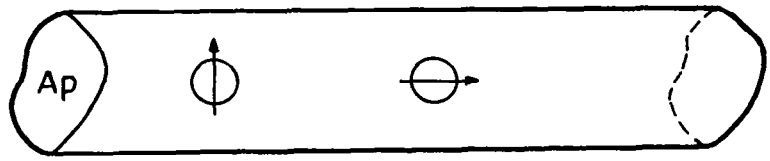

b) DIPOLE SOURCE MODEL

FIG. 3 EFFECT OF SOURCE ENCLOSURE WITHIN A PIPE

II. EXPERIMENTAL METHODS

The purpose of this study is to examine the sound power radiated from a model jet pipe into which are inserted a variety of flow spoilers at some distance from the exit plane. Of particular interest is the way in which the level and spectrum of this power changes with the flow and geometric parameters. In this chapter, we describe the experimental techniques that have been used in the study.

2.1 Total Power Measurement

The measurement of total radiated sound power, although easy to envision in principal, in practice is considerably complicated by the three-dimensional character and highly directive nature of the radiation field. In the past, many experimenters have been content to describe the sound radiation on the basis of a few fixed microphone locations arranged in a fixed pattern around the jet source. Such measurements, however, have a very limited interpretation when we consider the continuously changing character of the sound field with flow velocity, frequency, and flow geometry. That there is an inherent difficulty in obtaining accurate measurements of total power cannot be doubted.

Two methods of measurement of the total radiated sound are available. The first, the "free-field" method, is limited only by the completeness with which the microphone can survey the radiation field and the subsequent accuracy with which one can manipulate the "sound-pressure" readings. The "anechoic" chamber is ideally suited to these measurements, removing the

"ground-plane" effect normally present in outside measurements.

The second method may be called the "reverberation-chamber" method. The successful use of this method requires only the measurement of the diffuse sound-pressure level at one or two locations within the chamber. These readings may then be related to the total power via the room calibration. Such a technique has been used by Waterhouse and Berendt (ref. 15) and Fitzpatrick and Lee (ref. 4) in their studies. The use of a reverberant space for measuring the total sound power radiated by a source is valid only on the assumption that the reverberant portion of the sound field is diffuse. Such a diffuse condition is only established if the primary sound wave suffers many reflections before being significantly attenuated. It is also necessary that the chamber be shaped in such a way that degeneraries in the resonance frequencies are minimized. For these and other reasons, the reverberant-chamber technique ceases to be of value both at very low frequencies, when the modal density is low and low-order modes govern the spatial distribution of sound energy, and at high frequencies when the absorption of sound energy by the air becomes significant. At these higher frequencies it becomes increasingly difficult to separate the "reverberant" portion of the sound field from the "direct" field of the source and eventually, of course, the sound field ceases to be diffuse.

In the experiments described in this study a large part of the total radiated power is observed to lie in the high-frequency region for which a reverberant-room technique cannot accurately be used. Following some preliminary tests, therefore, it was decided that a free-field technique should be employed.

2.2 Free Field Survey

The study has been carried out with the jet source located in an "anechoic" chamber. Experiments have shown that, in general, the sound field radiated by the experimental jet system is axially symmetrical. Thus the sound field may be completely described by a simple planar traverse of the radiation field, the traverse being centered on the exit plane where the sound sources are effectively located.* Experimentally this is achieved by a self-powered rotating microphone boom. The output of the microphone defines the radiation field and the "weighted" integration of this output gives an accurate measure of the total radiated power.

In order to minimize the effects of fluctuations in the running speed of the air-flow equipment, the total noise signal from the traversing microphone was recorded on magnetic tape while the microphone was swept from the downstream (0^{o}) position to the upstream (180^{o}) position and back to the downstream (0^{o}) position. The traverse in the reverse directions provides a useful check on the constancy of the radiation pattern and also serves to detect malfunctions of the apparatus. This procedure was repeated for each of several flow velocities over the range available from the air-flow equipment. The data was then available for spectral analysis and power computation. Calibration of the instantaneous spatial position of the microphone during the

---

* As we shall see later in the report, "spoiler" noise is generated in the vicinity of the spoiler and propagates from there as an acoustic wave. From the viewpoint of the free-field radiation, the spoiler sources are located at the exit plane, unlike the free jet "quadrupole" sources which are distributed spatially along the free jet region.

sweep was obtained by simultaneously (with the magnetic recording) recording the microphone output on a pen recorder which also carried a position marker triggered by the microphone boom.

2.3 Power Computation

Computation of the total radiated sound power from free-field measurements involves the "weighted" integration of the axially symmetric "directivity pattern" after the manner

$$P_A = \frac{2\pi R^2}{\rho c} \int_0^{\pi} \overline{p^2} \sin \theta d\theta \quad , \tag{24}$$

where P_A is the acoustic power, R the source/microphone distance, $\overline{p^2}$ the mean square sound pressure measured by the microphone at an angle θ relative to the downstream axis, and ρ and c atmospheric density and the sound speed, respectively.

Generally, the farfield sound pressures generated by a jet source are strongly dependent upon angular position relative to the jet axis. Under these conditions, the graphical integration by hand of Eq. (24) is extremely laborious and is, thereby, liable to inaccuracy.

III. EXPERIMENTAL EQUIPMENT

In this chapter, we describe the hardware used in the experimentation and the air-flow facility and measurement chamber.

3.1 Air-Flow Equipment

The source of air flow consisted of the supercharger section of a Pratt and Whitney model R-2800 aircraft engine driven by a 600 HP Cummins diesel engine. This equipment was capable of producing an air flow up to 6000 standard cubic feet per minute at pressures up to about 15 psi. The air output from the supercharger was passed through an aftercooler, a 12-in.-diameter pipe, and a 12-ft-long noise muffler, into the measurement chamber via a 6-in.-diameter flexible hose. A schematic of this equipment is shown in Fig. 4. The flow of air to the experimental jet system was controlled both by controlling the speed of the diesel engine and by dumping air from the aftercooler.

3.2 Measurement Chamber

The measurement chamber as used in these studies had dimensions of about 12 ft by 12 ft by 7 ft high and is shown in plan schematic in Fig. 5. The walls of the chamber were partially treated with 18-in.-deep "anechoic" wedges to suppress the major reflections. The remaining surfaces (including jet pipe and support brackets) were treated with a 4-in.-thick sound-absorptive blanket. Tests have shown that with the jet pipe

located, as shown, at a distance of about 2 ft from the chamber wall and with a source/microphone distance not exceeding 4 ft, the chamber was effectively "anechoic" at sound frequencies of 300 cps and greater.

The microphone boom by which the radiation field of the source is scanned, was located close to the ceiling of the chamber. The microphone was suspended from the boom and moved in the horizontal plane of the jet exit. Throughout the studies, the distance between the microphone and the jet exit plane was 3 ft and the speed of rotation of the boom was about 1 rpm. Movement of the microphone was limited to between 10^{o} and 150^{o} measured relative to the downstream axis of the pipe, the lower limit being set by the need to keep the microphone clear of the jet stream. A photographic view of the measurement chamber, showing the absorptive treatment, the experimental jet, and microphone boom, is given in Fig. 6.

3.3 Experimental Jet System

The air supply was passed to the jet system via the 6-in.-diameter flexible hose and transition sections shown in Fig. 5. Throughout most of the studies, the jet pipe into which the spoilers were inserted had a nominal diameter of 2 in. (1.875 in. actual). The total length of the jet pipe from transition to exit plane was 36 in. Thus, at the exit plane, fully developed pipe turbulence was established.

The jet system was designed in such a way that spoilers could be easily inserted into and removed from the jet pipe. Furthermore, any particular configuration could be reassembled, exactly, at any stage during the study. The design chosen to

satisfy these requirements is shown in Fig. 7. Each spoiler configuration was constructed within a 6-in.-long unflanged pipe. This could then be inserted into the pipe system using the removable flanges and "O" rings as shown. The flanged construction also allowed the distance of the spoiler from the exit plane to be adjusted over a range from zero to 18 in. To minimize structural vibration of the spoilers, they were constructed in the form of two layers of aluminum, sandwiching a layer of structural damping material. A more detailed description of the spoiler geometries as they apply to the various experiments appears in a later chapter of this report. A photographic view of a selection of spoilers is given in Fig. 8.

3.4 Instrumentation

A block diagram of the instrumentation used is shown in Fig. 9. The signal from the traversing condenser microphone (Bruel and Kjaer 1/2 in.) was fed via the appropriate amplifiers and a high-pass filter to a magnetic tape recorder (Kudelski Nagra III B) and a graphic level recorder (Bruel and Kjaer type 2305). The high-pass filter served to remove that part of the acoustic signal below 250 cps, for which the measurement chamber was not anechoic. The frequency response of this total system was linear from 250 cps to 20 Kcps. The upper limit was set by the high-frequency cut off of the magnetic-tape system.

3.5 Flow Measurement

Air flow was measured using a single pitot static tube centrally located in the jet pipe at a distance of about 22

in. from the exit plane, as shown in Fig. 7. Water and mercury manometers were used as necessary to read static and velocity pressure heads.

3.6 Data Reduction

When it was considered that each experiment in this study might involve seven or eight different flow conditions and that, at a minimum, the data reduction — involving the linear and octave-band spectrum analysis — would require seven graphical integrations, of the form of Eq. (24), under each flow condition (the total experiment, therefore, giving of the order of 50 sound-pressure level versus angular position charts), it became apparent that a faster and more accurate method of data computation was required.

The "Grafacon" is an analogue/digital device which allows the user to "draw" a plot or graph into the computer where it is stored in digital form. The data is then directly available to the computer for further analysis. A computer program was written embodying the integration involved in Eq. (24). The graph of sound-pressure level versus angle was then read into the computer using the "Grafacon". The computer then typed out the answer to the required integration.

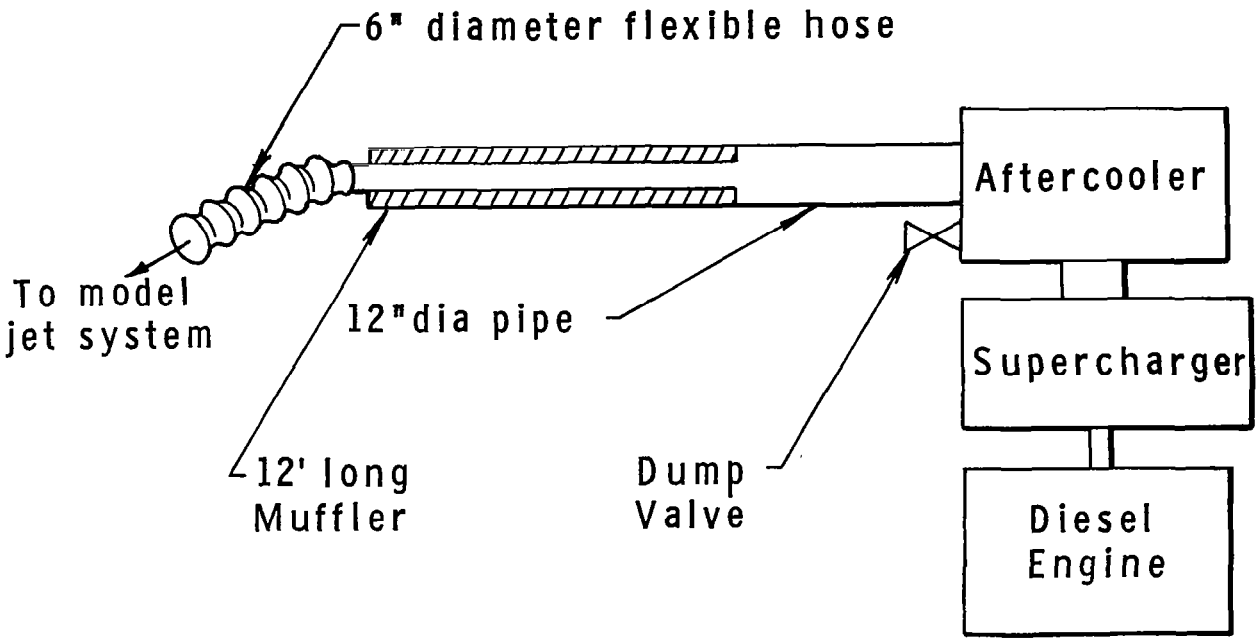

FIG. 4 AIR-FLOW EQUIPMENT SCHEMATIC

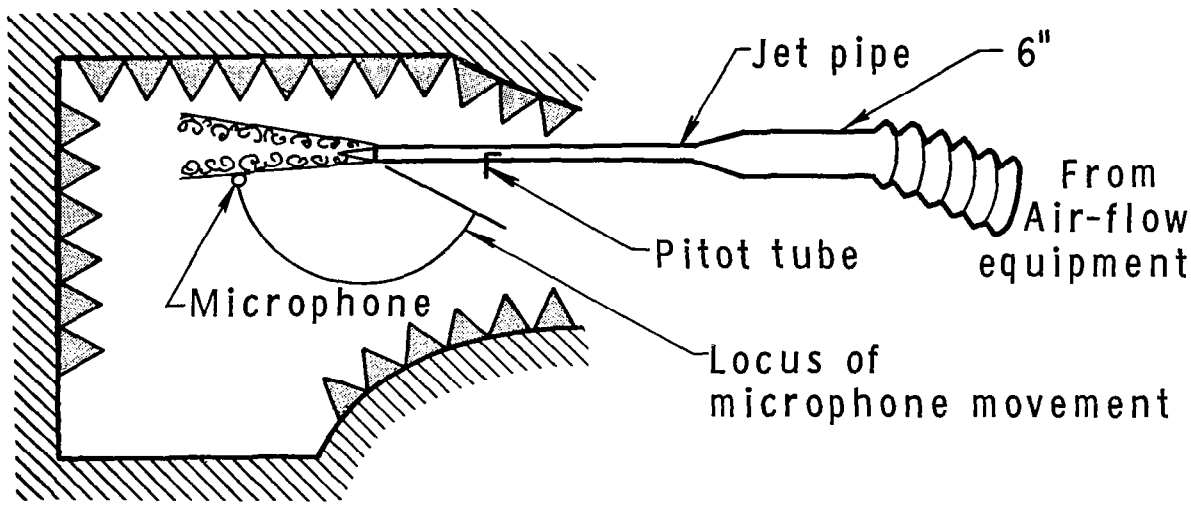

FIG. 5 MEASUREMENT CHAMBER SCHEMATIC

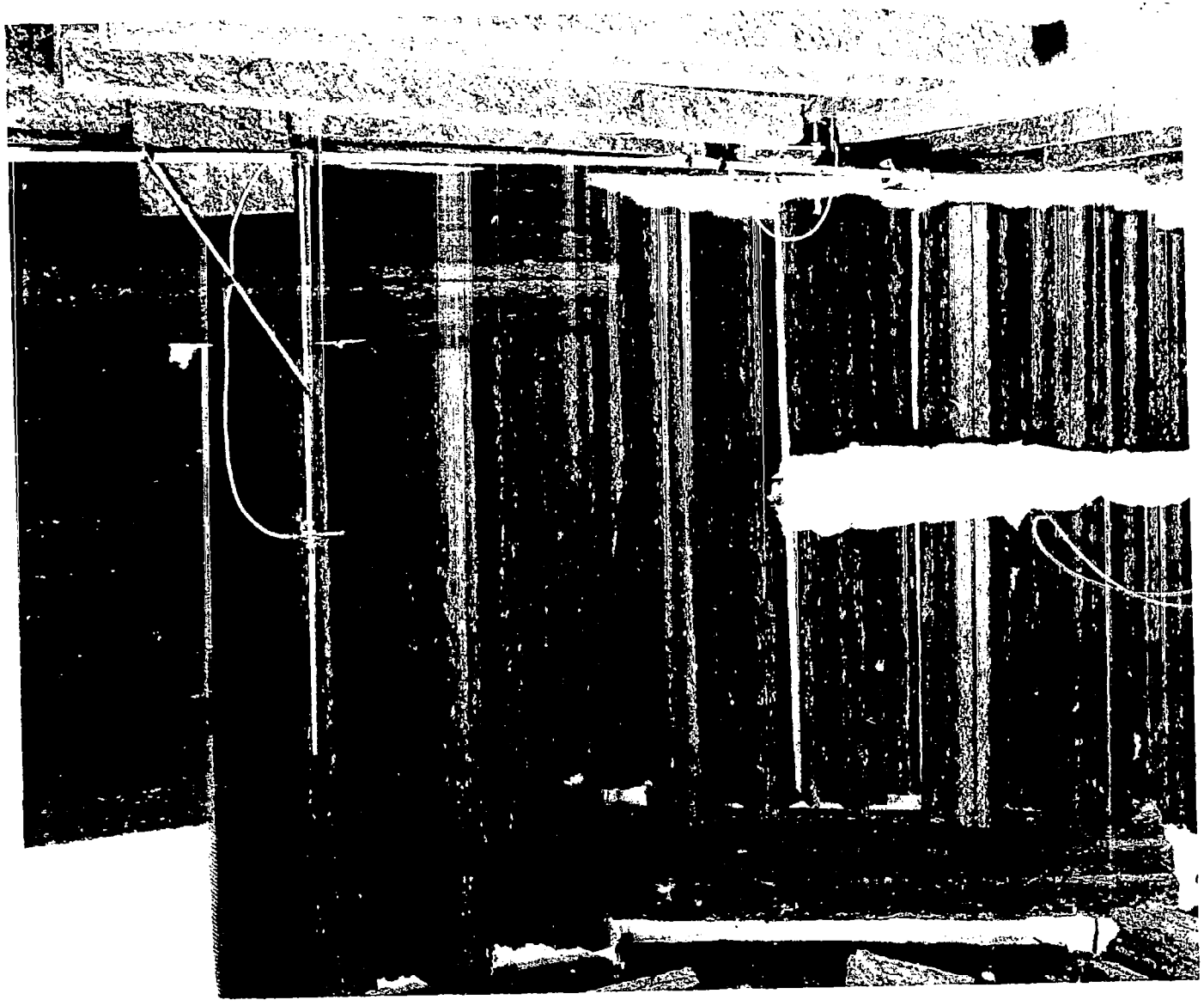

FIG.6 VIEW OF MEASUREMENT CHAMBER

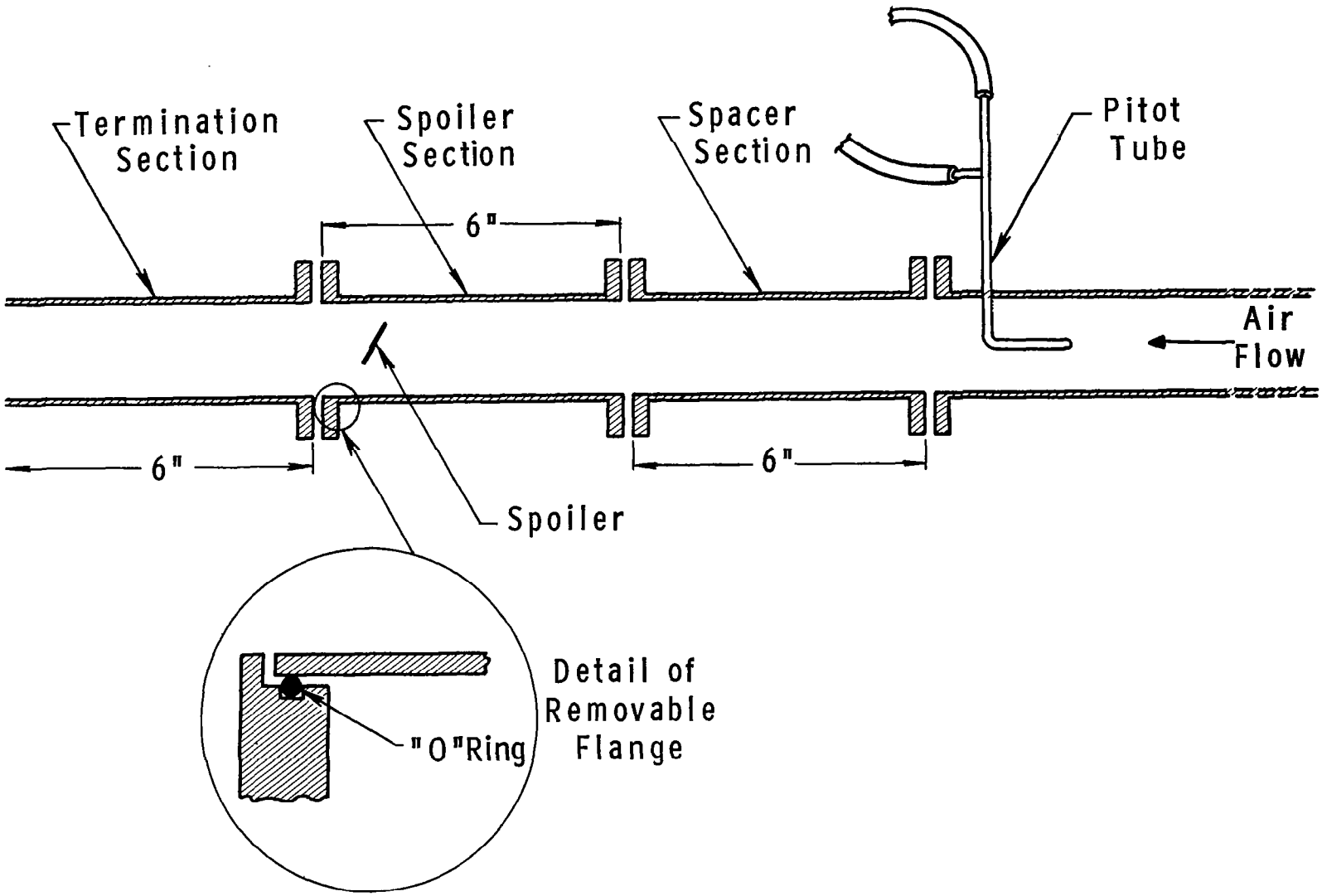

FIG.7 EXPERIMENTAL JET

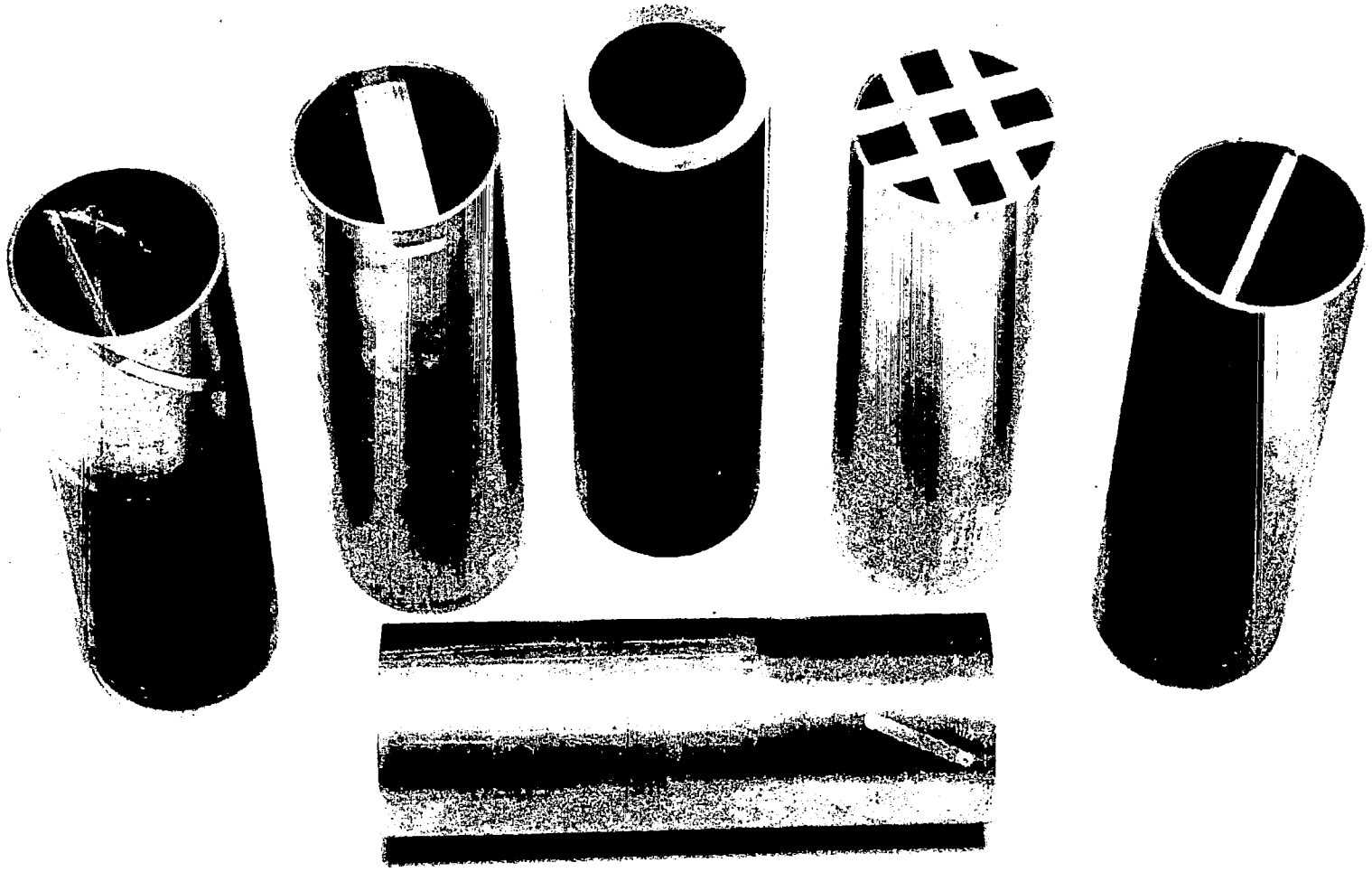

FIG.8 A SELECTION OF FLOW SPOILERS

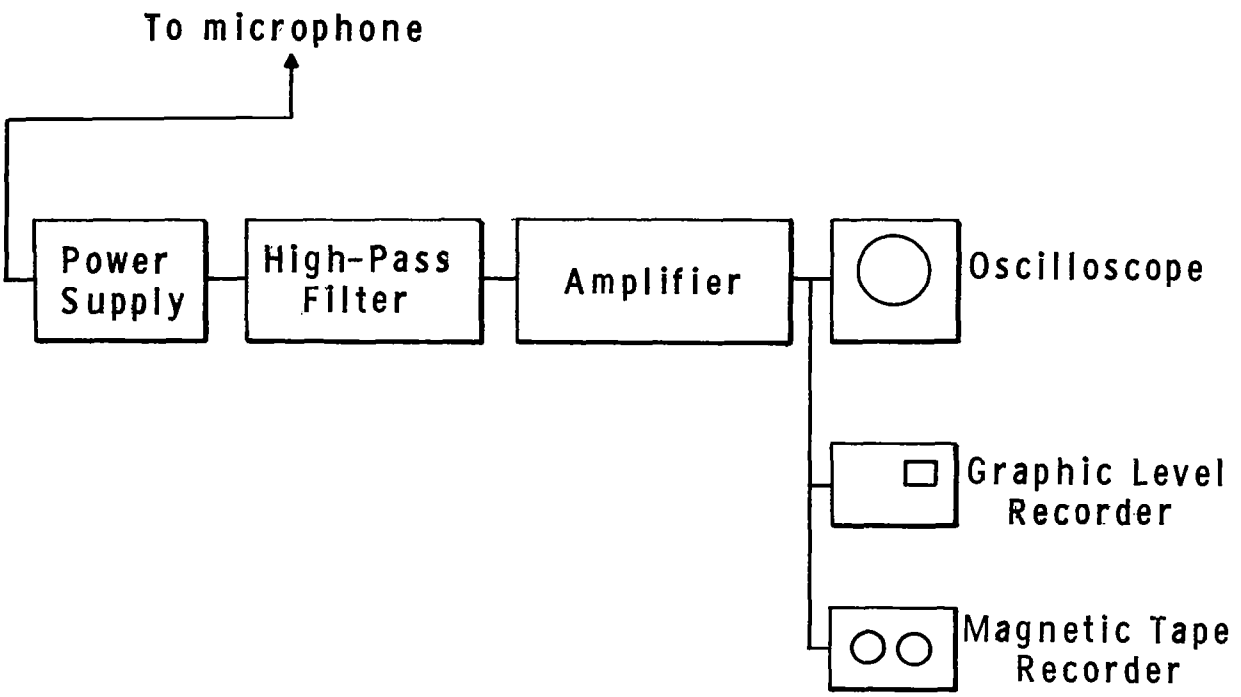

FIG.9 INSTRUMENTATION SCHEMATIC

IV. PRESENTATION OF RESULTS

The study described in this report is an examination of the power radiation from a model jet system into which are inserted, in turn, a variety of flow spoilers at some distance from the exit plane. The purpose of the study is to examine the effect of such insertions upon the radiated sound power in a highly controlled environment.

It is our purpose in this chapter to review some of the findings of this study and to present in a logical sequence experimental configurations leading from the quadrupole-dominated plain jet pipe to the spoiled jet flow. An accumulation of observations regarding the location and empirical description of in-pipe noise sources is also presented.

4.1 The Plain "Unspoiled" Jet System

The level of radiated sound power from an unspoiled jet-pipe flow is shown in Fig. 10 as a function of the exit-plane velocity. Results are shown for three separate experiments made over a four month period. This result demonstrates the high order of repeatability obtained from the experimental equipment. The plain pipe radiation shows a sixth-power of velocity dependence at the lower velocities changing into an eighth-power dependence at the higher velocities. The latter is identified with the free-jet turbulence and agrees closely with theoretical predictions (solid line) based on constants determined experimentally by Fitzpatrick and Lee (ref. 4). The accuracy of the data collection and reduction schemes appears to be satisfactory.

4.2 Spoiled Pipe Flow

When a spoiler is inserted into the pipe, the radiated power increases as shown in Fig. 11 and a sixth-power of velocity now becomes established (solid line) over the total operating flow range. It is relevant at this stage to note that throughout these studies a sixth-power-of-velocity law has been consistently and accurately observed for most spoiled-flow configurations (just as the eighth-power law has been experimentally observed for the plain jet pipe).

Accepting for the moment the assumption that a sixth-power of velocity is indicative of dipolelike sources, (as described in Chapter I), at least two sources of noise can be postulated. They are located, respectively, in the close vicinity of the spoiler and at the exit plane of the jet pipe. The latter has been referred to as "lip noise" and is generated by the interaction of the spoiler wake with the pipe wall.

4.3 Source Location

Figure 12 describes the results of an experiment in which an acoustic muffler was inserted immediately downstream of the flow spoiler. The muffler was constructed of a cylinder of porous sintered Fibremetal* backed by a 1-in.-deep air space. The purpose of the experiment was to remove the acoustic energy propagating downstream from the spoiler without affecting the turbulent wake. The experiment indicates quite conclusively that the dominant spoiler noise must be located close to the

* by Huyck Metals, Inc.

spoiler rather than at the exit lip. A second experiment in which flow straighteners were added to reduce the turbulent wake but not the acoustic wave was also carried out and led to the same conclusion; i.e., that spoiler noise is generated in the vicinity of the spoiler itself rather than in the exit-plane region. Thus the noise generated by a spoiler propagates as an acoustic wave along the jet pipe and into the surrounding space. The acoustical parameters of the jet pipe must, therefore, be important in controlling spoiler-generated noise.

4.4 Effect of Spoiler Dimension

Having gained some idea of the mechanisms and location of the spoiler-generated sources, the next step in this presentation is to examine the forms of sound radiation for a variety of spoiler configurations and sizes.

In Fig. 13, the results of measurements on three forms of "strip" spoiler* are shown plotted against exit flow velocity. It is apparent and, perhaps, not surprising that although a sixth-power-of-velocity dependence is approximately applicable to each experiment, there is a very considerable spread (about 20 dB) from one to the other.

---

* More-detailed descriptions of these spoilers are given elsewhere. At present, it is sufficient to know that they lie in the radial plane of the pipe and present the forms shown (as hatched) in Fig. 13 to the flow. Their thickness is about 1/8 in.

4.5 Correlation of Data

Studies of this and other data have shown that a very close correlation between unlike experiments is possible on the basis of the total pressure drop across the spoiler. Total pressure drop is given by $(p_o - p_a)$, where p_o is the total stagnation pressure on the upstream side of the spoiler -- as measured by a pitot tube -- and p_a is the atmospheric pressure. The results of Fig. 13 are plotted to this abcissa in Fig. 14.

The total acoustic power radiation from a spoiler inserted in a jet pipe may be described apparently by a relation having the form

$$P_A = K(p_o - p_a)^3 D^2 / \rho_a^2 c_a^3 \quad , \tag{25}$$

where ρ_a and c_a are the atmospheric density and sonic velocity, respectively; D is the pipe diameter and K is a constant having a value of about 2.5×10^{-4}. It is interesting to note that this formulation does not include specifically any information regarding the flow spoiler -- this information is already implicit within the pressure drop. The formulation of Eq. (25) is almost exactly that of Yudin (ref. 14) described earlier. [Eq. (25) is obtained from Eq. (21) by setting $A_F \simeq \delta D$].

In the next chapter, we shall consider the development of this empirical formulation and consider the basis on which we shall normalize the experimental data.

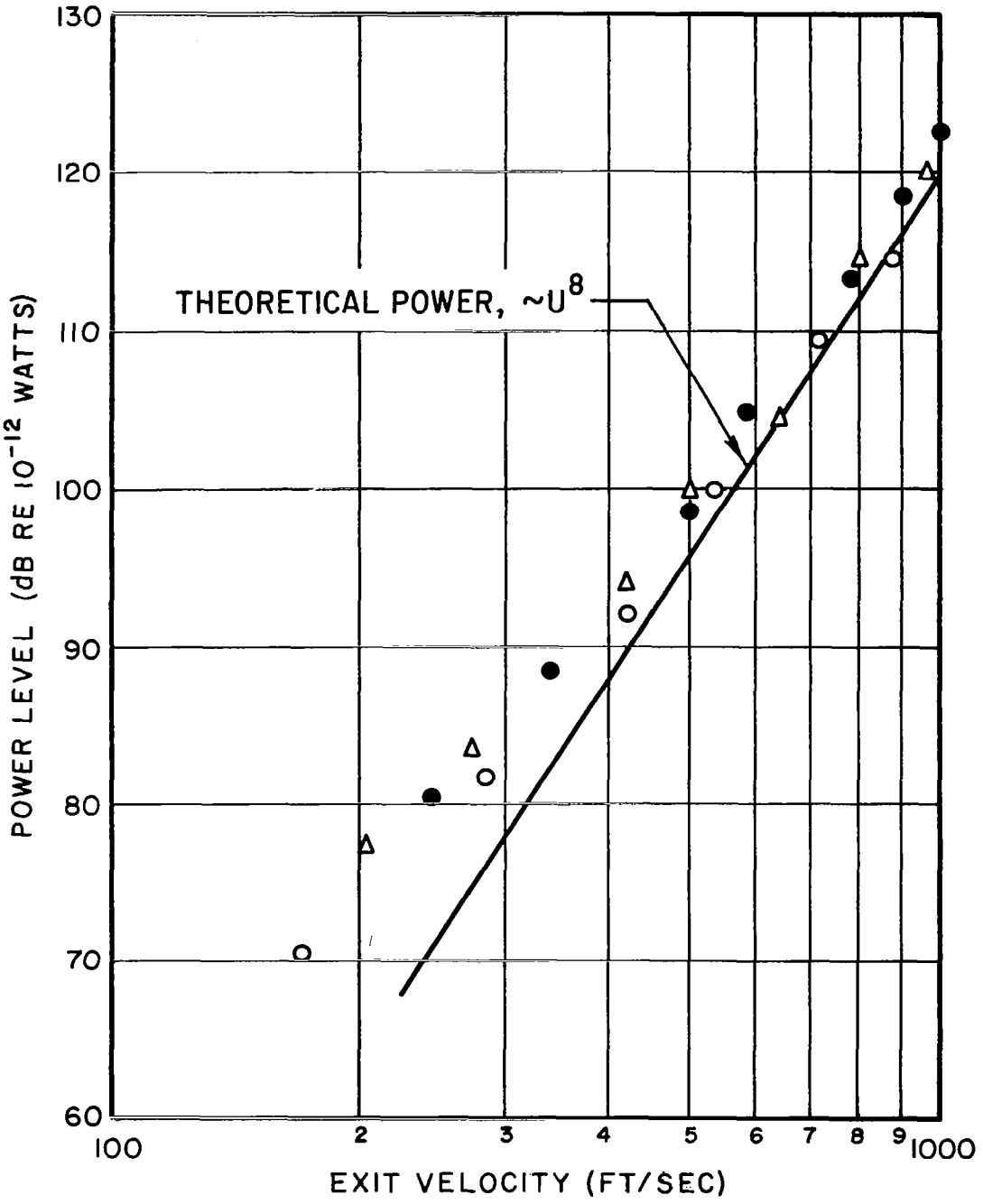

NOISE RADIATION FROM PLAIN JET PIPE

FIG.10

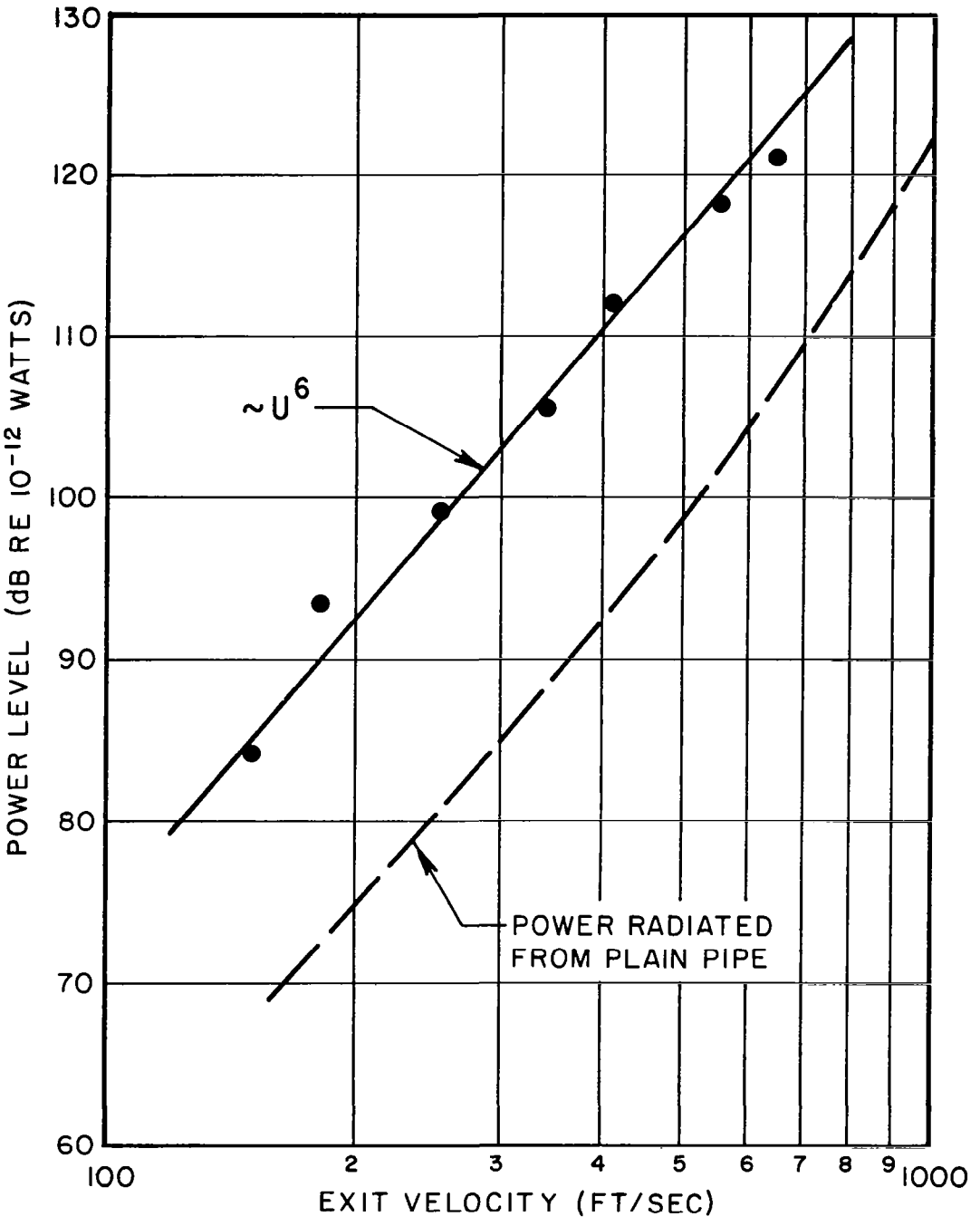

EFFECT OF FLOW SPOILER UPON POWER RADIATION

FIG. 11

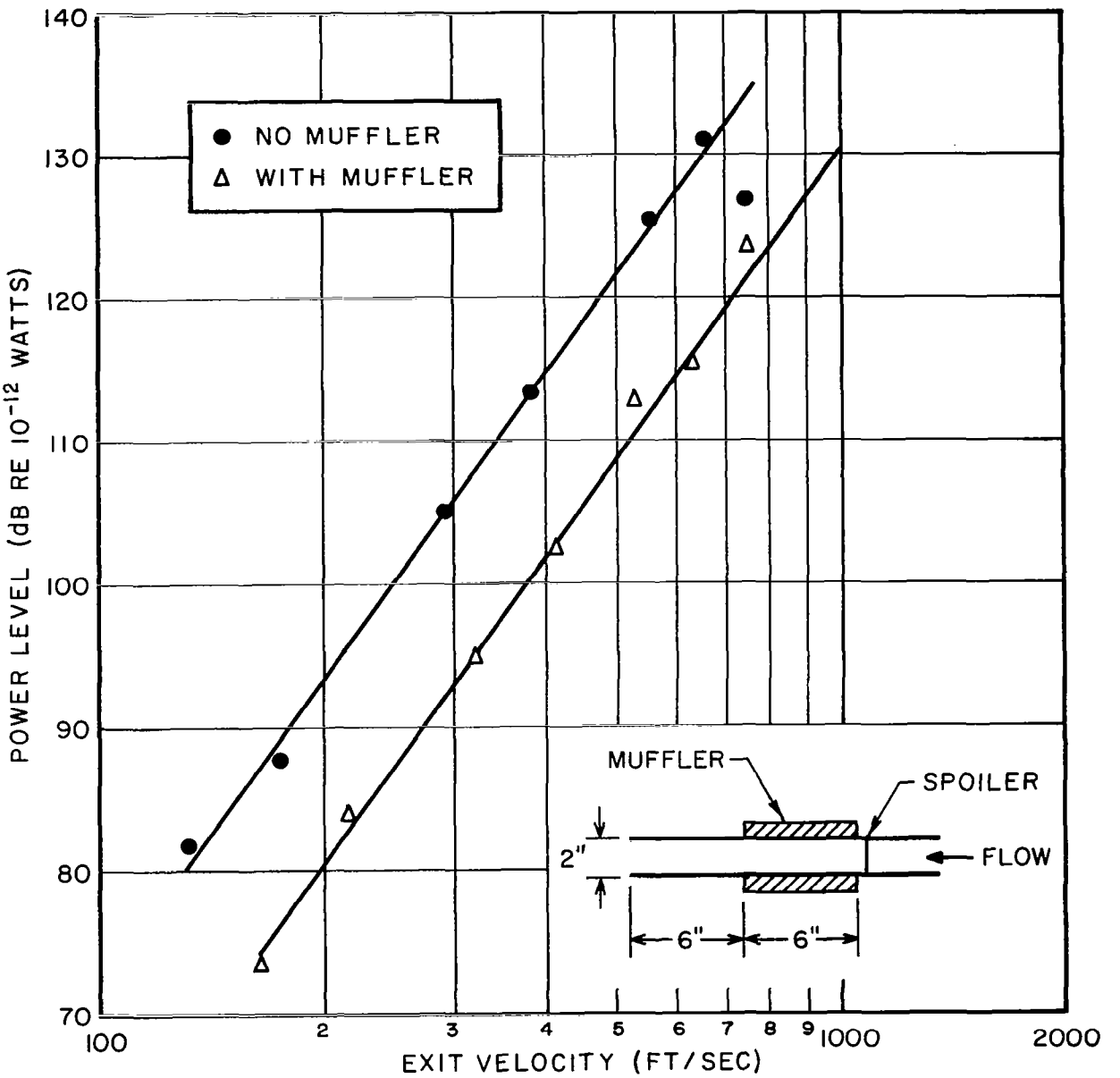

EFFECT OF MUFFLER ON RADIATED SOUND POWER

FIG. 12

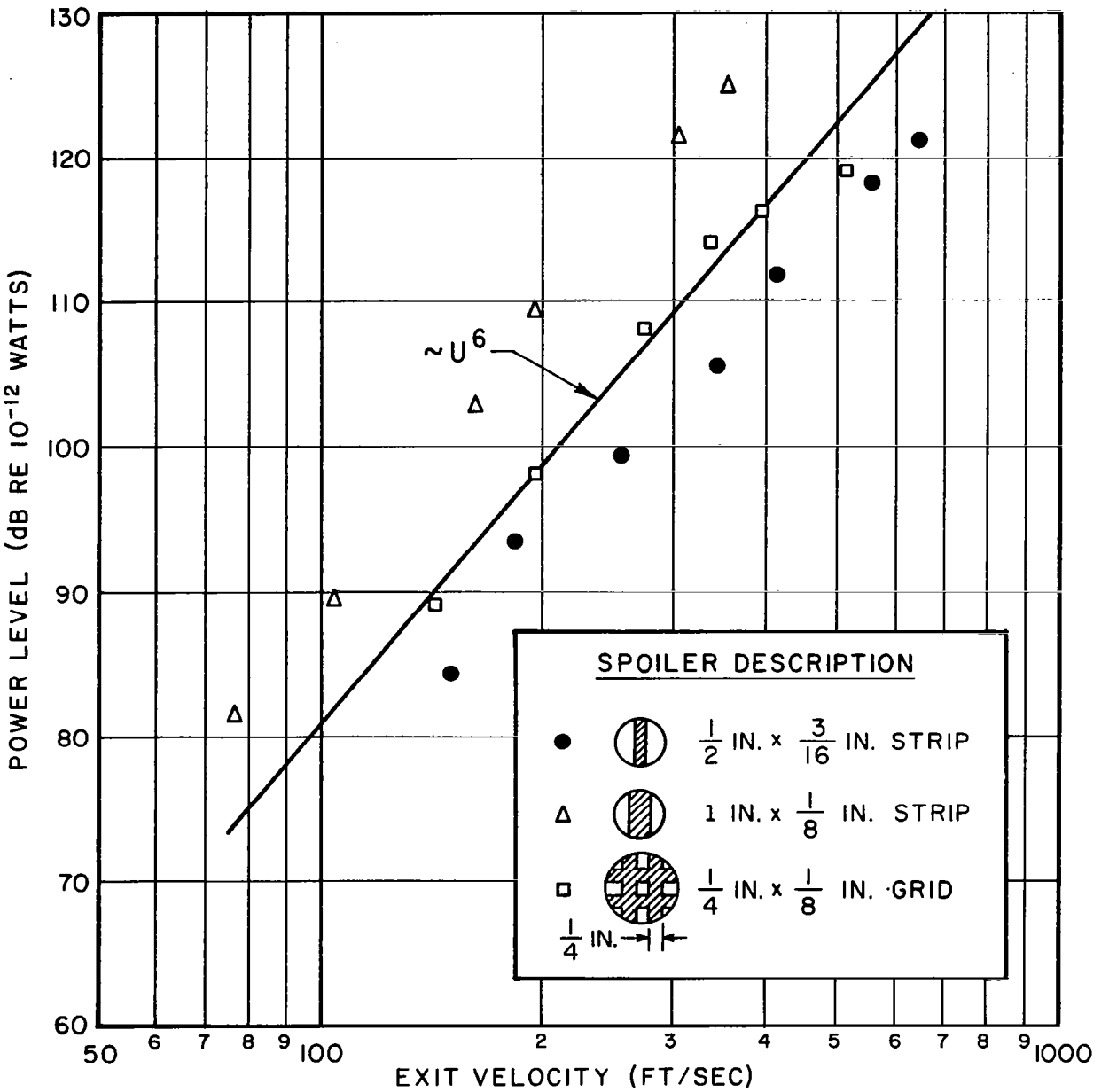

EFFECT OF SPOILER DIMENSION ON RADIATED POWER

FIG. 13

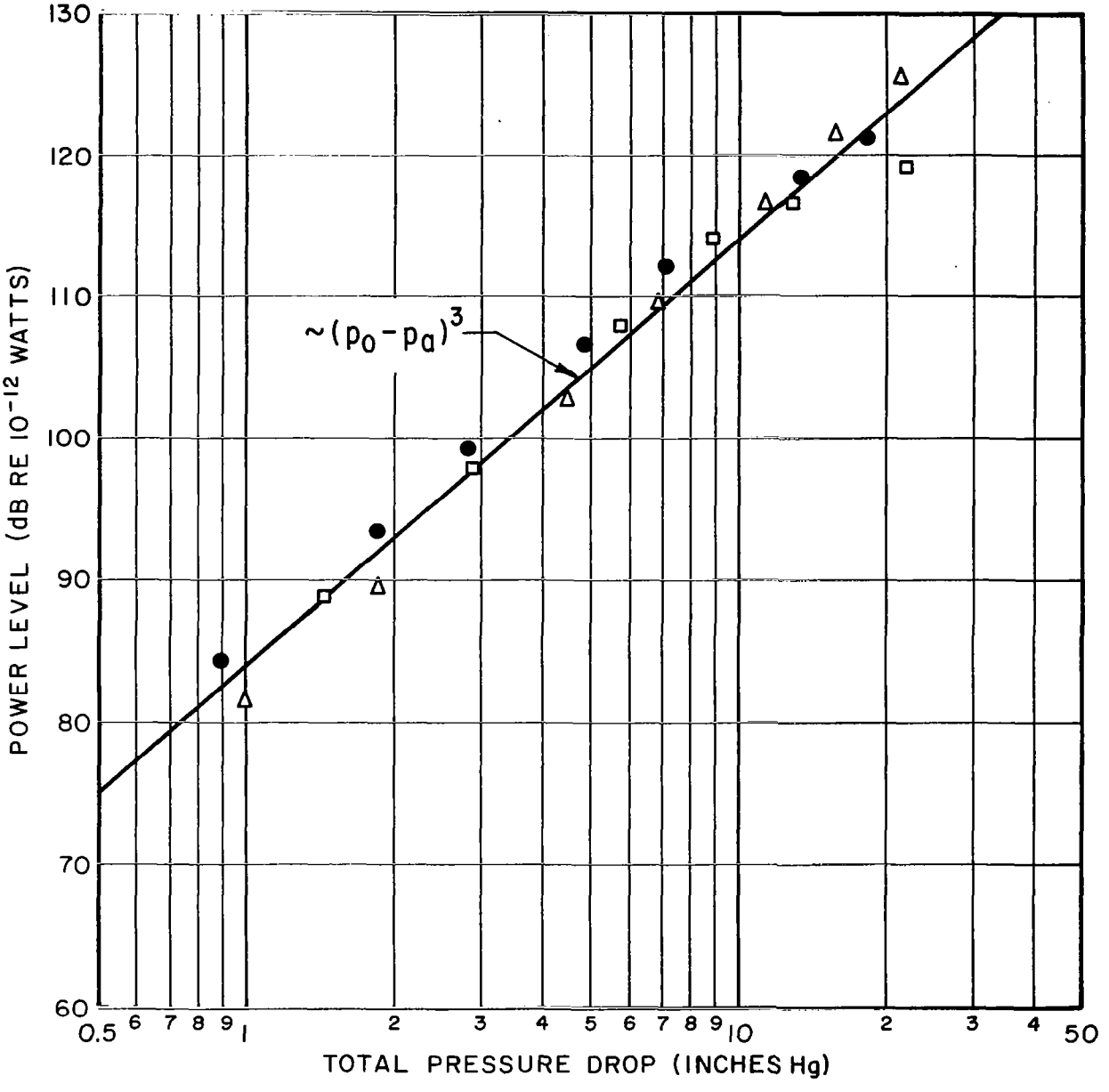

COLLAPSE OF DATA OF PREVIOUS FIGURE WHEN PLOTTED AGAINST THE TOTAL PRESSURE DROP THROUGH SPOILER.
For spoiler geometry and identification see Fig.13

FIG.14

V. NORMALIZATIONS OF RESULTS

In the preceding chapter, it has been shown that the noise generated by a flow spoiler is generated within the jet pipe and that the sound power is related to the sixth-power of typical flow velocity or to the third-power of total pressure drop across the spoiler. In the present chapter, we wish to develop a semiempirical formulation of spoiler-generated sound upon which the normalization of the experimental results may be based.

5.1 A Dipole Model of Spoiler Noise

In the earlier theoretical dissertation on aerodynamic noise sources and also in Appendix A of this report, the validity of applying a free-field solution to an in-pipe (one-dimensional) environment has been very seriously questioned. The fact remains, however, that, notwithstanding the apparent constrictions upon the environment, the experimental appearance of the sixth-power-of-velocity law is a strong indication of dipolelike activity of a more or less conventional sort.

This conclusion is further strengthened by the observation that Eq. (25) is very easily derived from the free-field dipole relation (ref. 11):

$$P_A \sim F^2 f^2 / \rho_a^2 c_a^3 \quad , \tag{26}$$

where F is the steady hydrodynamic force and f is a typical frequency. Here, we assume a constant proportionality between steady and fluctuating components of the force field.

Consider the jet-pipe configuration shown schematically in Fig. 15. The upstream static pressure and velocity are p_1 and U_1, and p_a and U_a are the downstream atmospheric conditions. The quantity (p_o-p_a), the total pressure drop, describes the local constricted velocity U_ℓ if we assume that the flow is virtually potential down to the constriction point and that the atmospheric pressure p_a penetrates up toward the spoiler location. Thus,

$$\frac{1}{2}\rho_a U_\ell^2 = p_1 + \frac{1}{2}\rho_1 U_1^2 - p_a = p_o - p_a \quad . \tag{27}$$

Returning to Eq. (26), the hydrodynamic drag can be described by the product of the local-velocity head and the projected area (wake area) of the spoiler:

$$F \sim (p_o-p_a)\, D\ell \sin\alpha \quad , \tag{28}$$

where D is the pipe diameter, ℓ is the width, and α is the angle of attack of the strip spoiler. The typical force frequency is described by the local velocity and the thickness of the wake:

$$f \sim U_\ell/\ell \sin\alpha \quad . \tag{29}$$

The total acoustic power can therefore be described in terms of the total pressure drop:

$$P_A \sim (p_o-p_a)^3 D^2/\rho_a{}^2 c_a{}^3 \quad . \tag{30}$$

This formulation is identical to that given in Eq. (25). It is found, experimentally, to satisfy much of the experimental data.

5.2 Form of Data Presentation

In the formal presentation of results in subsequent chapters, the normalization employed is based on Eq. (30). The normalized power level (PWL_N) for total and octave-band data is given by

$$PWL_N = 10 \text{ Log } \left[\frac{P_A \rho_a{}^2 c_a{}^3}{(p_o - p_a)^3 D^2} \right] \quad , \tag{31}$$

where P_A is the measured total or octave-band acoustic power [see Chapter I].

The major results presented include normalized data for the total (linear frequency response) sound power and for octave-band spectra. The total sound-power data are shown plotted against the Reynolds Number of the constricted flow where

$$\text{Reynolds Number} = U_\ell \, \delta/\nu \quad ; \tag{32}$$

the typical dimension, δ, is taken as the thickness of the wake ($\ell \sin \alpha$ in Fig. 15), and ν is the kinematic viscosity. Octave-band normalized data is shown plotted against Strouhal Number defined by

$$\text{Strouhal Number} = f\ \delta/U_{\ell} \quad , \tag{33}$$

where f is the octave-band center frequency.

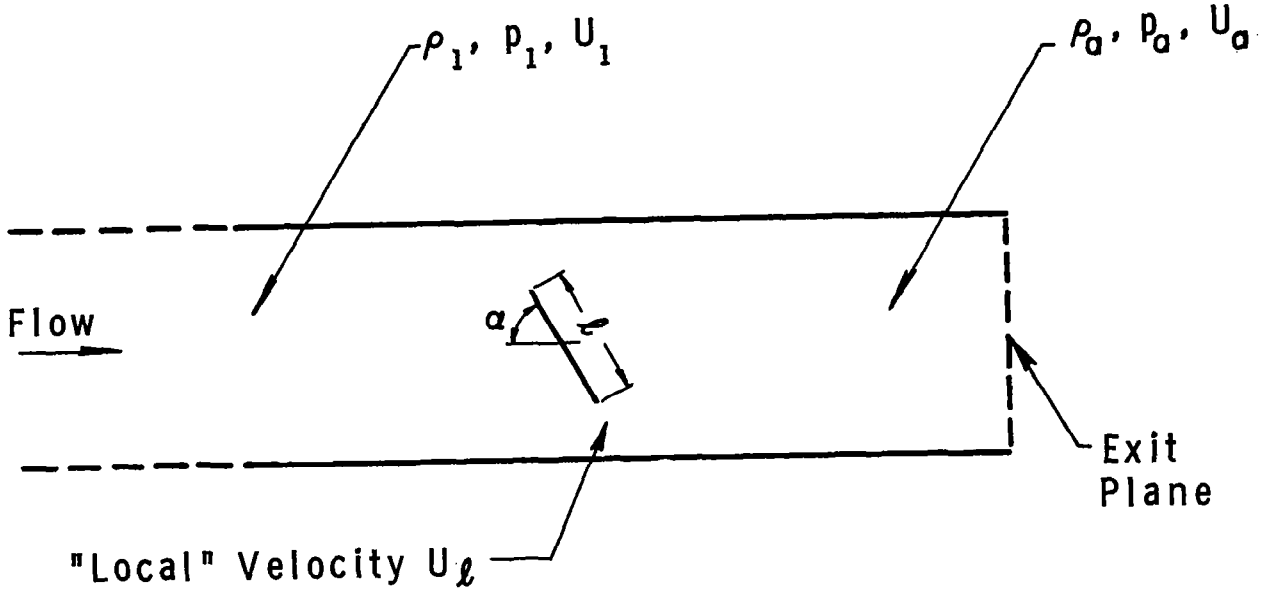

FIG. 15 SCHEMATIC OF STRIP SPOILER IN PIPE

VI. RESULTS: STRIP SPOILERS

A strip spoiler, in the context of the present experimentation, is described as a spoiler of width ℓ and thickness t, placed radially across the pipe from one side of the pipe to the other at a distance x from the exit plane and presenting an angle of attack α to the flow. Such a configuration is shown schematically in Fig. 16. In this chapter, we present the results of a number of experiments in which the parameters relevant to the noise of strip spoilers have been studied.

6.1 Effect of Angle of Attack

A series of experiments was performed with a 1-in.-wide laminated spoiler inserted across the 2-in.-diameter jet pipe at a distance of 6 in. from the exit plane, and arranged at a number of different angles of attack ranging from 0^{o} to 90^{o}. The schematic arrangement is that of Fig. 16.

A plot of the normalized total power level versus Reynolds Number [with $\delta = \ell \sin \alpha$ in Eq. (32)] for the values of α studied is shown in Fig. 17. The approximate independence that the normalized total radiated power bears to the Reynolds Number is an indication that the data are in support of the relation

$$P_A = k(p_o - p_a)^3 D^2 / \rho_a^2 c_a^3 \quad , \tag{34}$$

where k is a constant [see Eq. (21)]. The mean value of k is about 2.5×10^{-4}.

It is interesting to note that the lowest values of k occur both when the spoiler is parallel to the flow and when it is at right angles to the flow. In the first case, it is not certain that, in fact, the noise is being dominated by the spoiler. In the second, it is apparent that as the constriction gets more severe the total spoiler area cannot participate in the noise-generation process — an obvious limiting case is that of a pinhole in an otherwise blocked jet pipe. Such a configuration will, of course, tend to be dominated by quadrupole radiation associated with the local jet flow. As the results of Fig. 17 show, there is already an indication that with the 90° angle of attack, quadrupolelike noise is causing the normalized power level (normalized, that is, on the assumption of dipolelike radiation) to increase with increased flow.

The normalized octave-band frequency spectra, for each angle of attack, plotted as a function of Strouhal Number, are given in Figs. 18 - 22. The normalization is based on a dipole-dominated radiation [see Eqs. (20), (21)]. Dipole-based normalization is assumed throughout, unless otherwise stated. It is observed that the degree of correlation is, in general, satisfactory. However, in certain ranges of the Strouhal Number some discrepancies are apparent. These are particularly pronounced at the higher Strouhal Numbers for values of α above zero and at the lower Strouhal numbers when α is equal to zero. To account for these discrepancies, it may be necessary to postulate that more than one type of source and/or more than one mechanism is involved in the sound production as discussed in Chapter I. Nevertheless, it is clear from the data that the dipolelike component is the dominant sound-producing source. A further study of these data is discussed in a later chapter.

6.2 Effect of Spoiler Width

In Fig. 23, the normalized total power from the 1-in.-wide spoiler set across the flow (previous experiment, $\alpha = 90^{\circ}$) is compared with the sound power from a 1/2-in. spoiler also set at $\alpha = 90^{\circ}$. The mean result is again consistent with a value of k of about 2.5×10^{-4}.

The normalized frequency spectra for these two configurations are given in Figs. 24 and 25. The degree of data collapse is seen to be better for the 1/2-in.-wide spoiler than it is for the 1-in.-wide spoiler. For both, we see again evidence of nondipole source activity in the range of high Strouhal Number.

6.3 Effect of Downstream Dimension

As a final experiment in this series, we have examined the form of the radiation from a strip spoiler arranged parallel to the flow ($\alpha = 0^{\circ}$) and having a variable width (ℓ).

As we have seen in an earlier chapter, the plain unspoiled jet pipe displays dipolelike radiation characteristics at the lower exit velocities. Since it was felt that the flow-aligned spoiler does not significantly interrupt the flow and that for this geometry the sound intensity might be dominated by lip noise, the measured results for the plain unspoiled geometry are included in the discussion of this experiment.

The form of the total normalized power is plotted in Fig. 26 against Reynolds Number with $\delta = t = 1/8$ in. (for purposes of comparison this same value of δ is used in describing the plain jet pipe.) It is observed that at the higher velocities

(high Reynolds Number) the normalized power for the plain jet pipe increases. This is expected since the noise at the higher velocities is dominated by the free-jet quadrupole sources. At the lower velocities, a dipole-producing mechanism seems to be active having a value of k of about 5×10^{-5}, significantly lower than the 2.5×10^{-4} observed for spoiled flow. This value might be associated with the so-called lip noise. A very interesting observation from Fig. 26 is that the short (ℓ = 1 in.) spoiler is noisier than the longer (ℓ = 6 in.) spoiler, the latter tending to the level of the unspoiled jet flow. A further observation is that the insertion of the 6-in. spoiler (and to a lesser extent, the 3-in. spoiler) leads to an apparent reduction in the level of generated free-jet quadrupole energy. A possible explanation of the first observation is that the turbulence generated at the leading (upstream) edge of the short spoiler interacts with the trailing edge. The extent of the interaction decreases as the spoiler length is increased. The second observation may be related to the influence of the long spoiler upon the general level of turbulence of the pipe flow.

The normalized octave-band spectra for these configurations are shown in Figs. 27 - 30. The behavior of the spectra at low Strouhal Numbers is indicative of the generation of sound by the free-jet quadrupoles. In general, the collapse of data is good in the high Strouhal Number region. Here, apparently, the noise is dominated by the pipe-enclosed-surface dipole sources.

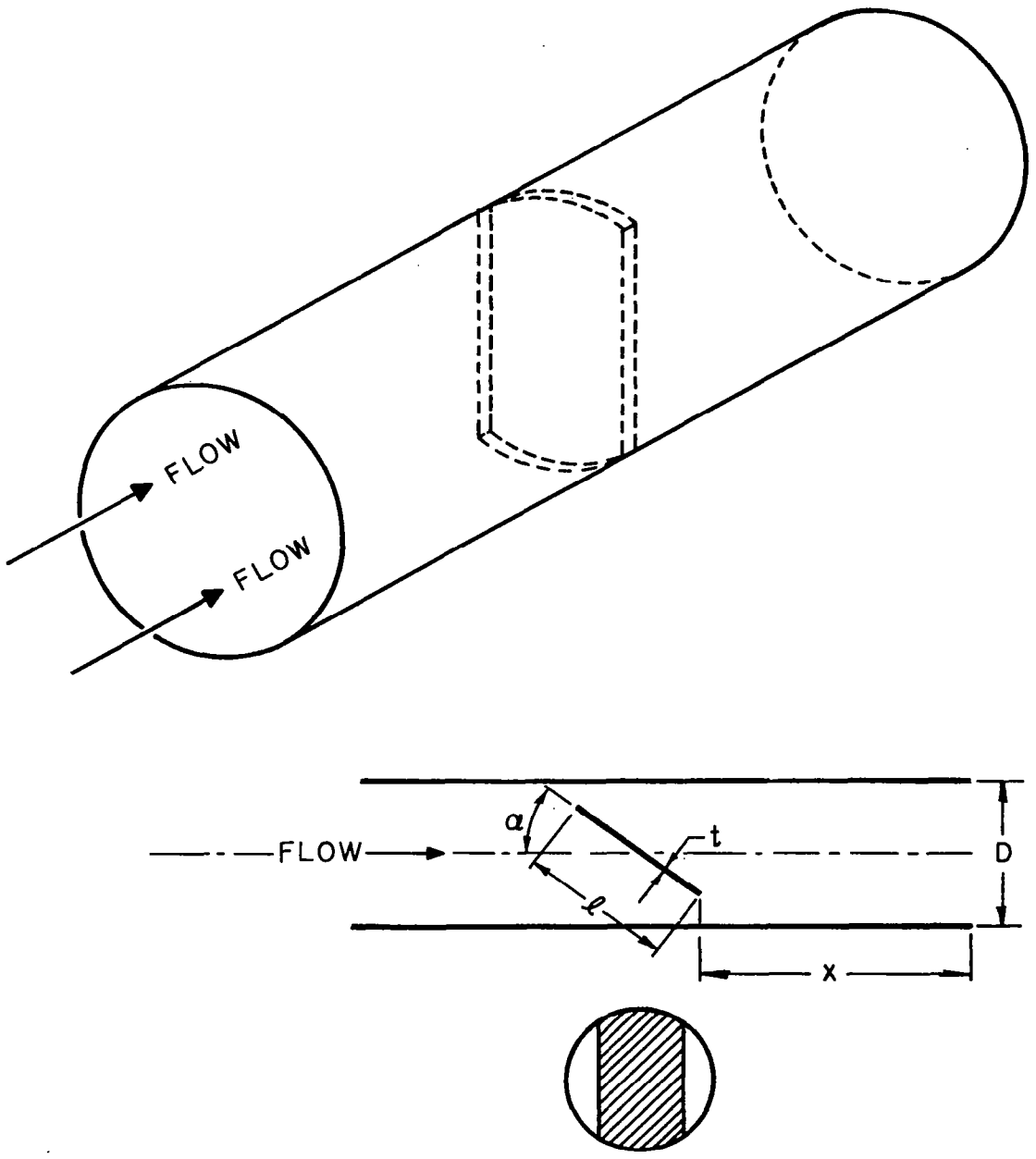

FIG.16 STRIP SPOILER SCHEMATIC

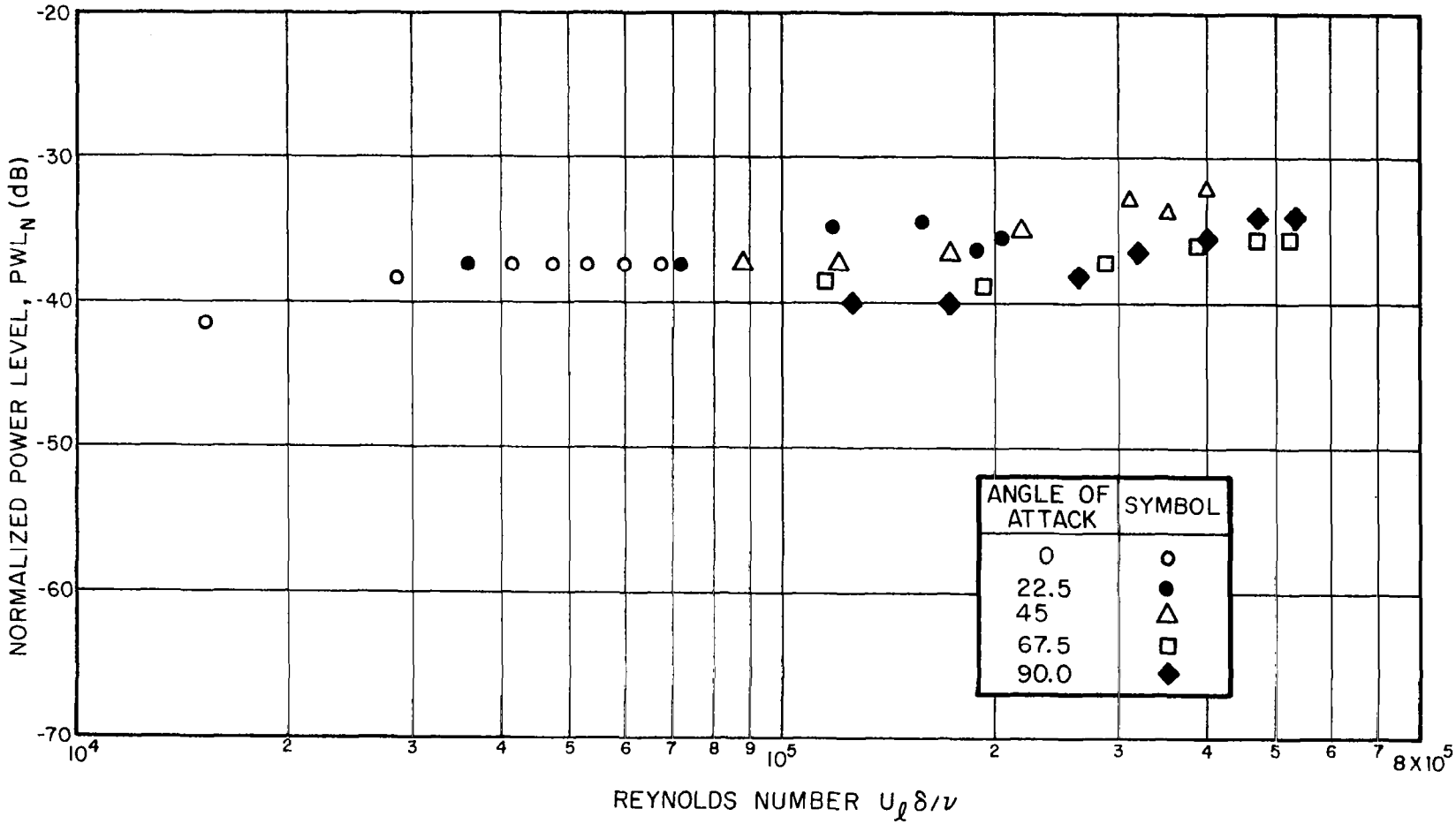

FIG. 17 NORMALIZED POWER LEVEL VERSUS REYNOLDS NUMBER FOR STRIP SPOILER D = 1.875, ℓ = 1 IN., x = 6 IN., α = VARIABLE

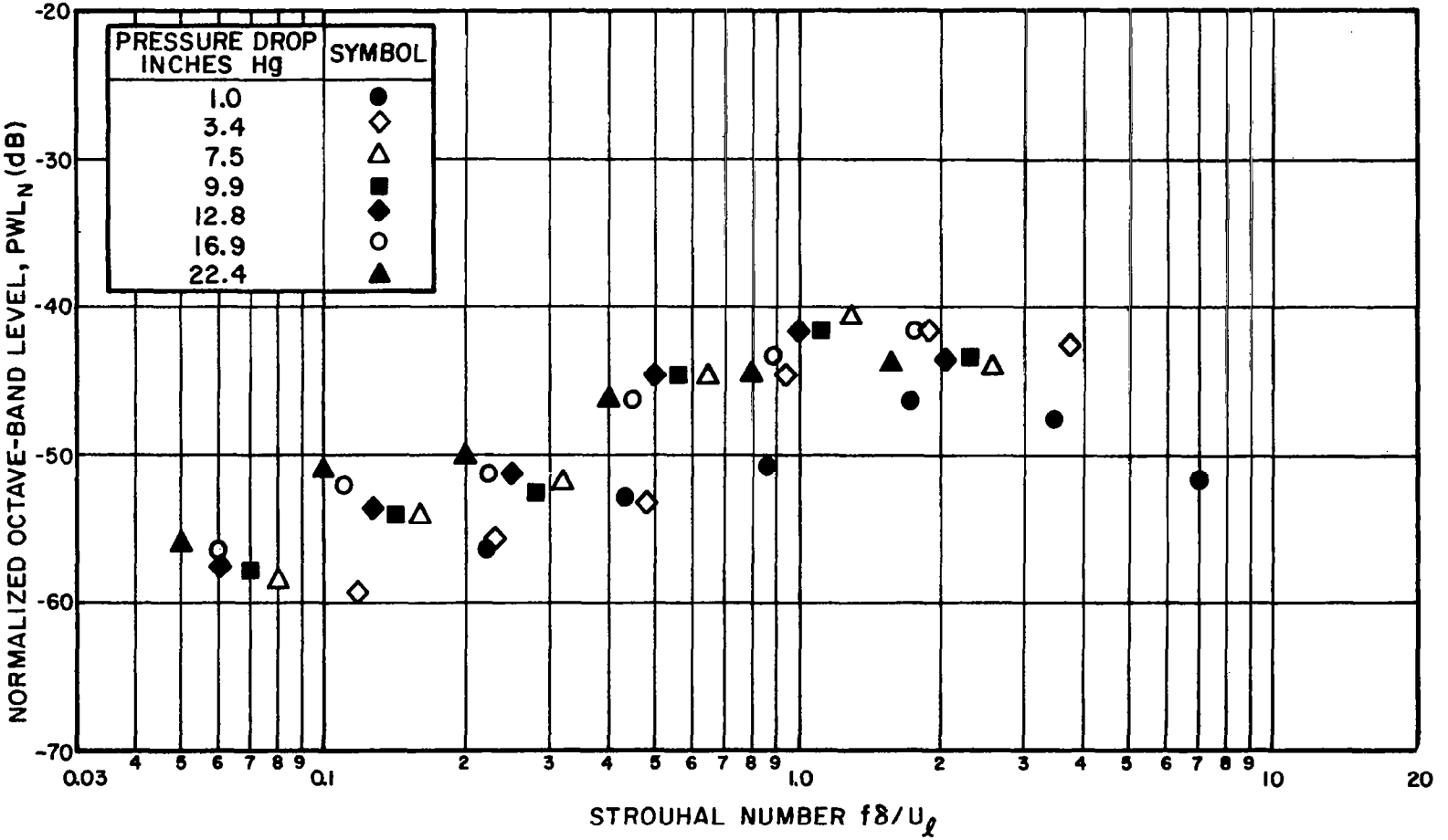

FIG.18 NORMALIZED OCTAVE-BAND POWER LEVEL VERSUS STROUHAL NUMBER FOR STRIP SPOILER
D = 1.875, ℓ = 1 IN., x = 6 IN., α = 0°

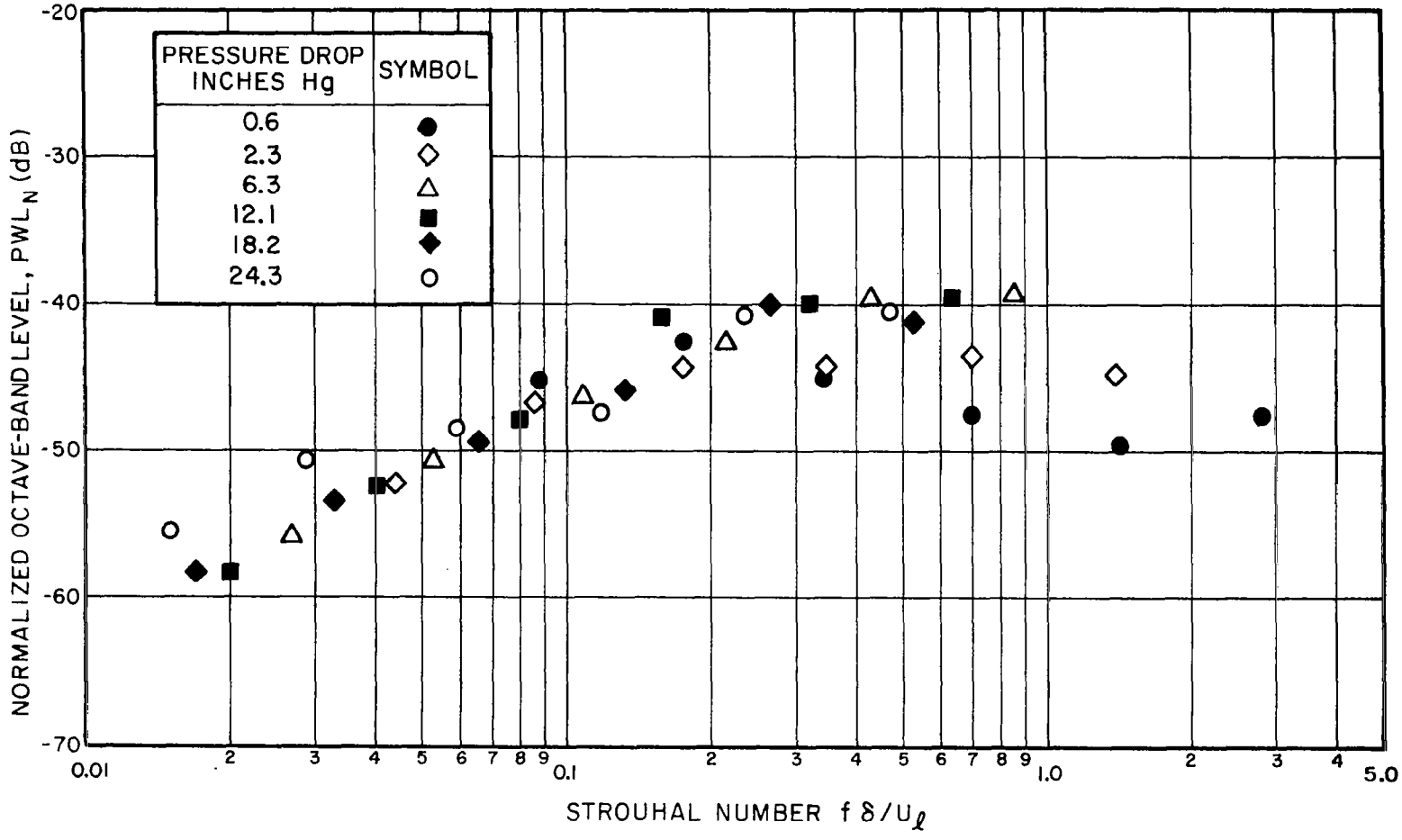

FIG.19 NORMALIZED OCTAVE-BAND POWER LEVEL VERSUS STROUHAL NUMBER FOR STRIP SPOILER
D = 1.875, ℓ = 1 IN., x = 6IN., α = 22.5°

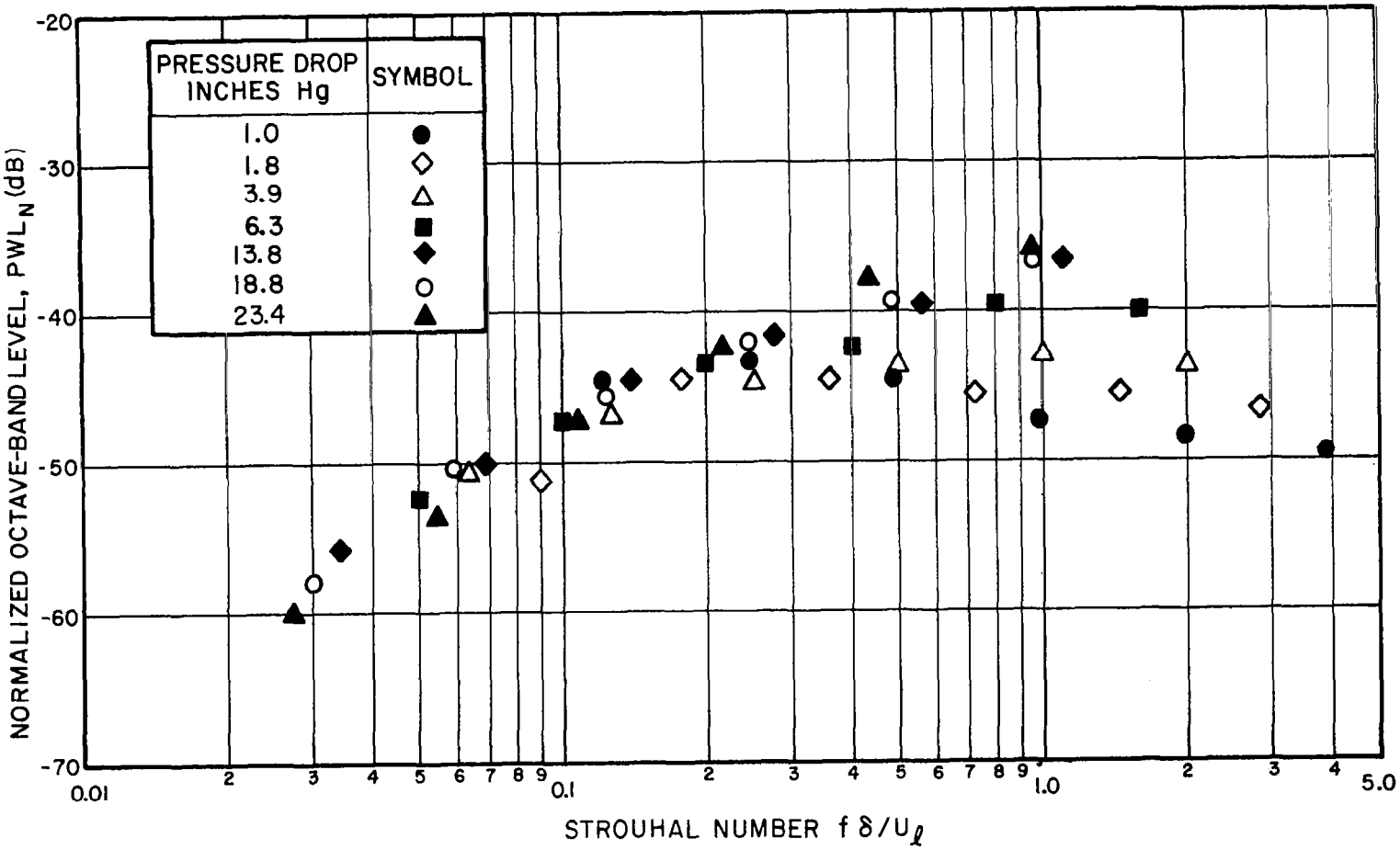

FIG. 20 NORMALIZED OCTAVE-BAND POWER LEVEL VERSUS STROUHAL NUMBER FOR STRIP SPOILER
D = 1.875, ℓ = 1 IN., x = 6IN., α = 45°

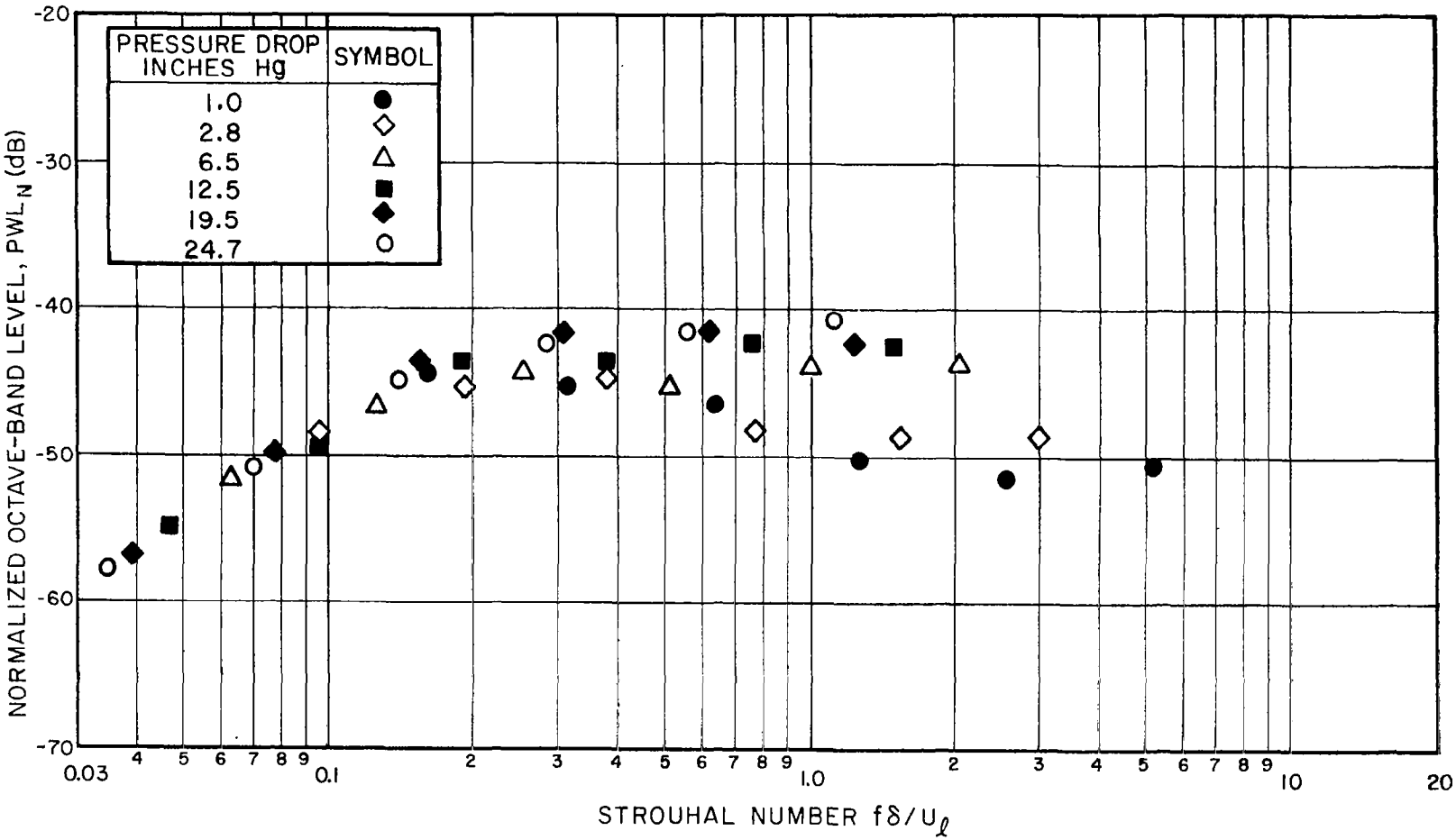

FIG.21 NORMALIZED OCTAVE-BAND POWER LEVEL VERSUS STROUHAL NUMBER FOR STRIP SPOILER
D = 1.875, ℓ = 1 IN., x = 6 IN., α = 67.5°

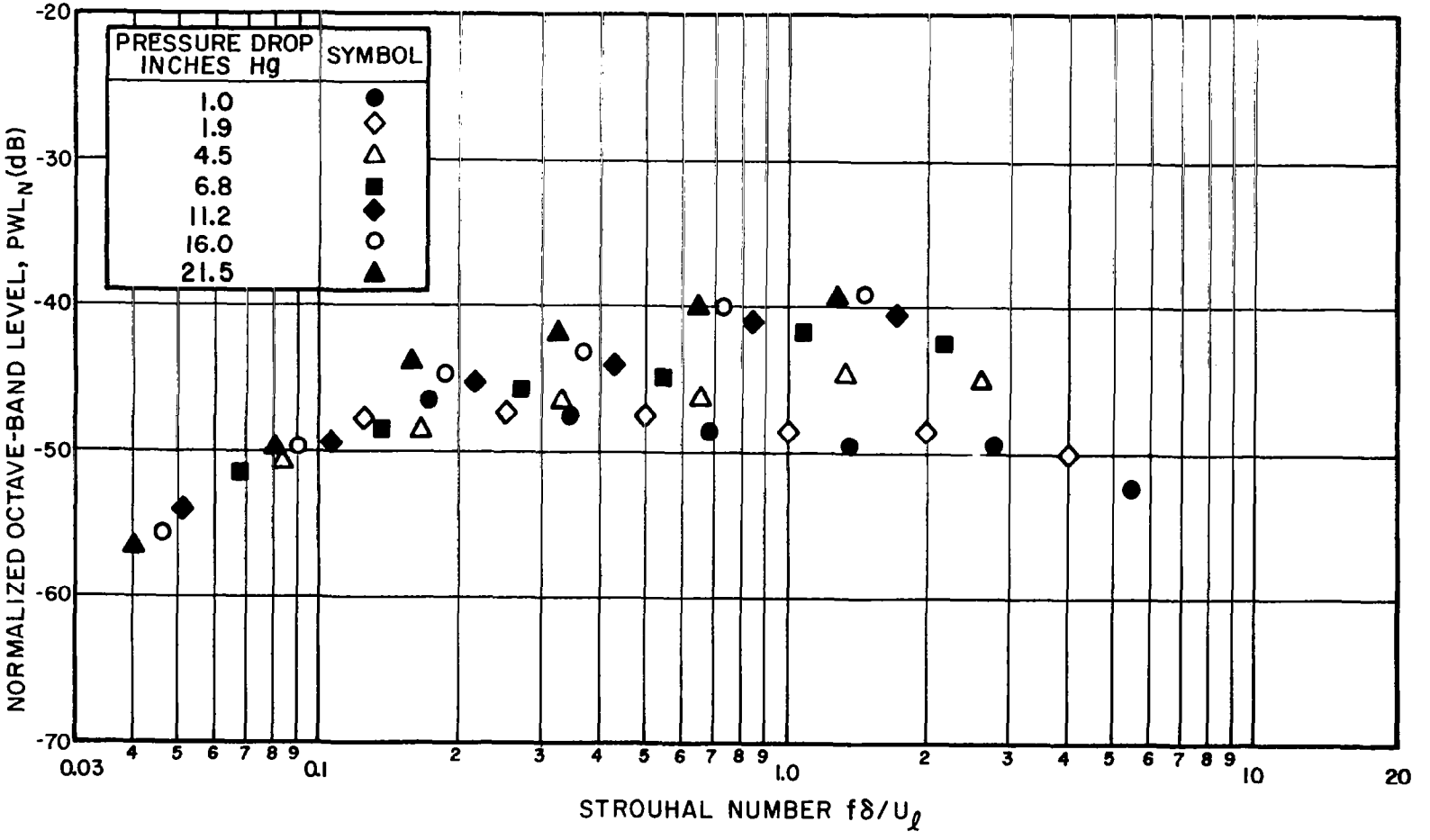

FIG.22 NORMALIZED OCTAVE-BAND POWER LEVEL VERSUS STROUHAL NUMBER FOR STRIP SPOILER
D = 1.875, ℓ = 1 IN., x = 6 IN., α = 90°

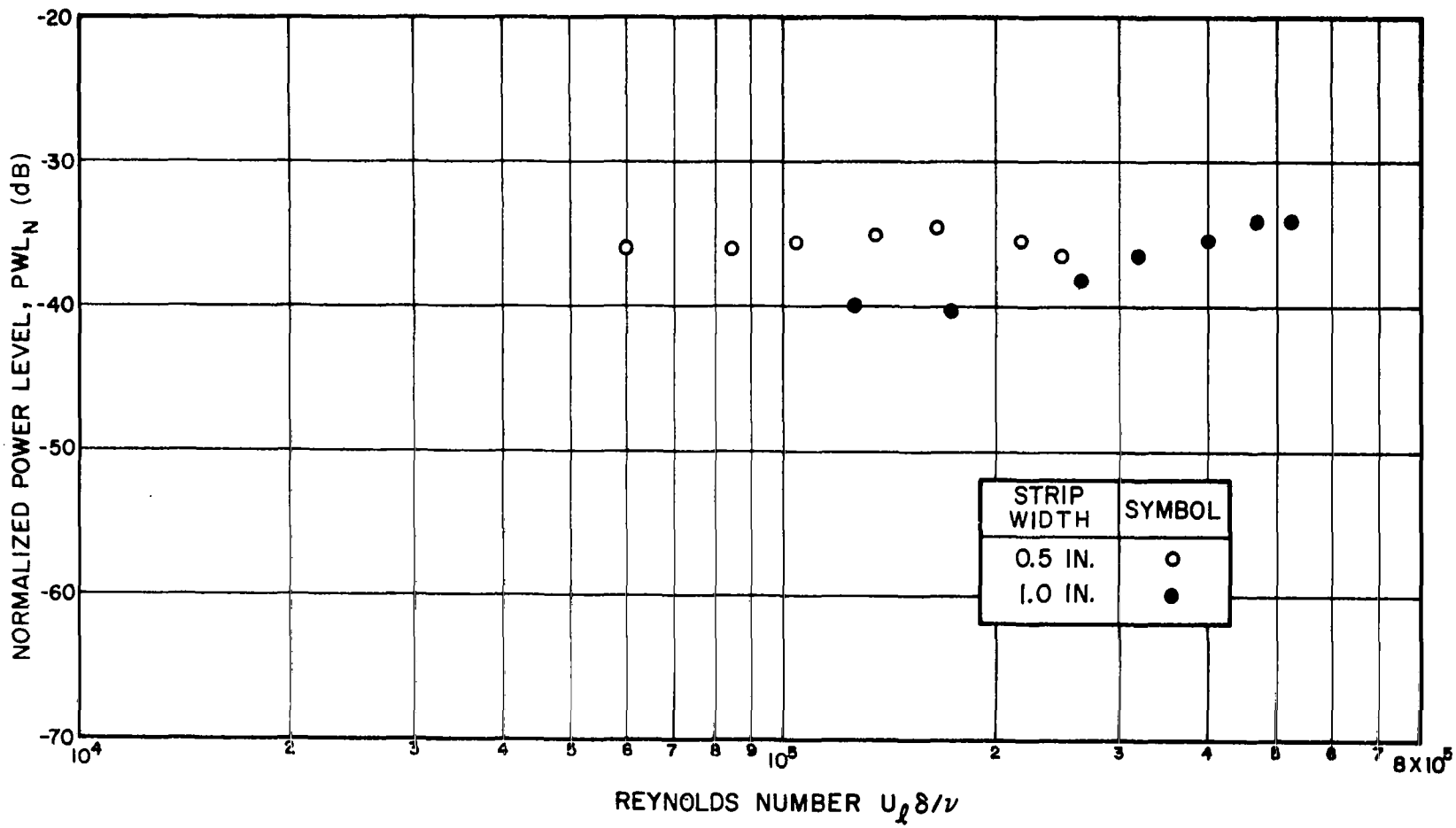

FIG. 23 NORMALIZED POWER LEVEL VERSUS REYNOLDS NUMBER FOR STRIP SPOILER D = 1.875, x = 6 IN., α = 90°, ℓ = VARIABLE

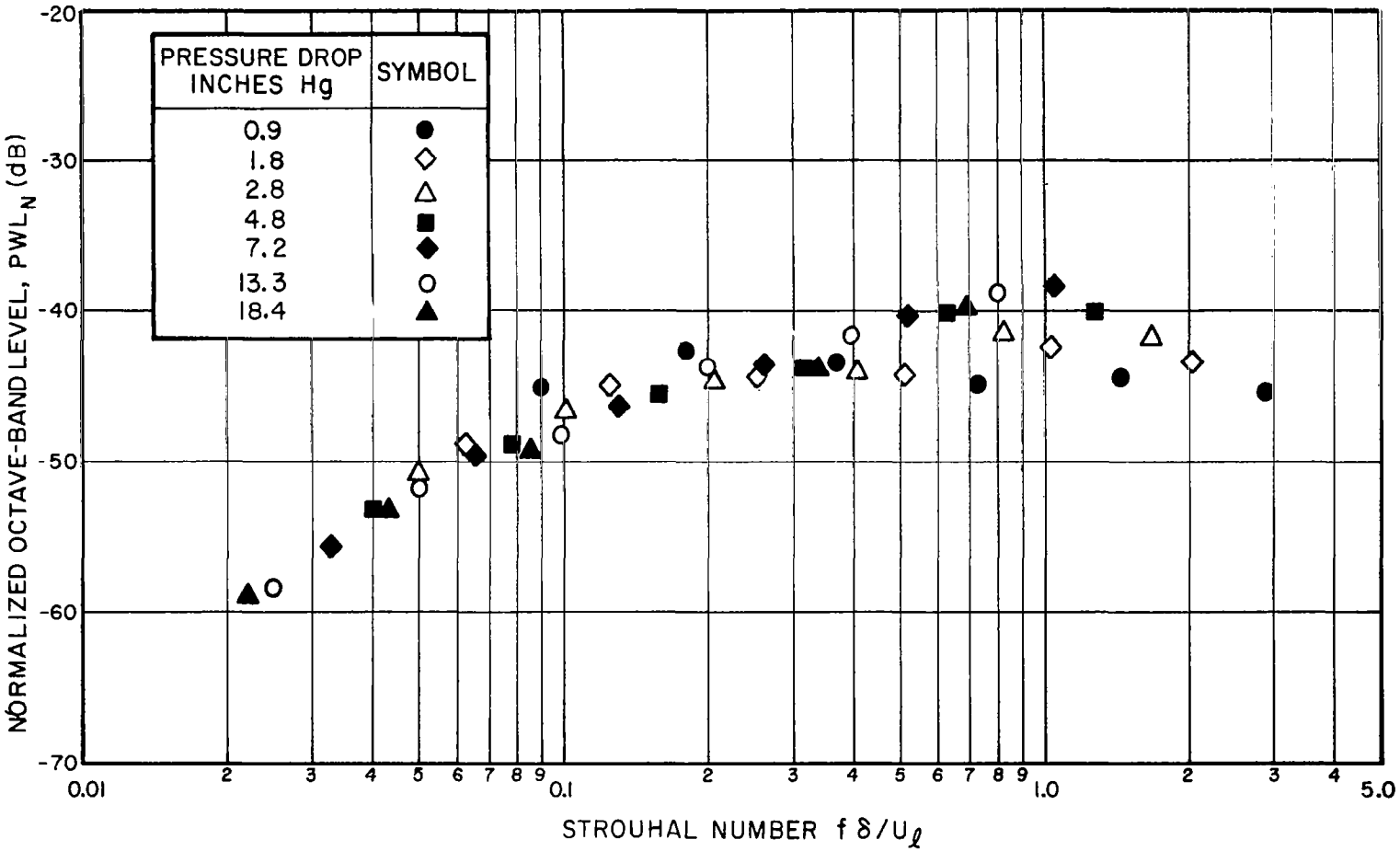

FIG.24 NORMALIZED OCTAVE-BAND POWER LEVEL VERSUS STROUHAL NUMBER FOR STRIP SPOILER
D = 1.875, ℓ = 0.5 IN., x = 6IN., α = 90°

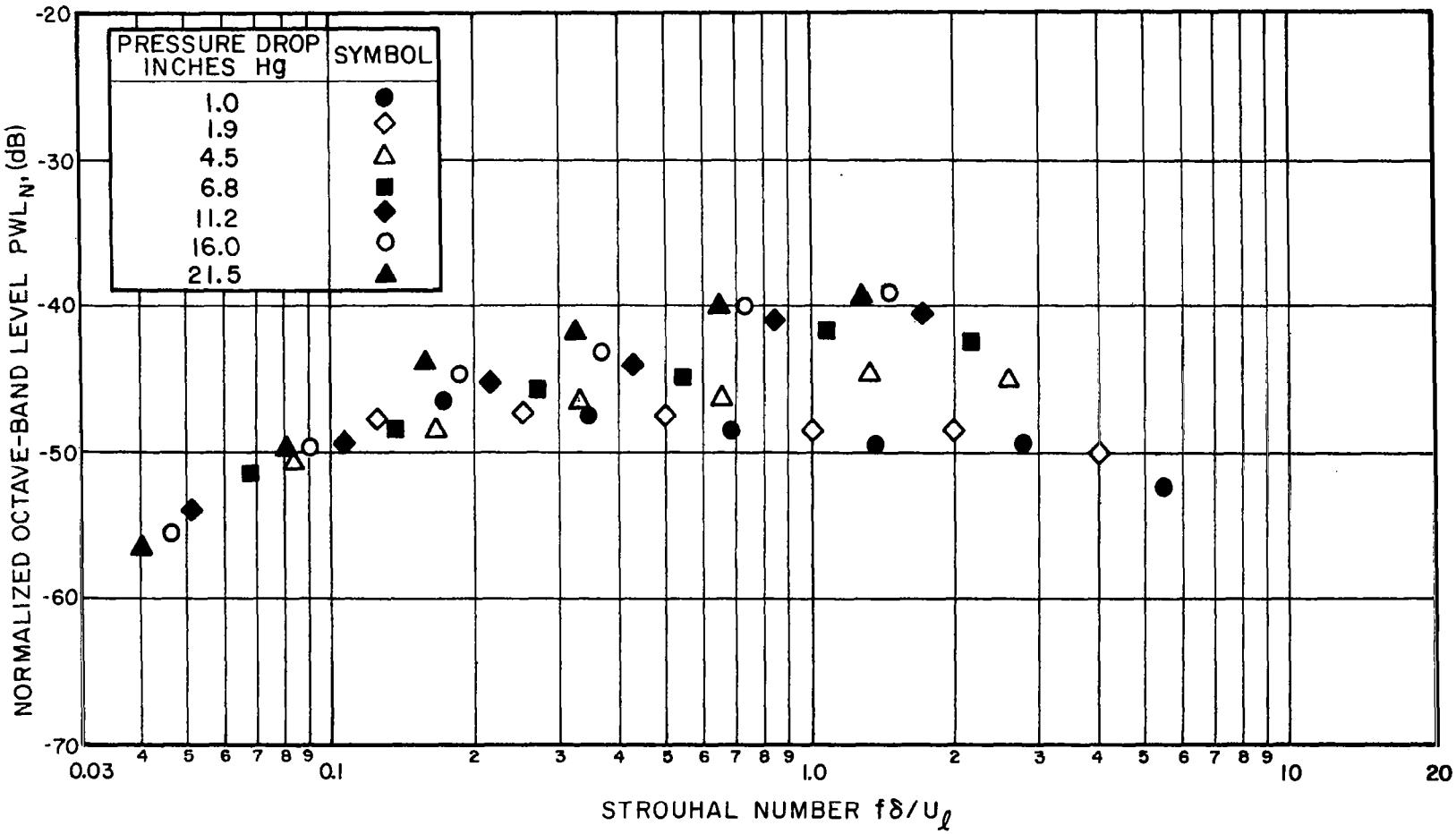

FIG.25 NORMALIZED OCTAVE-BAND POWER LEVEL VERSUS STROUHAL NUMBER FOR STRIP SPOILER
D = 1.875, ℓ = 1 IN., x = 6 IN., α = 90°

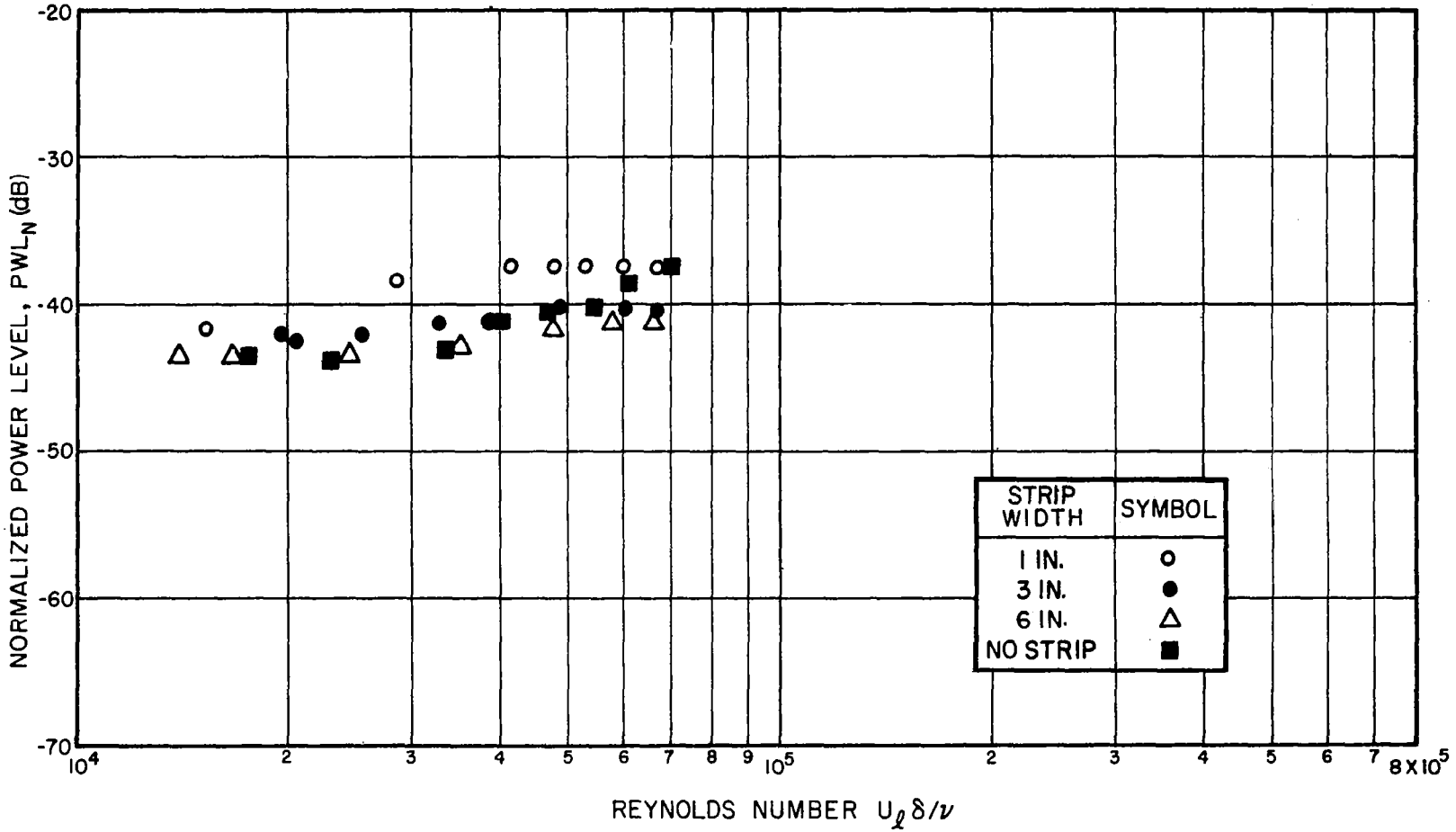

FIG. 26 NORMALIZED POWER LEVEL VERSUS REYNOLDS NUMBER FOR STRIP SPOILER D= 1.875, x= 6 IN., α = 0°, ℓ= VARIABLE

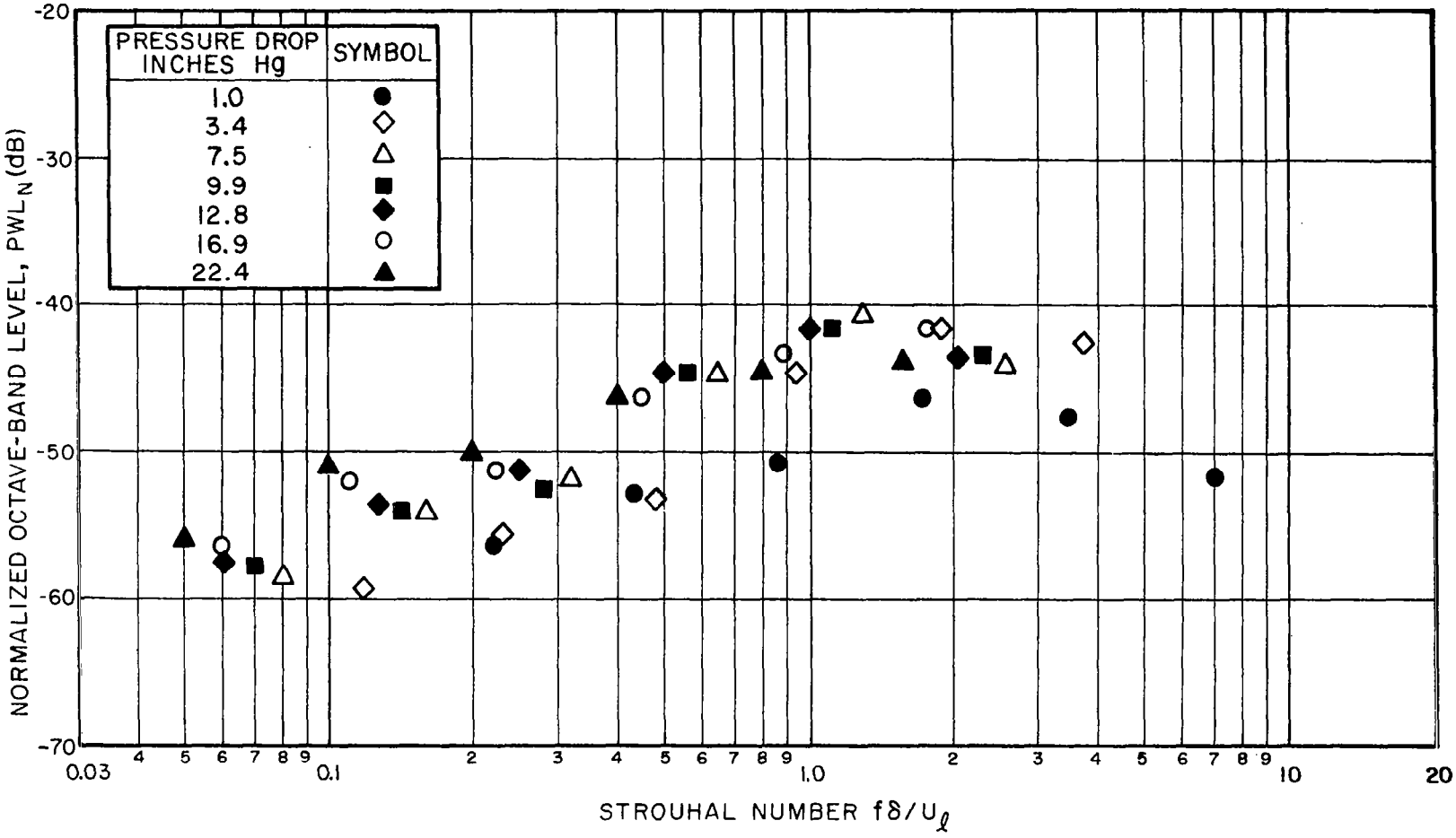

FIG.27 NORMALIZED OCTAVE-BAND POWER LEVEL VERSUS STROUHAL NUMBER FOR STRIP SPOILER
D = 1.875, ℓ = 1 IN., x = 6 IN., α = 0°

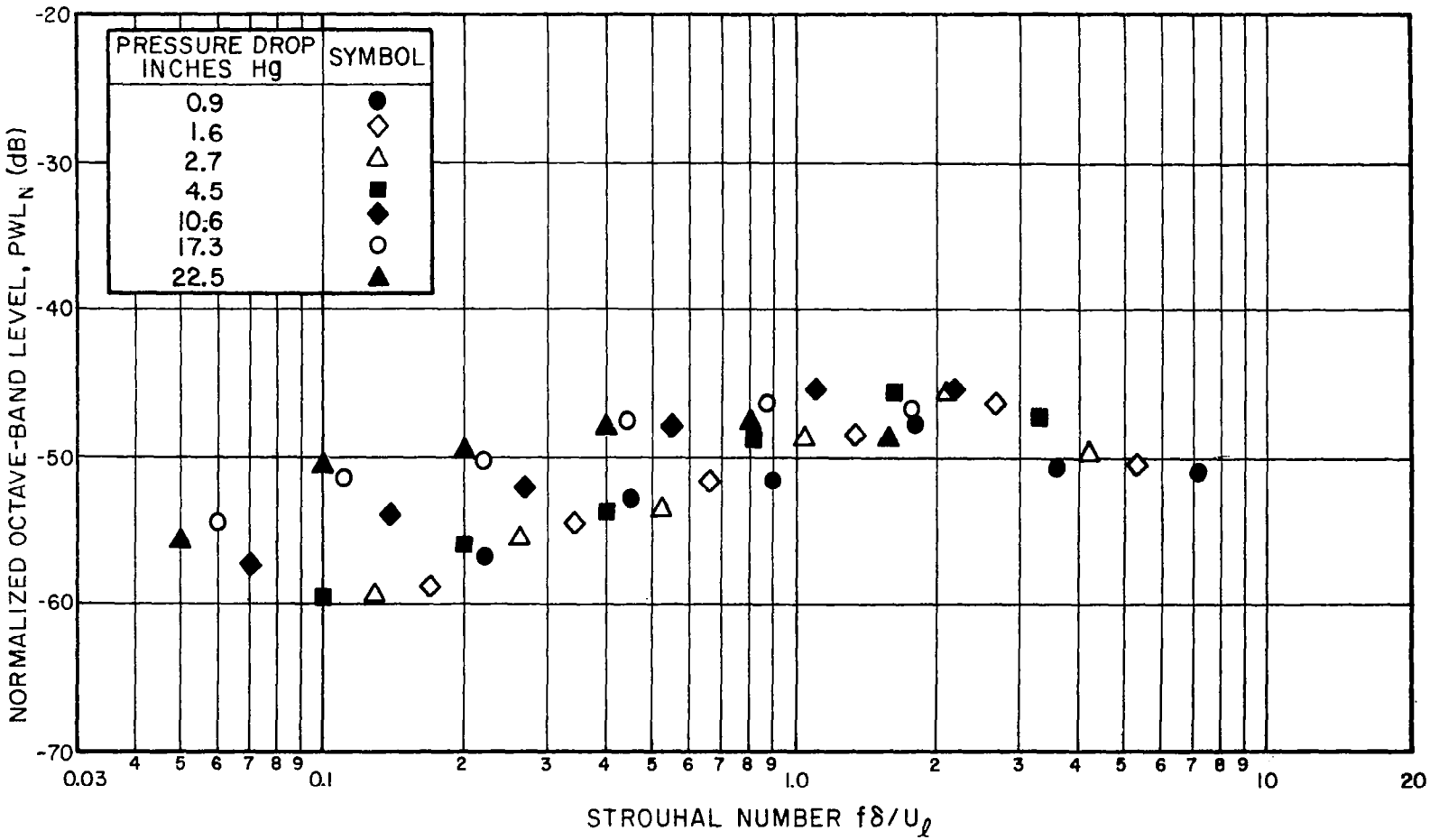

FIG.28 NORMALIZED OCTAVE-BAND POWER LEVEL VERSUS STROUHAL NUMBER FOR STRIP SPOILER
D = 1.875, ℓ = 3 IN., x = 6 IN., α = 0°

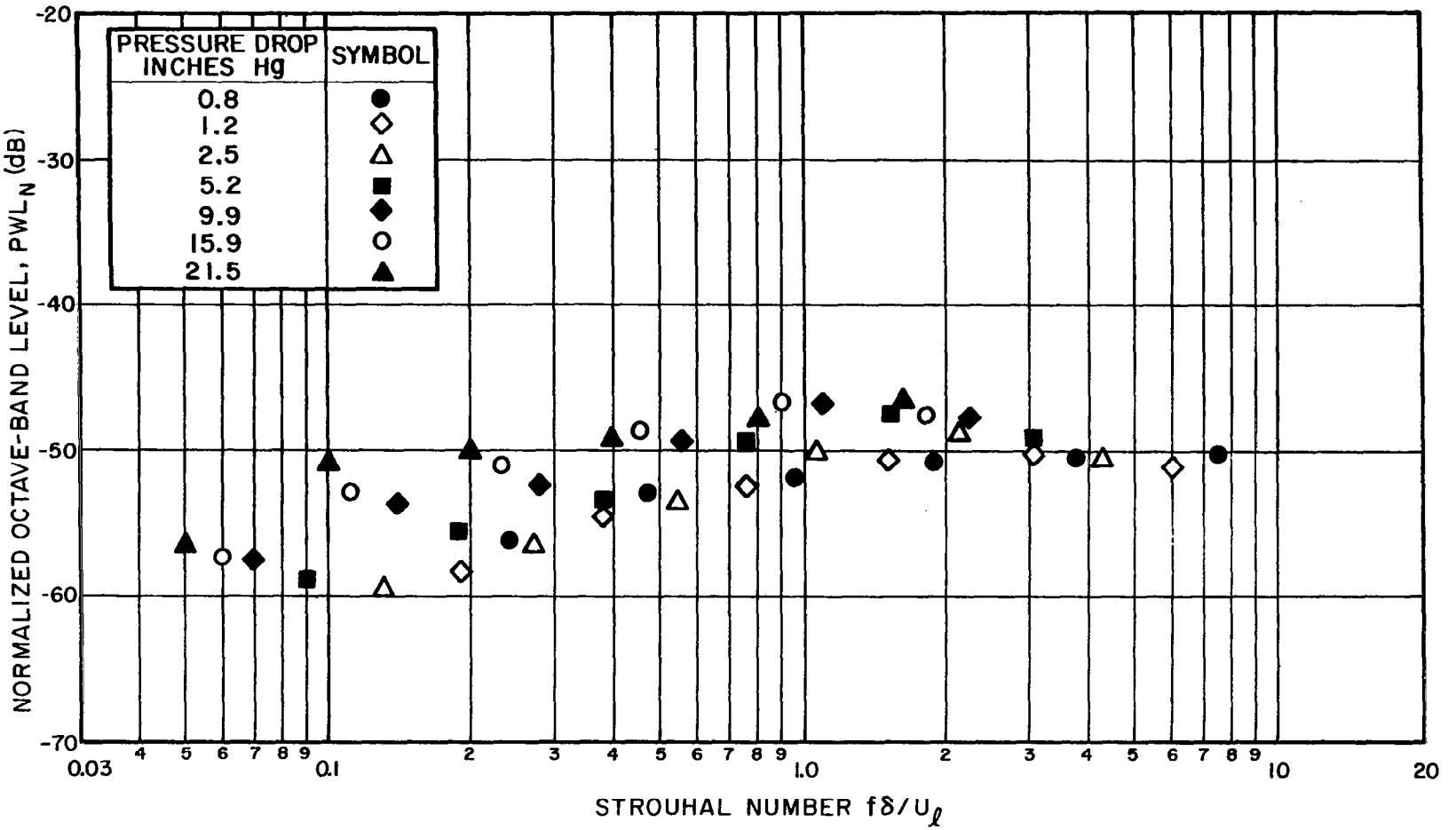

FIG.29 NORMALIZED OCTAVE-BAND POWER LEVEL VERSUS STROUHAL NUMBER FOR STRIP SPOILER
D = 1.875, ℓ = 6 IN., x = 6 IN., α = 0°

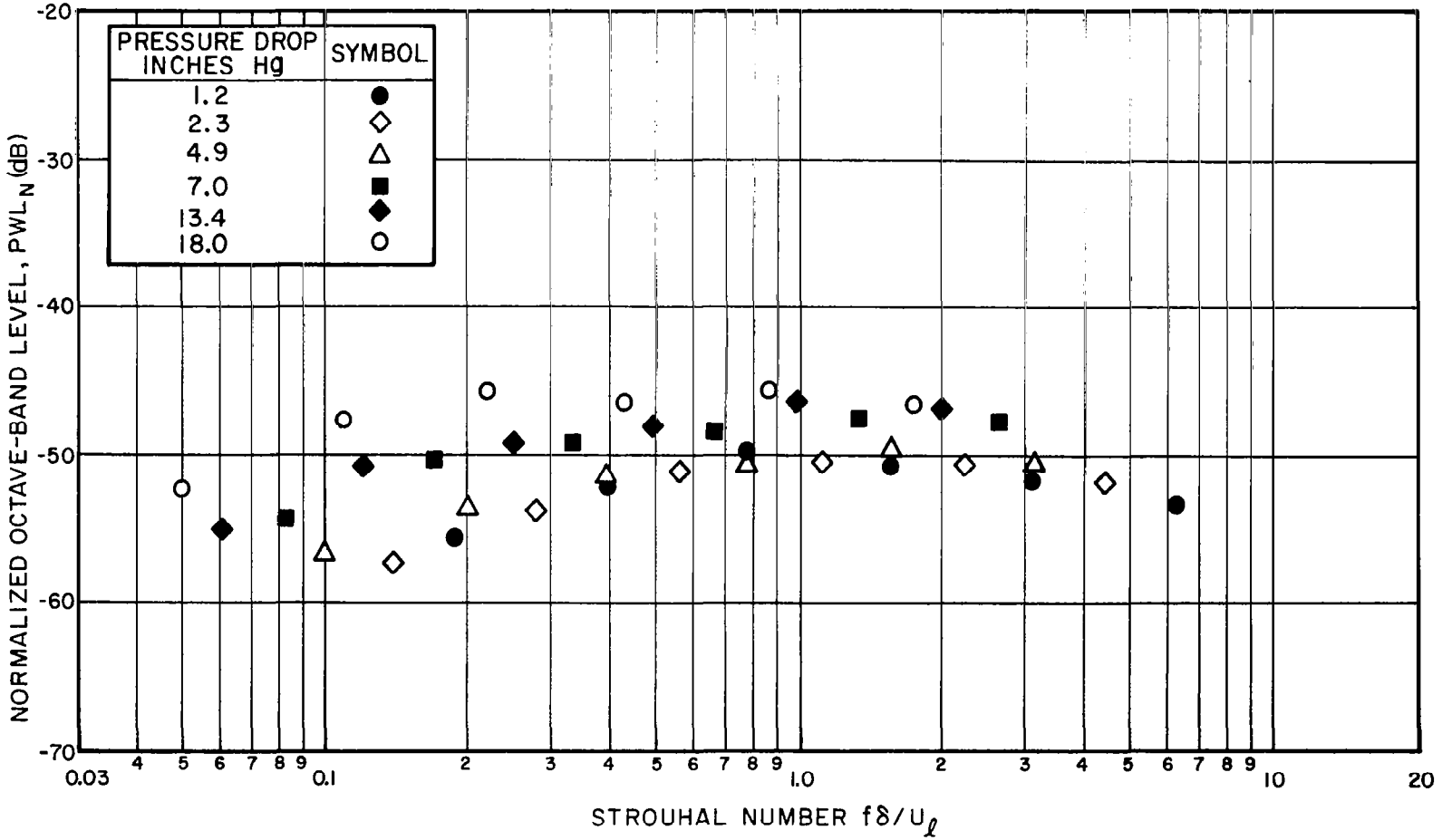

FIG.30 NORMALIZED OCTAVE-BAND POWER LEVEL VERSUS STROUHAL NUMBER FOR PLAIN PIPE
D = 1.875

VII. RESULTS: RING SPOILERS

A ring spoiler in the contex of the present experimentation is described as a spoiler placed at right angles to the flow in the form of a peripheral ring of thickness t having an inner diameter d and an outer diameter equal to that of the jet pipe D. The spoiler is placed at a distance x from the exit plane. Such a configuration is shown schematically in Fig. 31. In this chapter, we present the results of a number of experiments in which various parameters relating to the spoiler-induced noise are examined.

7.1 Effect of Ring Diameter

Figure 32 shows the normalized total power for two different ring inner diameters. The results are plotted against Reynolds Number based on $\delta = \frac{1}{2}$ (D-d). The results for the large-diameter ring indicate a dipolelike behavior having a value of k close to 2.5×10^{-4}. The smaller-diameter ring, however, displays a quadrupolelike behavior over most of the operating range. At the lower Reynolds Numbers, where, presumably, a dipolelike mechanism is active, the value of k is significantly lower (6×10^{-6}) than for more-conventional spoiler arrangements. It would seem that as the ring diameter gets smaller, the influence of the downstream pipe wall on the sound-generating mechanisms decreases. Such an observation is consistent with the idea that spoiler noise arises from the expanding jet region (following the constriction) rather than from the region of accelerating flow leading up to the constriction point. The observation is also made that, if the data for the 0.5-in.-diameter ring were normalized on the basis of a value of D of

0.5 in., rather than 2 in., the resulting value of k at the low flow velocities would be approximately 7×10^{-5}, which lies between these values identified in the previous chapter with spoiler noise and lip noise.

7.2 Effect of Upstream Distance

A further indication of the part played by the interaction of the constricted flow with the downstream pipe wall is given by a comparison of the sound radiation of the 1.5-in.-diameter ring spoiler placed in turn 6 in. upstream and at the exit plane (x = 0 in.). The total normalized power for each of these configurations is shown in Fig. 33. When the spoiler was moved to the exit plane, the value of k decreased by an order of magnitude (to 3×10^{-5}) and at the higher velocities the noise was dominated by the free-jet quadrupoles. This leads to the observation that a spoiler immersed in the jet pipe is noisier than the same spoiler located at the exit plane.

Again, it is observed that if the normalization were based on the orifice diameter, rather than the pipe diameter, when the spoiler is at the exit plane, the value of k would correspond closely with that associated with lip noise in the previous chapter. The normalized octave-band spectra for these two configurations are shown in Figs. 34 and 35. The former shows some lack of correlation at the high Strouhal Numbers, which is again consistent with a non-dipolelike source mechanism. The latter shows some spread at the lower Strouhal Numbers. This is consistent with the presence of free-jet quadrupoles.

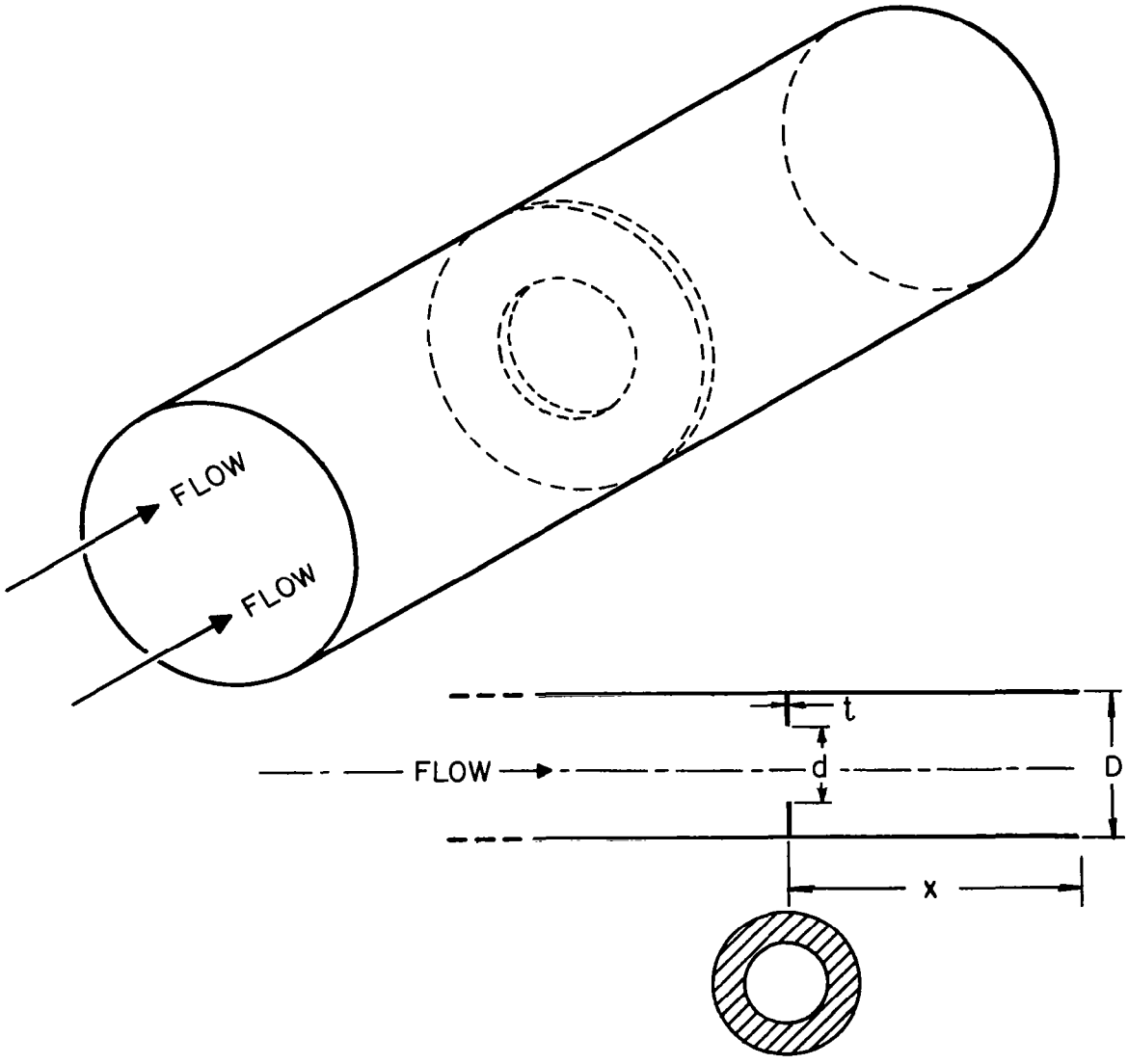

FIG.31 RING SPOILER SCHEMATIC

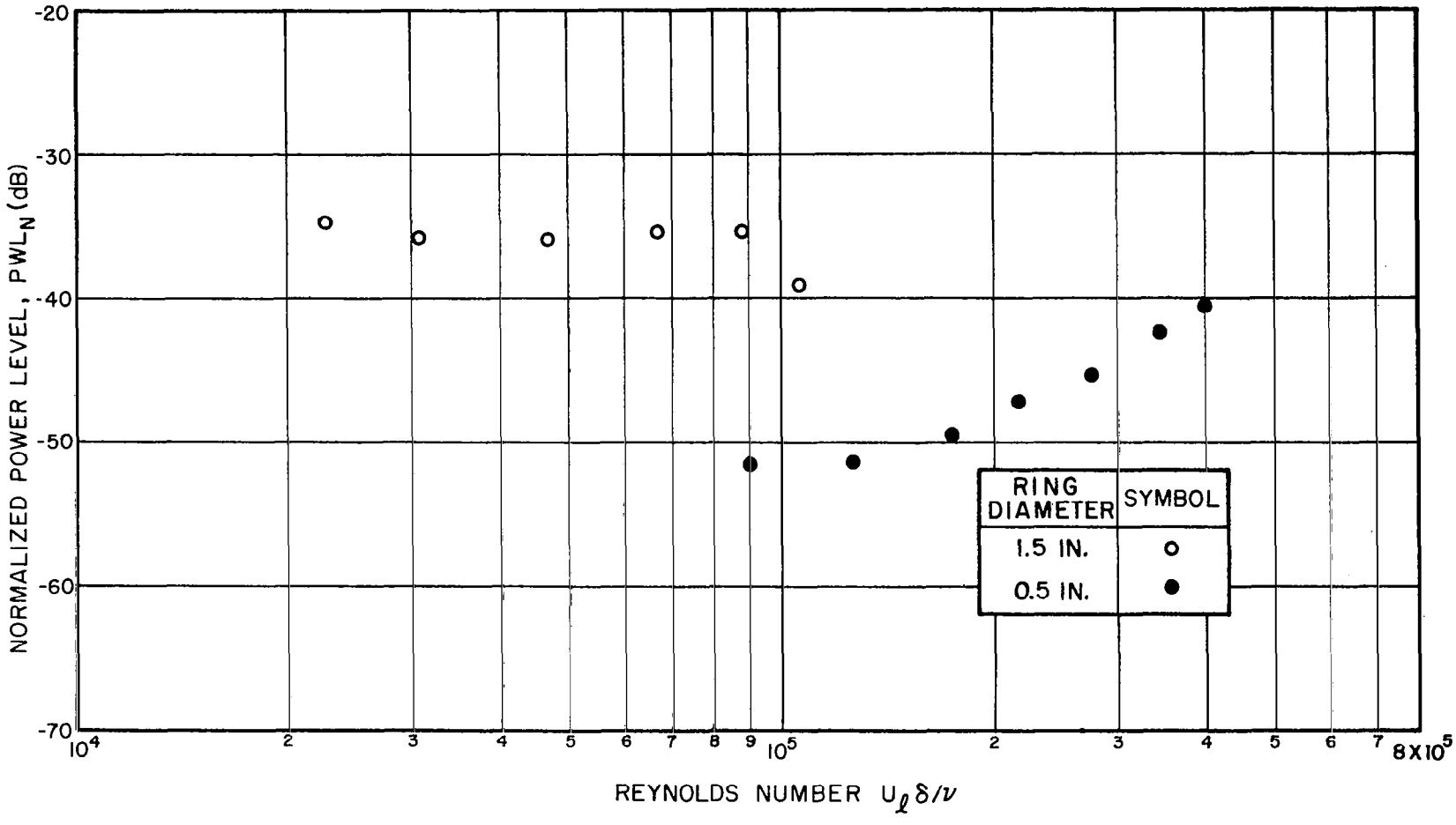

FIG. 32 NORMALIZED POWER LEVEL VERSUS REYNOLDS NUMBER FOR RING SPOILER D = 1.875, x = 6 IN., d = VARIABLE

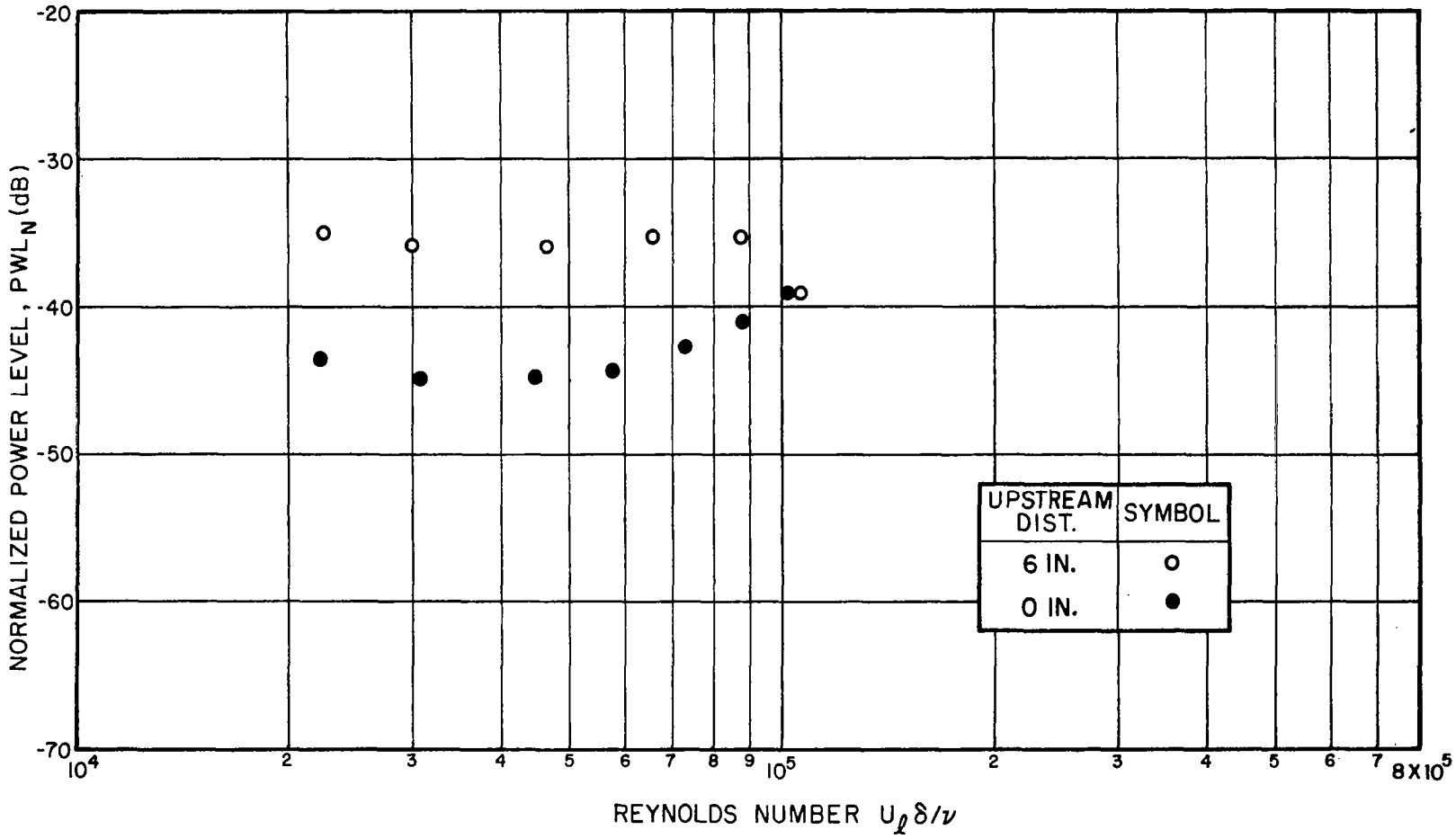

FIG. 33 NORMALIZED POWER LEVEL VERSUS REYNOLDS NUMBER FOR RING SPOILER D = 1.875, d = 1.5 IN., x = VARIABLE

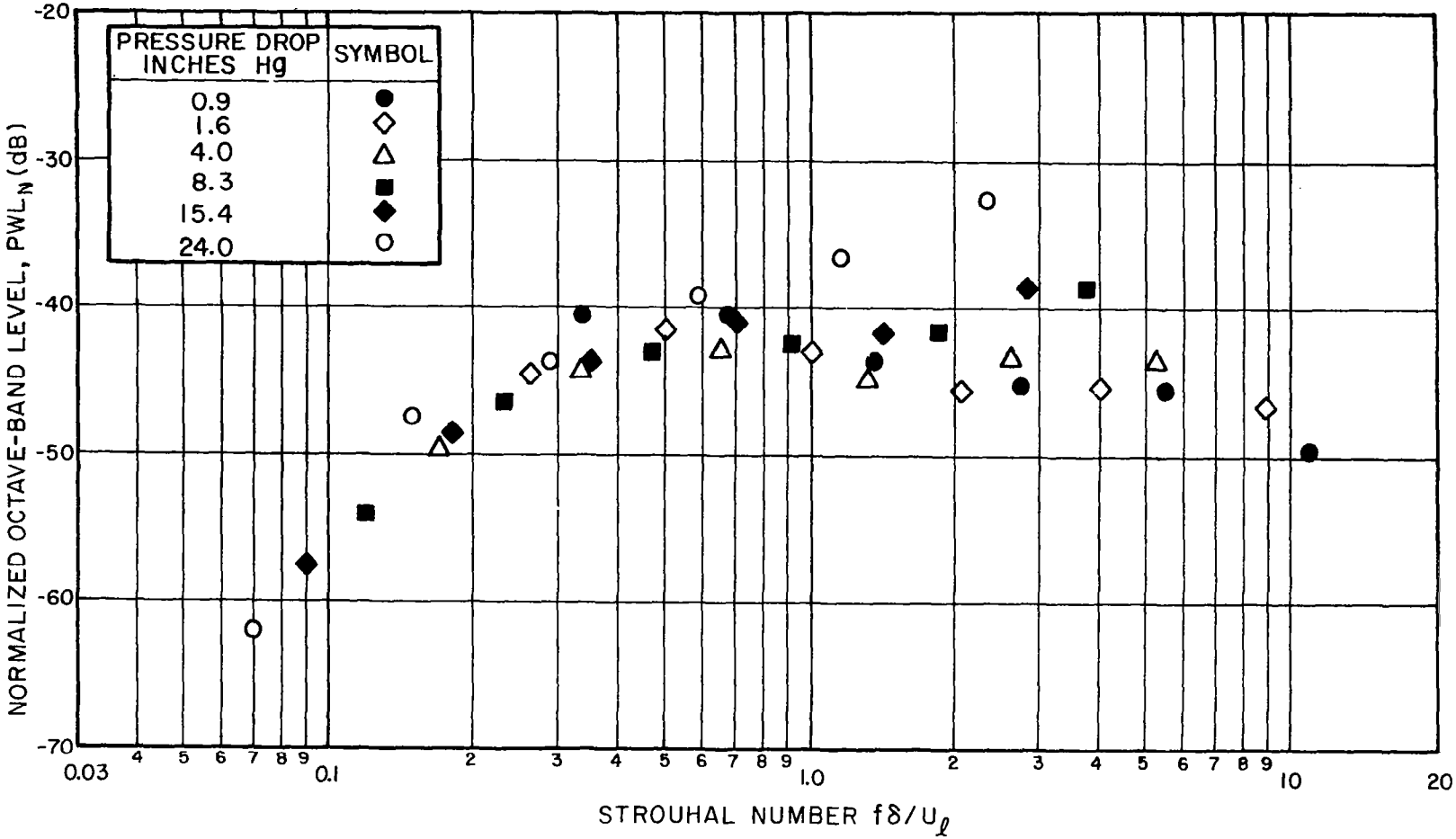

FIG.34 NORMALIZED OCTAVE-BAND POWER LEVEL VERSUS STROUHAL NUMBER FOR RING SPOILER
D = 1.875, d = 1.5 IN., x = 6 IN.

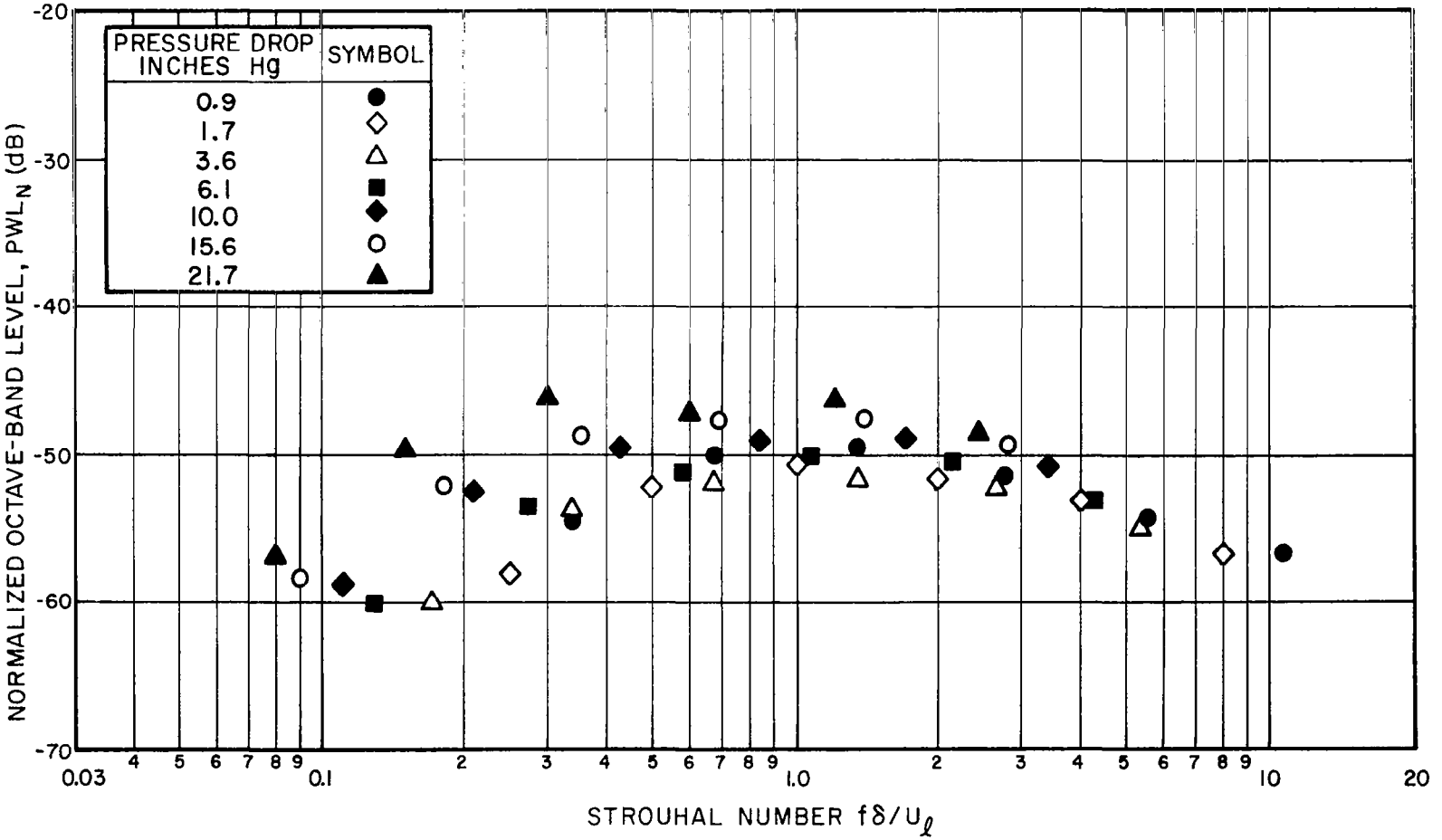

FIG.35 NORMALIZED OCTAVE-BAND POWER LEVEL VERSUS STROUHAL NUMBER FOR RING SPOILER
D = 1.875, d = 1.5 IN., x = 0 IN.

VIII. RESULTS: EFFECTS OF SCALING

The results presented so far have indicated that within a wide range of spoiler dimensions and geometries the radiation from a 2-in.-diameter "spoiled" pipe is given by an expression of the form

$$P_A = k(p_o - p_a)^3 D^2 / \rho_a^2 \, c_a^3 \quad ,$$

where D is the pipe diameter (2 in.) and k is nearly constant having a value of order 2.5×10^{-4}. Some idea of the limitations of this formulation have also been presented — the spoiler must be immersed within the pipe and the constriction that it presents to the flow must be moderate.

In this chapter, we present the results of measurements in which the 2-in.-diameter jet pipe was replaced by a 4-in.-diameter pipe and strip spoilers of, respectively, 1-in. width and 2-in. width, placed across ($\alpha = 90^o$) the flow at an upstream distance x of 12 in. The normalized total power is shown in Fig. 36 as a function of the Reynolds Number. For comparison, Fig. 37 reproduces the earlier measurements on the 2-in.-diameter pipe for scaled geometries — i.e., $\ell/D = 0.25$ and 0.5 respectively.

The scaling of the geometries between the two experiments was, unfortunately, not complete — the spoiler thickness in all instances was 1/8 in. The most serious discrepancy, however, probably lay in terms of the upstream scaling — the 4-in.-diameter configuration probably being influenced in terms of turbulence, velocity profiles, etc., by the air supply configuration.

It is interesting to note in this connection that the sound generated by inserting a 1-in.-wide spoiler in the 4-in.-diameter pipe shows a very distinct quadrupole characteristic. The sound frequencies generated, however (see Fig. 38), are very much higher than might be accounted for by conventional free-turbulence quadrupole noise. The 2-in.-wide strip spoiler shows a more-consistent dipolelike behavior, and the results indicate a value of k of about 2.5×10^{-4}. It is a rather strange observation that this behavior is exactly in reverse of that for the 2-in.-pipe, where some quadrupole activity was noted for a value of ℓ/D of 0.5 and more-consistent dipolelike radiation for an ℓ/D of 0.25. We cannot at present advance a satisfactory explanation of this result.

Normalized frequency spectra for these experiments are presented in Figs. 38 and 39 as functions of the Strouhal Number based on $\delta = \ell$. In both of these plots, there is a deviation in the data collapse at the high Strouhal Numbers. This is particularly so for the 1-in.-wide spoiler — the deviation having been already identified with quadrupole sources. A method of more complete normalization of these results is considered in a later chapter.

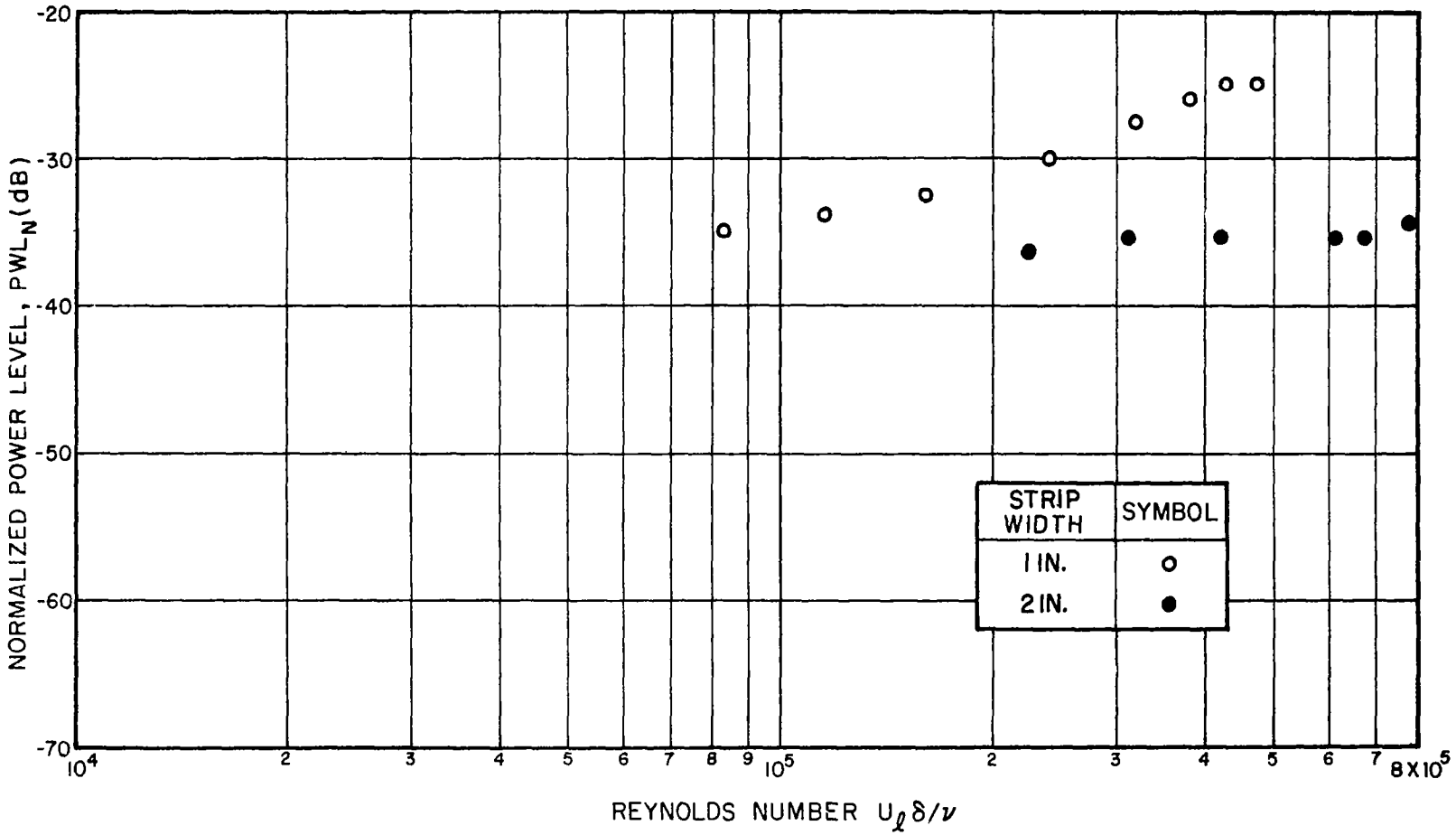

FIG. 36 NORMALIZED POWER LEVEL VERSUS REYNOLDS NUMBER FOR STRIP SPOILER D = 3.875, x = 12 IN., α = 90°, ℓ = VARIABLE

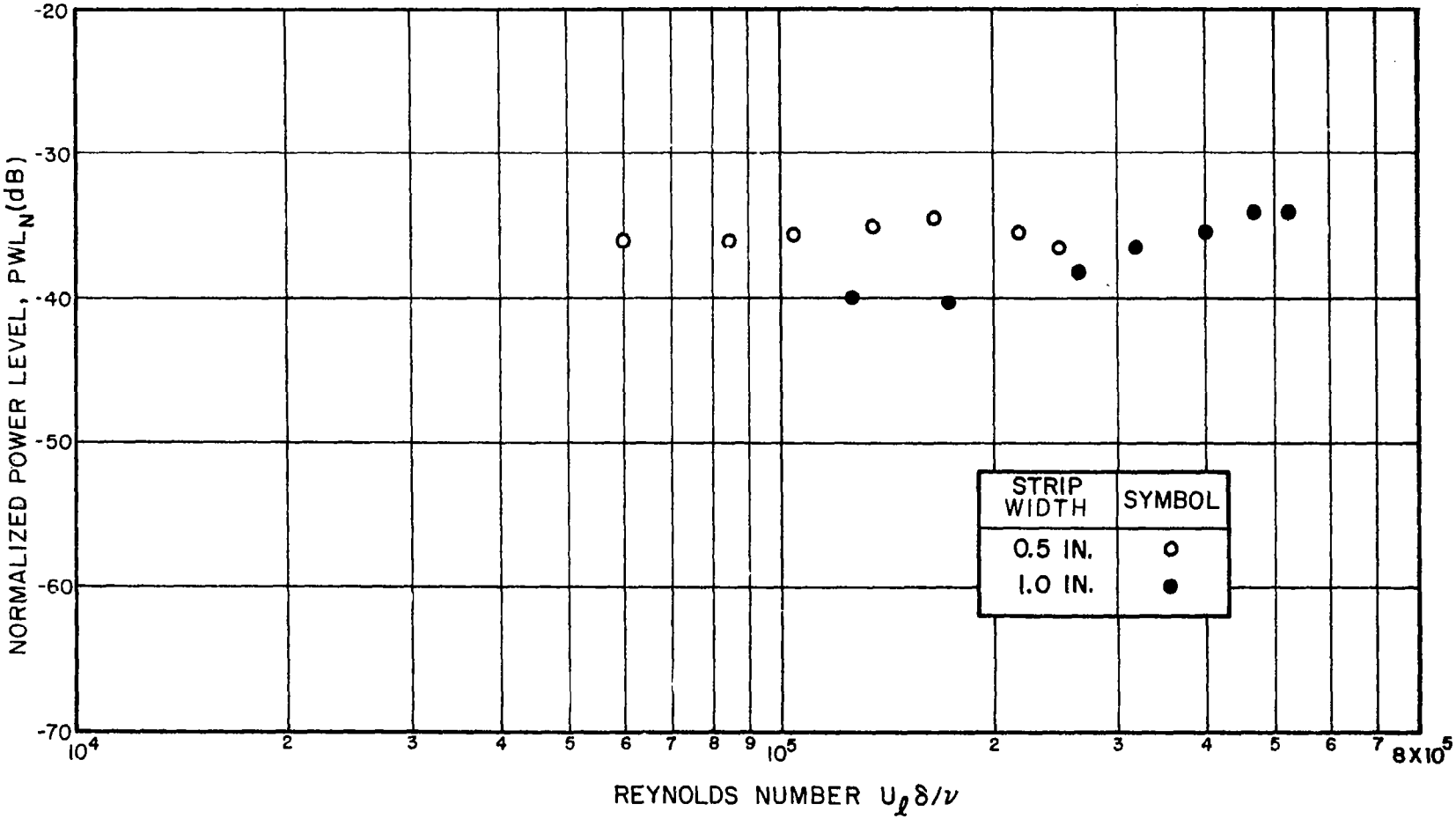

FIG. 37 NORMALIZED POWER LEVEL VERSUS REYNOLDS NUMBER FOR STRIP SPOILER D = 1.875, x = 6 IN., α = 90°, ℓ = VARIABLE

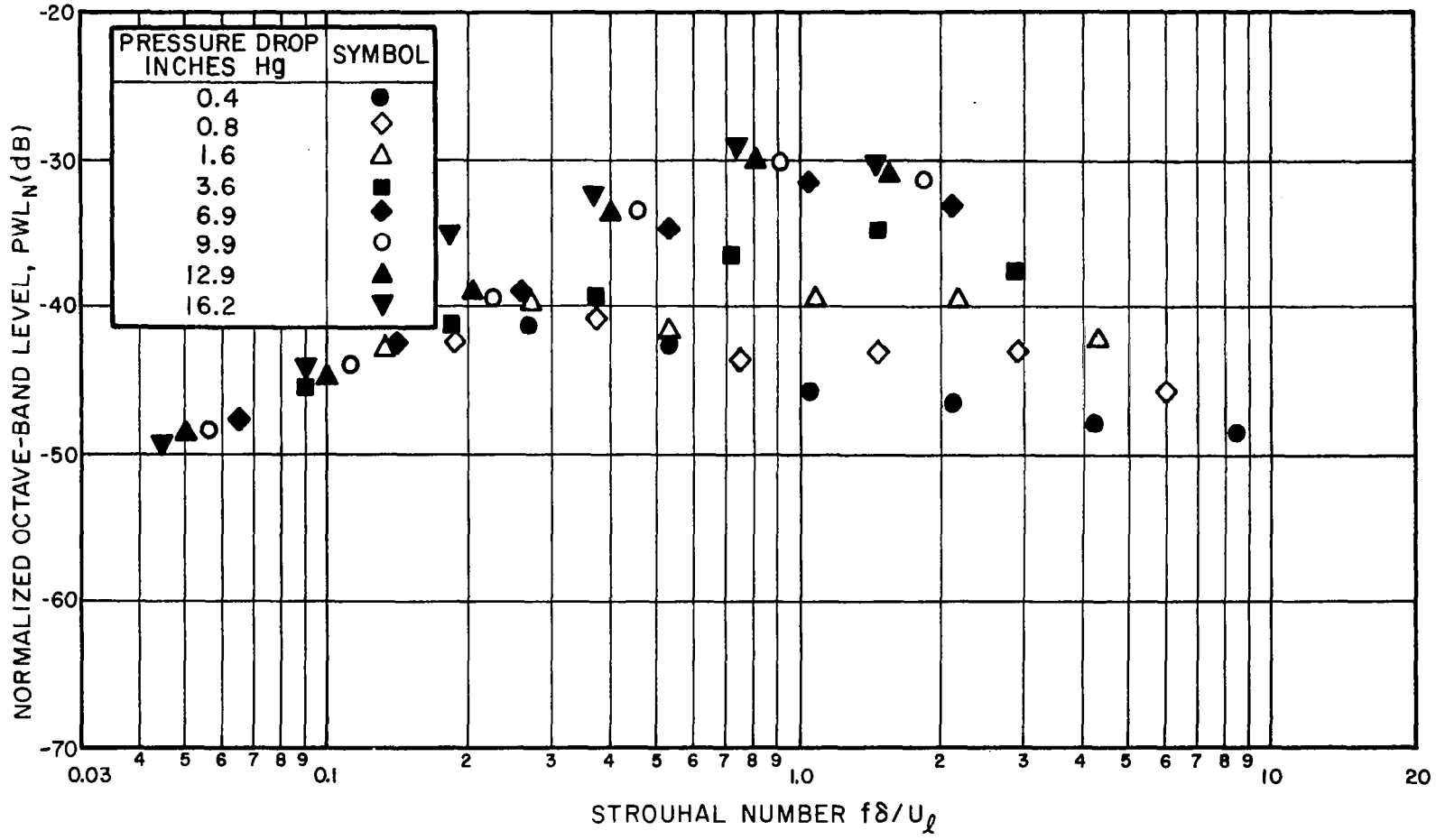

FIG. 38 NORMALIZED OCTAVE-BAND POWER LEVEL VERSUS STROUHAL NUMBER FOR STRIP SPOILER
D = 3.875, ℓ = 1 IN., x = 12 IN., α = 90°

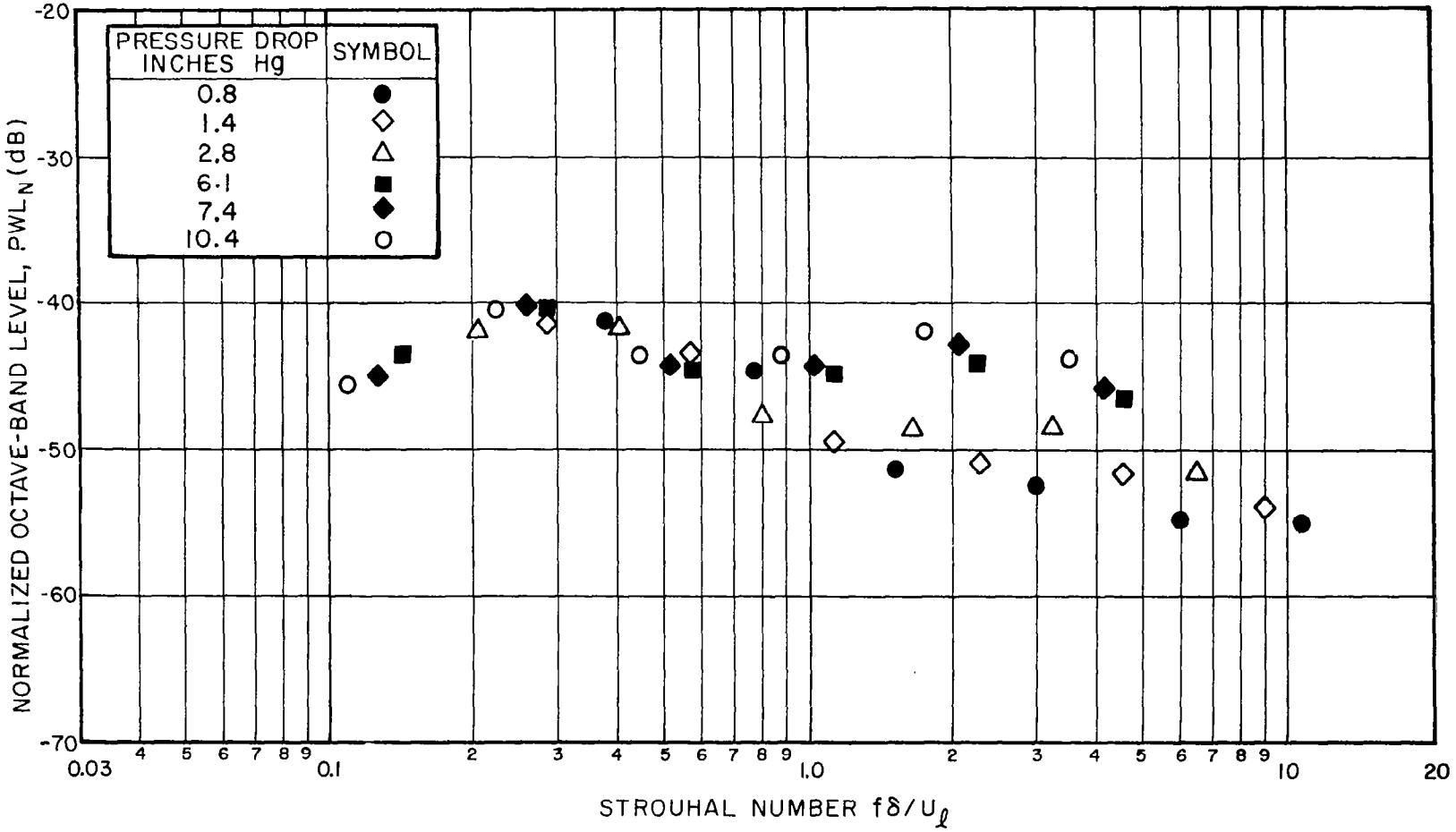

FIG. 39 NORMALIZED OCTAVE-BAND POWER LEVEL VERSUS STROUHAL NUMBER FOR STRIP SPOILER
D = 3.875, ℓ = 2 IN., x = 12 IN., α = 90°

IX. RESULTS: FURTHER OBSERVATIONS

In this chapter, we present the results of a variety of experiments designed to study specific configurations that do not fit directly under the preceding chapter headings but are relevant to the understanding of the mechanisms of noise production and to empirical description of these mechanisms.

9.1 Distributed Strip Spoiler

What happens when the flow discontinuity produced by a spoiler is distributed along the downstream axis or when the flow discontinuity is created by a plurality of flow spoilers? An experiment was carried out, using the configurations of Fig. 40, in which the spoiler was a flexible 1/2-in.-wide, thin steel strip: in Case (a), a single strip terminating at 3 in. from the exit plane; and Case (b), three strips all originating at the joint flange and terminating at, respectively, 3, 2, and 1 in. from the exit plane.

The normalized total power generated is shown in Fig. 41 as a function of Reynolds Number. Also included is the normalized data for a 1/2-in.-wide strip spoiler of the conventional sort ($A = 90^{\circ}$). The results correlate well and indicate a value of k of about 3×10^{-4}. We conclude that the mechanism of noise generation is essentially unchanged by the distributed spoiler geometry.

9.2 Change in Pipe Area

In yet another series of experiments, the effects of abrupt changes in the pipe diameter have been studied. The two basic configurations are shown in Fig. 42, being (a) an abrupt expansion to a 4.25-in.-diameter pipe for the final 6 in. of pipe length, and (b) a flow contraction to a 7/8-in.-diameter pipe, again for the final 6 in. of pipe flow. The results are shown in Fig. 43, together with the normalized results given earlier, for the plain 2-in.-diameter jet pipe. The values of D used in the normalization are tabulated. The abcissa for this plot is the total pressure drop $(p_o - p_a)$ in inches of mercury. At low velocities (low-pressure drop), the expanded flow is considerably noisier than either of the other configurations. Examination of the spectral data has indicated that this is associated with a quarter-wavelength acoustic resonance of the terminating cavity. This resonance is "washed away" as the flow velocity increases [see Chapter XI]. At the higher velocities, both the straight and contracted geometries begin to exhibit quadrupolelike behavior. Values of k in the range 5×10^{-5} to 10^{-4} are indicated.

A later experiment carried out with a 12-in. length of 4.5-in.-diameter pipe has indicated a value of k of about 2×10^{-4}. It is felt that the expanded flow geometry bears a very close similarity in total power generation to the conventional spoiler performance, so long as the length of expanded flow is sufficient to let the downstream flow become properly established. The suggestion is, again, that the noise-producing region lies in the immediate downstream expanding flow region of the "spoiled" system. The values of

k obtained for the "contracted-flow" configuration is more likely associated with lip noise.

9.3 Grid Configuration

As a more realistic type of spoiler geometry, the 1/4-in. grid system, discussed earlier in Figs. 13 and 14, has also been studied. The results have indicated a dipolelike sound-generating mechanism having a value of k of 2.5×10^{-4}.

9.4 Immersion of Sources in a Pipe

The theoretical analysis of aerodynamic sound sources within a hard-walled tube, given in Appendix A of this report, indicates a definite and drastic affect upon the radiation efficiency of such sources. Specifically, the analysis shows that eighth- and sixth-power-of-velocity dependencies exhibited by free-field quadrupoles and dipoles, respectively, should change to sixth- and fourth-power laws when these sources are immersed in a pipe. So far in the experimental study, there has been no evidence of such a fundamental change in source behavior, and the question arises as to how deeply immersed the sources must be in order for the analysis to be applicable.

An experiment was carried out in which the 0.5-in.-diameter ring spoiler was placed at the exit plane and then, in turn, at 6, 12 and 18 in. upstream. This spoiler, as we have shown earlier, behaves as a quadrupole generator over most of the operating range. It was hoped that by immersing this spoiler more and more deeply into the jet pipe, the predicted change in flow dependence of the quadrupole mechanism would be observed.

The results are shown in Fig. 44 where the total power (decibels re 10^{-12} Watts) is plotted against the total pressure drop (inches mercury). No change in slope from the quadrupolelike fourth-power of pressure drop, equivalent to the eighth-power of velocity, is indicated. (The change in level as the spoiler is moved from the exit plane has been commented on earlier). The theoretical analysis of the effects of immersion therefore remain unsubstantiated.

We must remember, however, that the acoustic energy is contained in frequency bands such that the acoustic wavelength is of the order of, or less than, the pipe circumference $2\pi D$. In this event, the radiated sound from the spoiler is controlled by "free-field behavior" and we would not necessarily expect to see the influence of immersion into the pipe.

9.5 Rotating Spoiler

A brief survey was made of the noise generated by a rotating "fan" in the jet pipe. The intent was to measure the radiated power as the effective angle of attack of the blades to the air flow was altered by "loading" or "driving" the rotating system over a wide range. The preliminary data indicated, as might be expected, that the system is essentially similar to the strip spoiler at variable angles of attack. The experimentation was limited to speeds of rotation such that the tip speed was in the low subsonic range. The experimentation was complicated by the problems of high background noise generated by the mechanical rotating parts (bearings, etc.) and no valid experimental data is available.

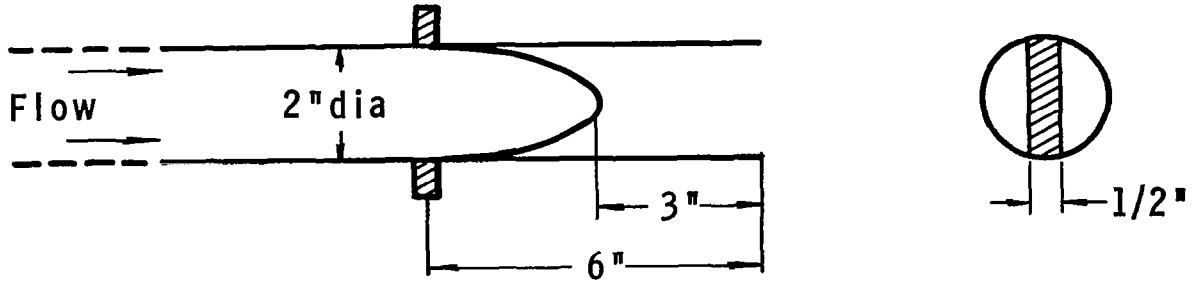

a) Single

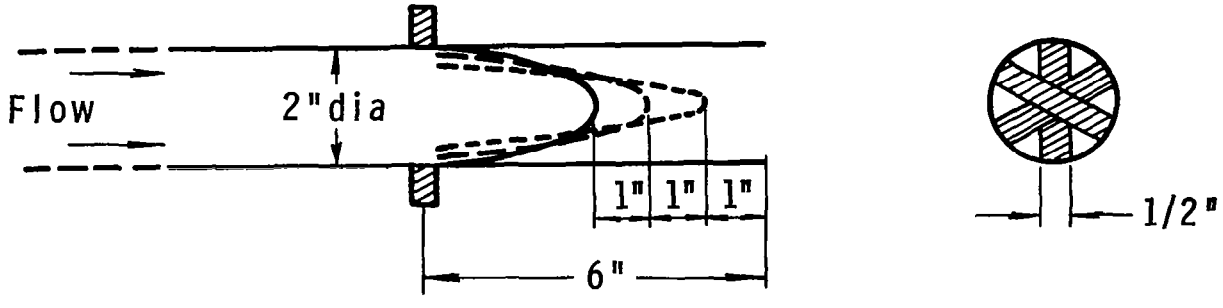

b) Triple

FIG. 40 DISTRIBUTED SPOILERS SCHEMATIC

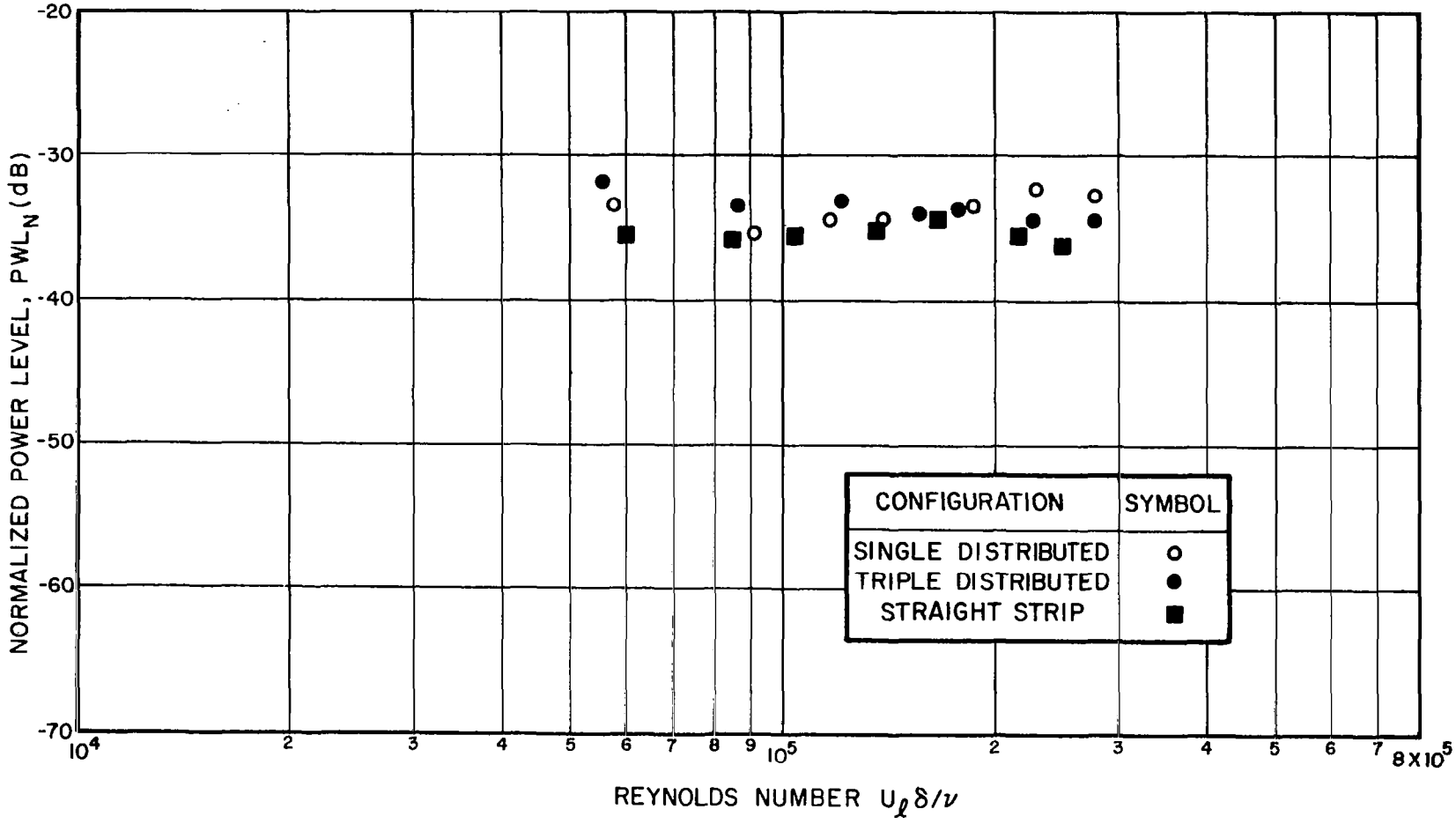

FIG. 41 NORMALIZED POWER LEVEL VERSUS REYNOLDS NUMBER FOR DISTRIBUTED AND MULTIPLE STRIP SPOILERS
D = 1.875, ℓ = 0.5 IN., α = 90°

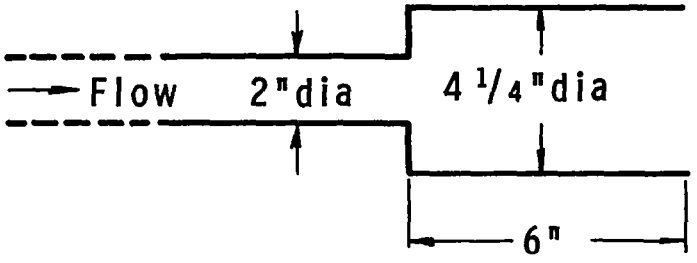

a) Expanded Flow

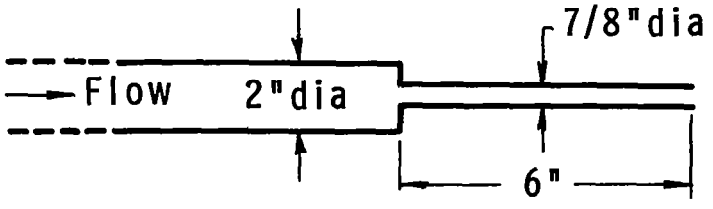

b) Contracted Flow

FIG. 42 CHANGE OF PIPE AREA

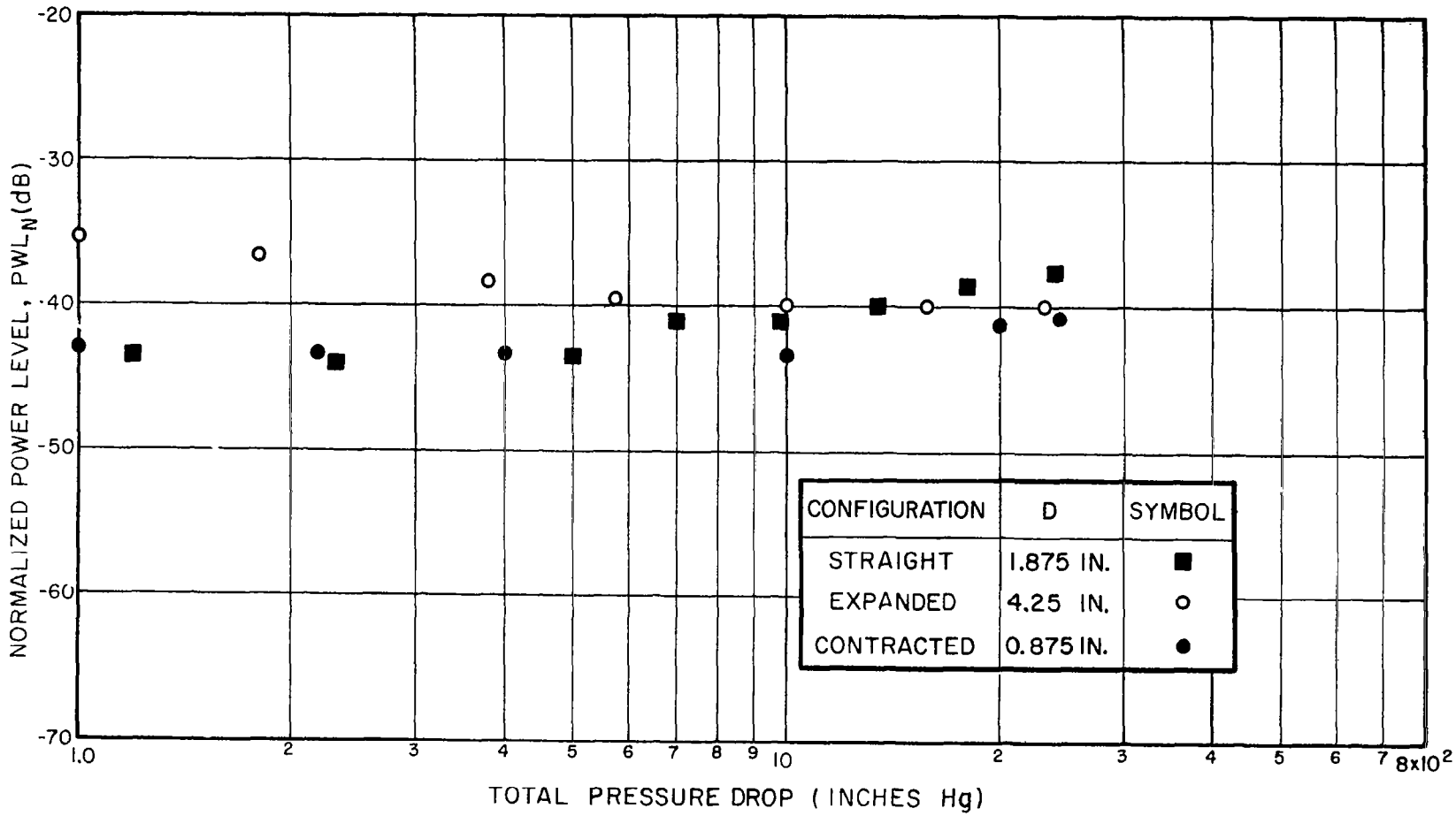

FIG. 43 NORMALIZED POWER LEVEL VERSUS TOTAL PRESSURE DROP FOR STRAIGHT, EXPANDED AND CONTRACTED PIPE CONFIGURATIONS

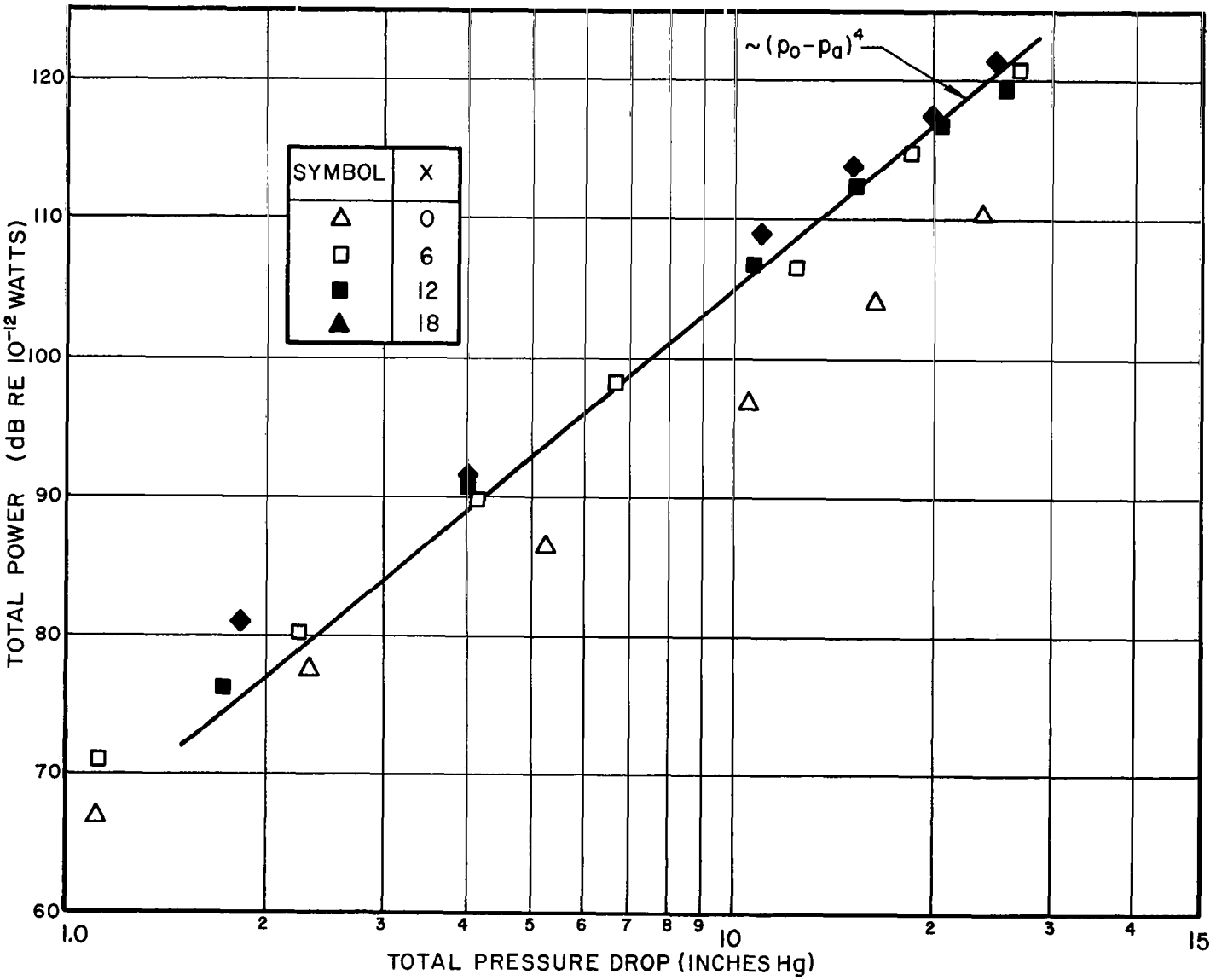

FIG. 44 TOTAL POWER LEVEL VERSUS PRESSURE DROP FOR RING SPOILER AT VARYING DEGREES OF IMMERSION IN JET PIPE D = 1.875 IN., d = 0.5 IN., x = VARIABLE

X. DIRECTIVITY PATTERNS OF SPOILED JET FLOW

The free-field study of the spoiler-generated noise also provides useful information regarding the directivity patterns associated with in-pipe noise sources. The comments below are based on the examination of a large quantity of experimental data.

Flow noise, generated by a spoiler in a pipe, radiates from the end of the pipe and produces a directivity pattern closely simulating the directivity pattern of noise injected into the pipe by means of a small loudspeaker in the absence of the spoiler. This fact supports the conclusion that air flow around a spoiler in a pipe generates noise in a region within the pipe close to the spoiler. One concludes also that the lobed directivity pattern is not, therefore, uniquely indicative of the sound-producing sources within the pipe but that the pattern arises as a result of refractive effects external to the jet pipe. The exit wake causes a decrease in the sound radiated along the axis of the jet by refracting the sound away from the axis. This effect increases with both the exit velocity of the air stream and the frequency of the sound.

A similar situation has been noted by Ribner and his colleagues (ref. 16) in their investigation of jet noise. A difference exists between Ribner's observations and those described here, because, in his case, the jet-noise source is external to the pipe, one or more pipe diameters downstream, whereas the present source is inside the pipe two to three diameters upstream. Ribner simulated jet noise by a point source 1 2/3 pipe diameters downstream and obtained a uniform directivity pattern in the absence of any flow. In the present

experiments, since the sound source is located in the pipe, there is a basic directivity pattern even in the absence of any refraction due to the exit-stream velocity. This is particularly so at high frequencies.

Even a very small flow (a few feet per second) causes a decrease in sound on axis and creates a peak in sound intensity at some relatively large angle. This angle increases with both flow velocity and frequency.

Figure 45 comprises an assembly of directivity patterns obtained for a 2-in.-diameter pipe at low exit flow velocity, Mach 0.15. Comparison is made between patterns obtained for the noise from a 1/2-in. spoiler at right angles to the flow (solid lines) and the noise injected into the pipe by a speaker upstream of the spoiler location but with the spoiler removed (dashed lines)*. Similarity is apparent between the patterns obtained for the two noise sources at each 5 frequency bands in the range of 1000 to 16000 cps. The pattern becomes more peaked at the higher frequencies and develops a deeper notch on axis. Similar agreement is shown at Mach 0.5, as shown in Fig. 46.

The angle of maximum radiation for different frequencies (related to the downstream axis) increases both with frequency and with flow velocity. This variation is shown in Fig. 47.

---

* It should be noted that the experiments with injected noise were made using third-octave bands of noise as opposed to the octave bandwidths for the spoiler data.

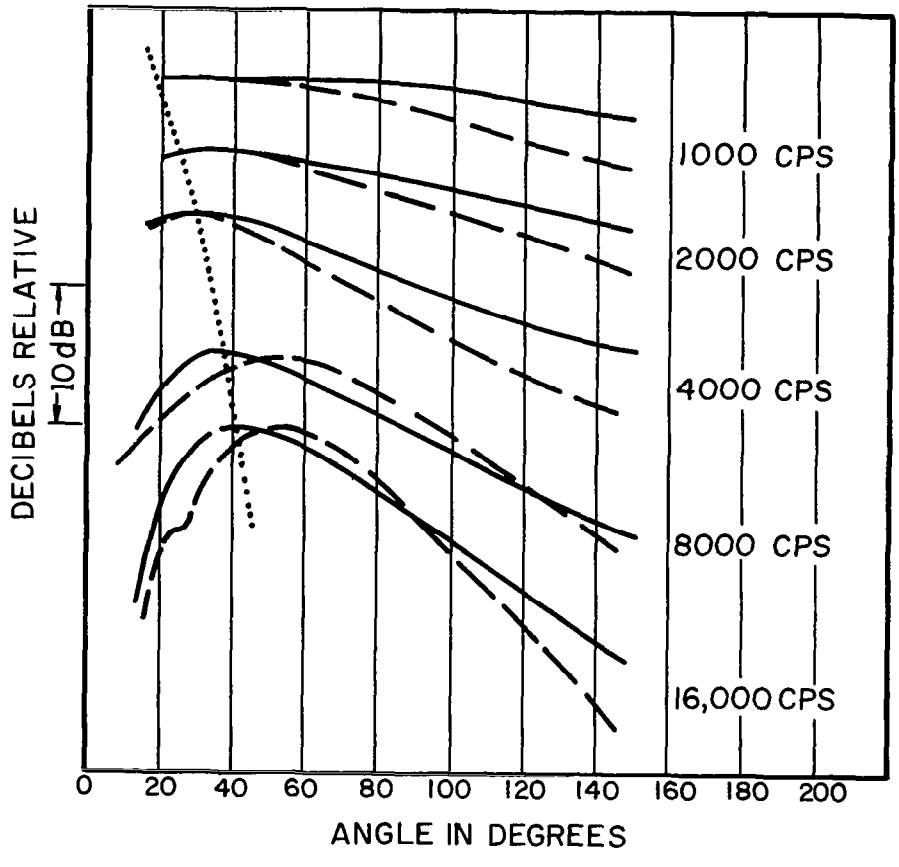

FIG. 45 DIRECTIVITY PATTERNS FOR M = 0.15
2" DIAMETER PIPE

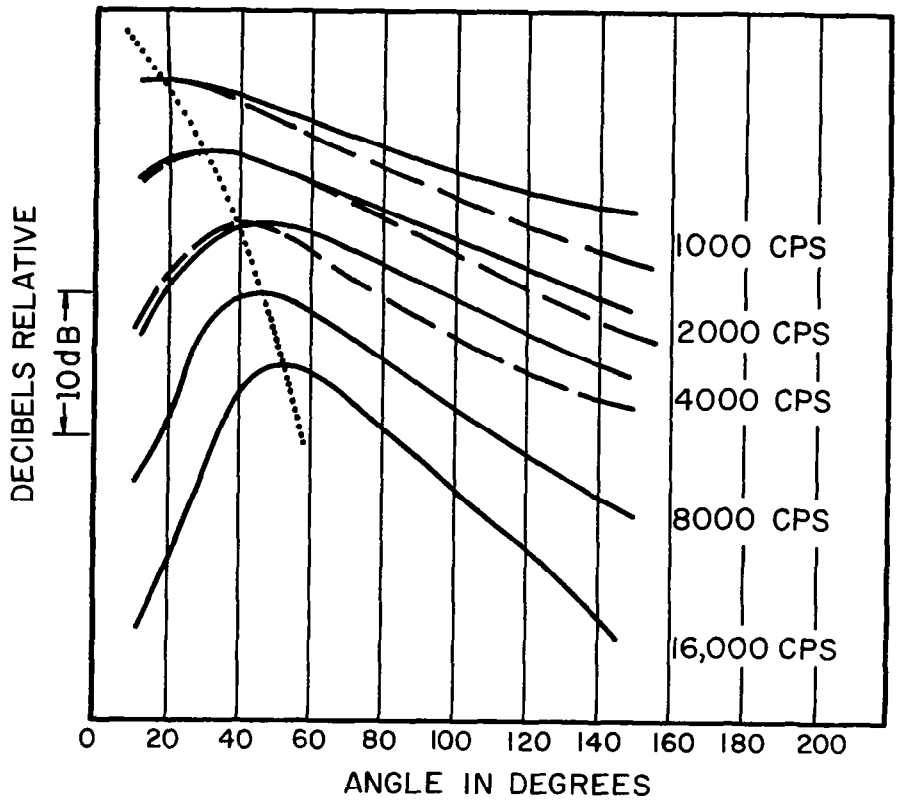

FIG.46 DIRECTIVITY PATTERNS FOR M = 0.5
2" DIAMETER PIPE

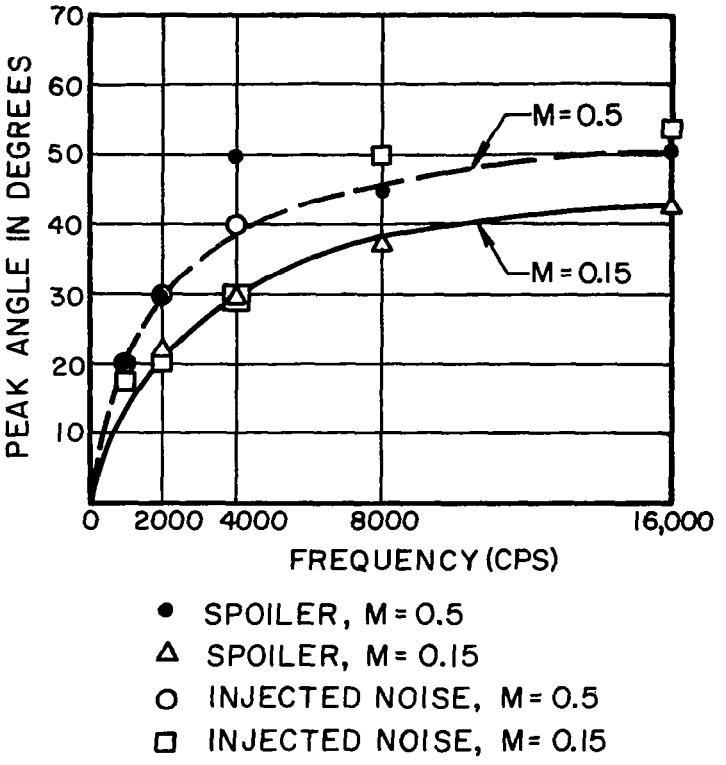

FIG.47 VARIATION OF PEAK ANGLE WITH FREQUENCY AND FLOW VELOCITY

XI. DISCRETE FREQUENCY PHENOMENA

Throughout the study, our interest has been centered specifically on the broad-band aspects of spoiler noise. Some of the spoiler configurations used during the study have caused the generation of discrete-frequency sound components [i.e. line spectra]. It is relevant here to describe three of these situations that are, perhaps, relevant to future studies of jet-engine noise.

11.1 Acoustic Resonances

The experiments have shown that the sound associated with flow spoilers is generated in the close vicinity of the spoiler. Thus the acoustic behavior of the jet pipe might be expected to influence the power radiation, particularly as it affects the radiation impedance of the in-pipe source array. Generally, however, the typical sound generated by the spoiler seems to interact little with the acoustic resonances of the pipe and no evidence of line spectra has been observed. This is with the exception of one experiment: that of the abrupt expansion in pipe diameter, (see Fig. 43). The typical sound spectra generated at the low flow velocities showed line components. At these low velocities, the jet "hooted". Analysis of the spectra revealed that the line components are associated with frequencies such that the acoustic wavelength is approximately four times the length of the expanded section of the pipe. These resonances, however, were "washed out" as the flow velocity increased. The suppression of these line spectra may arise from changes in the end impedance of the pipe at the higher flow velocities. It is suggested that this phenomenon

may also be related to the acoustic response of cavities in an aerodynamic flow (ref. 17).

11.2 Thin Spoiler Parallel to Flow

A series of experiments has already been described (see Chapter VI) in which the downstream length of a spoiler at zero angle of attack was varied. In setting up these experiments, very severe discrete frequencies were encountered, associated, apparently, with trailing-edge flow instability at the intersection of the spoiler with the pipe wall. Resonances were removed by radiusing the in-plane spoiler trailing edge at the points where it intersected with the pipe wall.

11.3 Spoiler-Spoiler Interaction

In an effort to determine the influence of the interaction of a spoiler with the turbulent wake of another spoiler, a series of experiments were conducted in which similar (1/2-in.-wide) spoilers were placed in series and the distance between them varied. A very strong discrete-frequency behavior was noted, particularly at the higher velocities. As the spacing between the spoilers increased (spacings up to 6 in. were studied), the flow velocity had to increase before evidences of the line spectra were established. When the spoilers were staggered relative to the tube axis, thus reducing the degree of wake interaction, the intensities of the line spectra were also reduced. These studies were in the form of a very cursory examination of interaction phenomena. They do indicate, however, the occurrence of the same phenomena noted by G. I. Taylor (ref. 7), with his toasting fork, and by Hubbard and

Maglieri (ref. 18), in their measurements of the noise of helicopter rotors. Similar interactions might be expected between rotor and stator stages of a compressor or turbine, although, here, the effect may be modified by the rapidly pulsating nature of the flow field.

XII. THE FREQUENCY SPECTRUM: RENORMALIZATION

If we examine many of the normalized octave-band frequency plots in previous chapters, it becomes obvious that the collapse of this data is often incomplete, particularly in the high Strouhal Number range. A typical type of spectrum is that of Fig. 21, examination of which shows a definite striation of the results in the higher Strouhal Number range. Studies of this data have shown that a vast improvement in data collapse may be obtained by modifying the normalization in accordance with the relation

$$P_A = k\,(p_o - p_a)^3 D^2 \left[1 + \left(\frac{f}{f_o}\right)^2\right] \Big/ \rho_a{}^2 c_a{}^3 \qquad (35)$$

and

$$PWL_N \text{ (normalized)} = 10 \log \frac{P_A \rho_a{}^2 c_a{}^3}{(p_o - p_a)^3 D^2 \left[1 + \left(\frac{f}{f_o}\right)^2\right]}, \qquad (36)$$

where f is the band center frequency of the data point in question, and f_o is some constant frequency, presumably based on the dimensions of the flow system [see Chapter I]. The modified normalization of the data of Fig. 21 is shown in Fig. 48, where a value of f_o = 4000 cps has been selected.

As a second example, we show in Fig. 49 the collapse of the spectrum data of Fig.37, this time reduced on the basis of a value of f_o = 1400 cps. Again, the data collapse is excellent.

A hint as to what might be happening is offered us by the observation that the latter result showed a definite eighth-power-of-velocity behavior over most of the operating range (see Fig. 36). A comparison of Eqs. (35) and (36) suggests that, while the first term of Eq. (35) describes a dipolelike source, the second term, having an extra frequency — squared (or velocity-squared) factor in it, does indeed resemble a quadrupolelike source. This aspect has been discussed in Chapter I.

If we look back at the earlier results relating to strip and ring (and other) spoiler configurations, it is observed that, in many instances, at the highest flow velocities there is a tendency for the total power level to increase a little beyond the normalized dipole level. This observation, together with the spectra, is a strong indication that a quadrupolelike mechanism is operative within the experimental jet system.

The term "within" is used advisably, because in most of these instances the frequencies (and levels) of this quadrupolelike behavior are well above that to be expected of the free-jet turbulence.

The summarized spectral data based on the modified normalization relation of Eq. (36) are shown in Fig. 50, for a selection of spoiler configurations. The relevant dimensional parameters and values of f_o used in the normalization are also presented in tabular form. It is observed that with the exception of the 1.-in. strip spoiler in the 4-in.-diameter pipe, the normalization constant f_o is, apparently, directly related to the ratio D/δ, where δ is the projected spoiler width given by $(\ell \sin \alpha)$.

The agreement between the renormalized spectra is excellent, the mean spectrum peaking at a Strouhal Number of about 0.2 (based on the projected spoiler width and the local velocity) and falling off at about a rate of 6 dB/octave at higher and lower Strouhal Numbers. It is clear from the collapse of the spectra that the total power, similarly renormalized [see Chapter I), will be essentially constant with respect to the Reynolds Number. It is remarkable that, in most cases, a single empirical parameter (f_o) is sufficient to induce such a thorough collapse in the data.

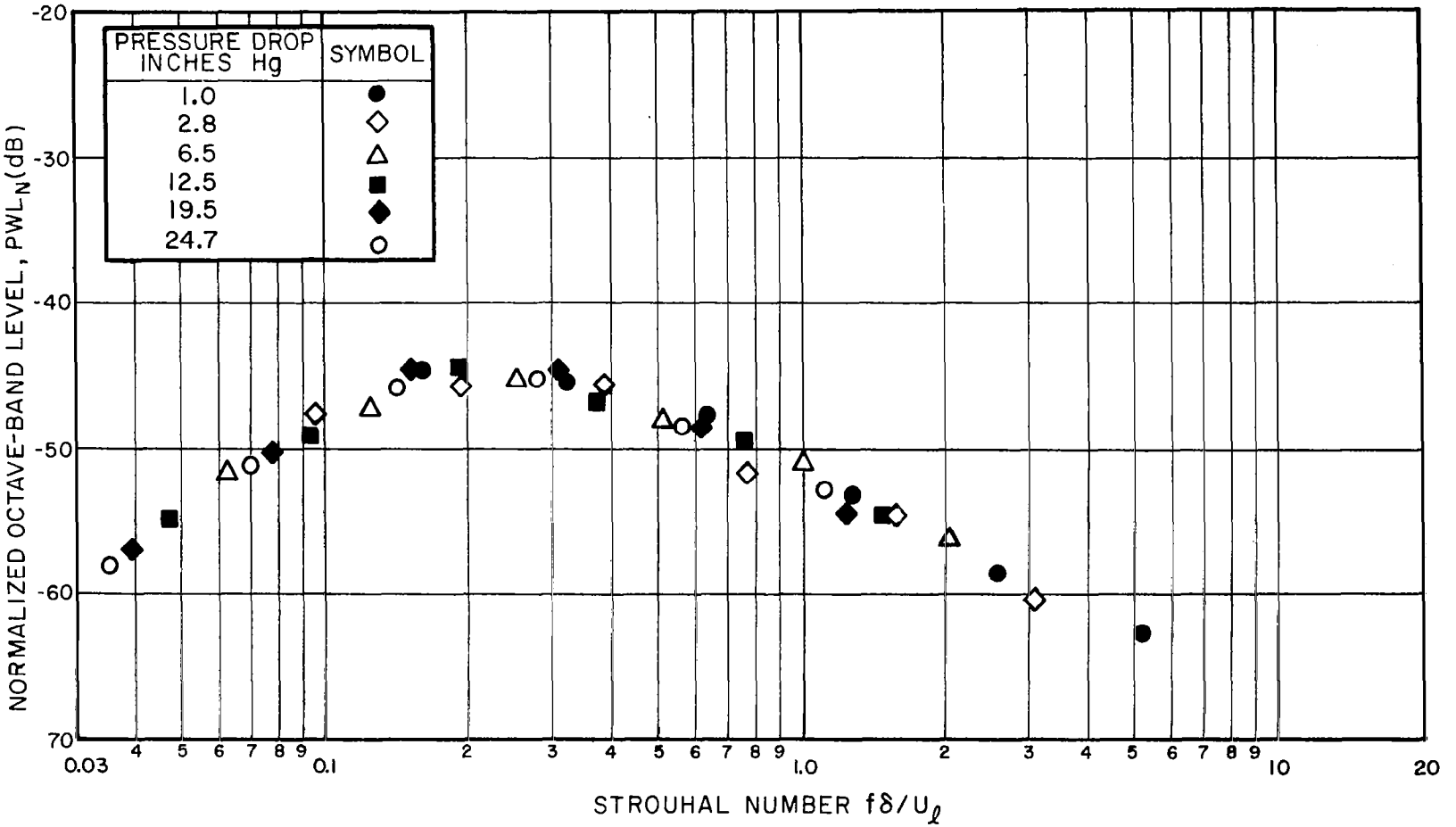

FIG. 48 MODIFIED NORMALIZATION OF THE RESULT OF FIG. 21 FOR f_0 = 4000 CPS, D = 1.875 IN., ℓ = 1 IN., x = 6 IN., α = 67.5°

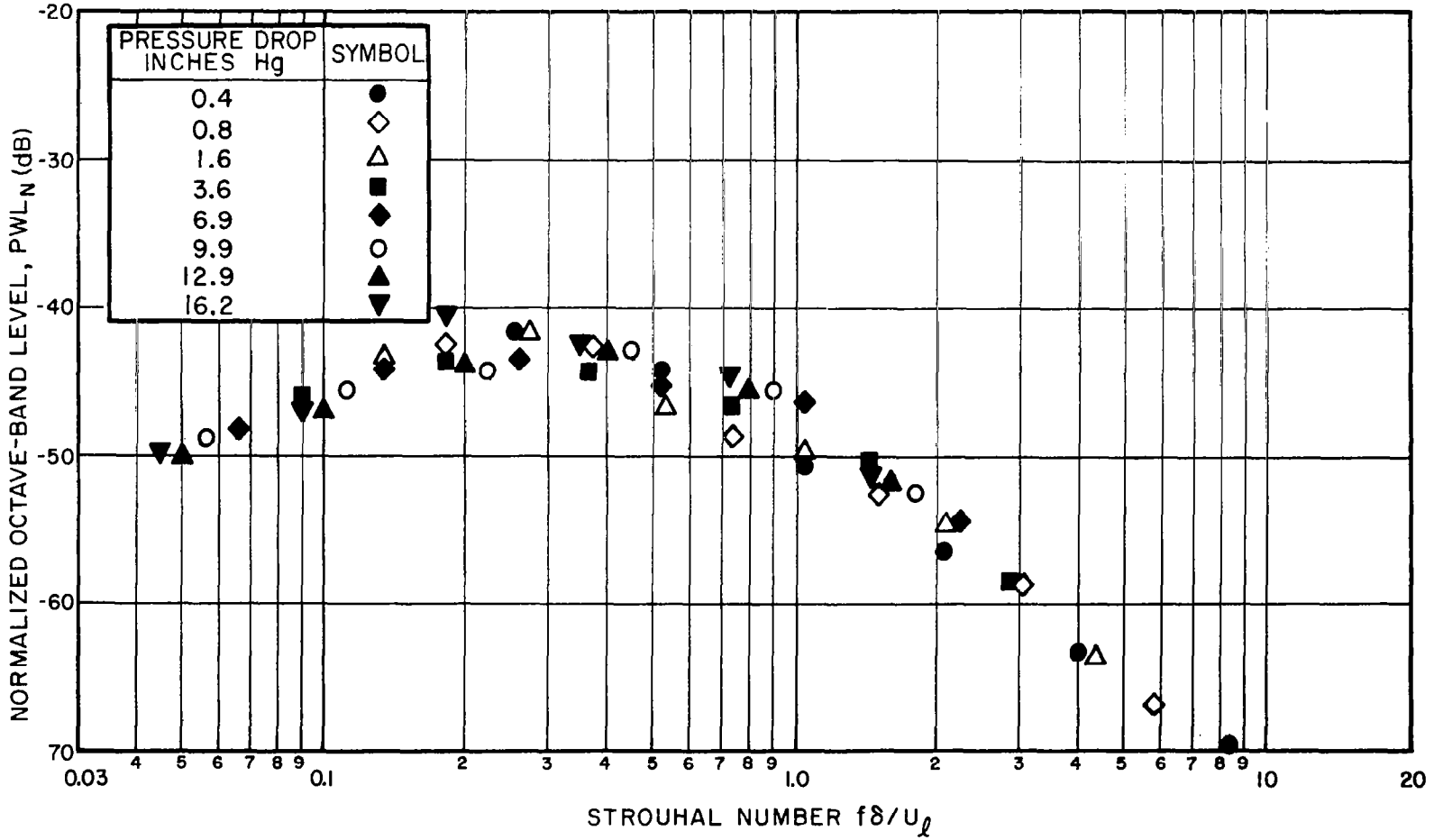

FIG. 49 MODIFIED NORMALIZATION OF THE RESULT OF FIG. 38 FOR f_0 = 1400 CPS, D = 3.875 IN., ℓ = 1 IN., x = 12 IN., α = 90°

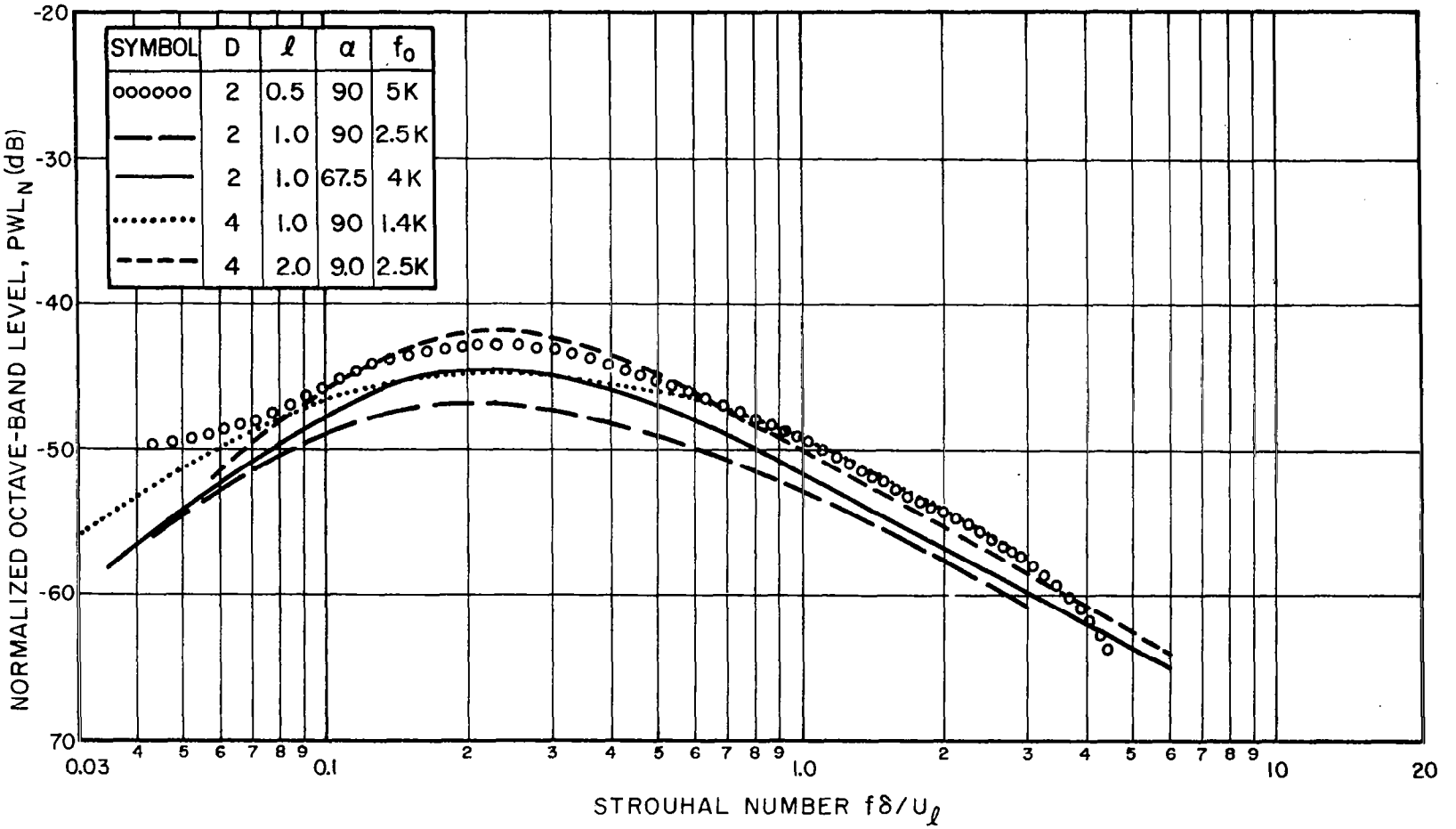

FIG.50 A COMPARISON OF MEAN SPECTRUM SHAPES USING MODIFIED NORMALIZATION

XIII. CONCLUSIONS

Within the scope of this study, we have examined the form of the acoustic radiation from a jet pipe into which spoilers have been inserted. We have examined the spectral and directivity characteristics of the radiation from such a system over a wide variety of spoiler configurations and sizes and have made observations concerning the location of the spoiler-generated sound sources. We have also looked at the effect of spoiler-spoiler interactions, the effect of the location of the spoiler within the jet pipe, and some other aspects pertinent to an understanding of the problem of spoiler-generated sound. Perhaps the establishment of an empirical formulism to describe the generation of "spoiler sound" is the most important practical achievement of this study. The effective collapse of the frequency spectrum data upon "re-normalization" - which indicates the presence of in-pipe quadrupole sources - must also be considered as particularly significant, although no theoretical explanation of the mechanisms involved can be presented at this time.

APPENDIX A. AERODYNAMIC SOUND SOURCES WITHIN A HARD-WALLED STRAIGHT TUBE

There are two distinctly different ways of approaching the problem of how the presence of pipe walls affect the radiation of turbulence-generated sound. The influence seems to be a definite and drastic one making it worthwhile to describe both approaches so that the effect is properly understood. Initially, we consider the turbulent flow deeply immersed in the tube, and leave until later the important and interesting transition that takes place when the sources are close to the tube exit.

The first approach is to consider the tube walls as reflecting surfaces. This procedure can hardly have rigorous generality, since the existence of suitable images is only established in particularly simple geometrical situations. On the other hand, one cannot foresee the detailed cross-sectional shape having any fundamental part to play in the problem; thus we choose, for simplicity, a tube of square cross section. The problem of estimating the radiation within the tube is then completely analogous to that of estimating the radiation in free space from an infinite but regular planar array of sources. For every source within the tube, there are perfectly identical sources arrayed throughout a plane perpendicular to the tube, with generators occurring once in every area equal to the tube area. The situation is depicted in Fig. A-1, the position of each source being indicated by a +.

Our intention is to indicate the radiation field of aerodynamic sources induced by turbulent flow over rigid surfaces within the tube. In a free field, the theories of Lighthill (ref. 1) and Curle (ref. 6) describe the situation. They indicate that the sound is generated by a volume distribution of quadrupoles of strength T_{ij} within the turbulence and that this is reinforced by a surface distribution of dipoles whenever the turbulence interacts with rigid surfaces. Discarding any nearfield effect, these theories predict the radiation at a point $(\underset{\sim}{x},t)$ to be the sum of all contributions from each individual source. From unit volume of turbulent flow at $\underset{\sim}{y}$, there radiates, according to Lighthill's theory, a distant density field of magnitude

$$\rho(\underset{\sim}{x},t) = \frac{1}{4\pi a_o^4} \frac{1}{r} \frac{\partial r}{\partial x_i} \frac{\partial r}{\partial x_j} \frac{\partial^2}{\partial t^2} T_{ij} \left(\underset{\sim}{y}, t - \frac{r}{a_o}\right) . \qquad (A.1)$$

The notation is the one usual to aerodynamic noise theory. The expression a_o is the speed of sound at $\underset{\sim}{x}$, and r is the distance separating source and observer (i.e., $r = |\underset{\sim}{x}-\underset{\sim}{y}|$). Curle extended the theory to show that, if P_i were the force exerted on the fluid by unit surface area at $\underset{\sim}{y}$, then that area was responsible for a distant density field of magnitude

$$\rho(\underset{\sim}{x},t) = \frac{1}{4\pi a_o^3} \frac{1}{r} \frac{\partial r}{\partial x_i} \frac{\partial P_i}{\partial t} (\underset{\sim}{y}, t-r/a_o) . \qquad (A.2)$$

Having transformed the pipe-noise problem to an analogous three-dimensional situation, we can regard these equations as the starting point of the analysis. The general problem is

clearly complicated by the directionality of the radiation field that is determined by details of the turbulent flow. This feature cannot be fundamentally important, so it is best ignored in this initial treatment, and this is effectively done by assuming both the volume stress field and the surface force field to be isotropic with magnitudes T and P, respectively. Eqs. (A.1) and (A.2) then become

$$\rho(\underset{\sim}{x},t) = \frac{1}{4\pi a_o^4 r} \frac{\partial Q}{\partial t} (\underset{\sim}{y}, t-r/a_o) \quad , \tag{A.3}$$

where $Q = \frac{\partial T}{\partial t}$ represents the volume quadrupole field, and $Q = a_o P$ represents the surface dipole field. By writing the equation in this way, we can treat the problem of both dipole- and quadrupole-generated sound in one step, taking the particular form of Q appropriate to the problem at a later stage. The problem now becomes one of simply summing all components of the field induced by sources of strength $\frac{\partial Q}{\partial t}$, arrayed at regular intervals throughout the source plane. This sum can be transferred to an integral over the area of the source area number density times the contribution from any one source, which is given by Eq. (A.3). Let the width of the tube by L so that the tube area is L^2. In every L^2 of area in the source plane, there will be found, according to Fig. A.1, one source. The source area number density is therefore constant at a value $1/L^2$. The total effect of all the sources will, therefore, be

$$\rho(\underset{\sim}{x},t) = \frac{1}{4\pi a_o^4 L^2} \int_s \frac{\partial Q}{\partial t} (\underset{\sim}{y}, t-r/a_o) \frac{ds}{r} \quad . \tag{A.4}$$

where v and s_o are, respectively, the volume and the surface over which the sources exist.

The usual dimensional analysis (where both the turbulence stress tensor and the surface stress field are supposed proportional to some typical dynamic pressure, and the operation $\frac{\partial}{\partial t}$ is like multiplying by a typical frequency U/L) predicts the mean square density field radiated by in-pipe volume quadrupoles and surface dipoles to be proportional, respectively, to

$$\rho_o^2 \frac{U^6}{a_o^6} \text{ and } \rho_o^2 \frac{U^4}{a_o^4} \quad . \tag{A.11}$$

These forms are to be compared and contrasted with the free-field predictions given by Lighthill and Curle, which are for the quadrupoles and dipoles, respectively:

$$\rho_o^2 \frac{U^8}{a_o^8} \frac{L^2}{r^2} \text{ and } \rho_o^2 \frac{U^6}{a_o^6} \frac{L^2}{r^2} \tag{A.12}$$

The behavior is fundamentally different, the magnitudes being greater by the large factor a_o^2/U^2 in both cases, and the field, as must be the case in a constrained region, displaying no decay with increasing distance from the source distribution.

Evidently, this behavior, which is quite different from usual, is established in regimes where the foregoing theory is a relevant description of the physical situation. Quite clearly, to an observer close to the turbulence, the theory is quite irrelevant, for two reasons. First, the farfield

form of the three-dimensional equations, Eqs. (A.1) and (A.2), formed the basis of the extension. The observation point is, therefore, supposed in the far field of each eddy, which implies it is several wavelengths downstream of the turbulence. Also, the formulation represented the image distribution as a continuous array of constant source density. Near a particular source, this model becomes inapplicable, so that the observer must be sufficiently distant from the source surface so that no one source has any distinctly greater influence on the field than do the neighboring sources at a distance L away. This condition places a further restriction: that the theory becomes relevant only when the observer is several tube widths downstream of the turbulence. Precisely how many is open to conjecture and is best left to be established by experiment.

The conclusions of this theory are therefore that the mean square density field several wavelengths and several tube widths downstream of a distribution of aerodynamic quadrupoles and dipoles becomes independent of distance along the tube and is proportional to $\rho_o^2 \, (U^6/a_o^6)$ and $\rho_o^2 \, (U^4/a_o^4)$, in the cases of quadrupoles and dipoles, respectively.

These conclusions are confirmed by a second form of analysis that is mentioned earlier. That analysis deals with the plane-wave mode of propagation down a tube of arbitrary cross section. The analysis is based on the equations of continuity and momentum.

If ρ is the mass contained in unit length of pipe, then a form of the continuity equation can be written

$$\frac{\partial \rho}{\partial t} + \frac{\partial}{\partial x} \int_S \rho U = 0 \quad , \tag{A.13}$$

where x is the coordinate along the pipe generator and $\int_s \rho U$ is the integral mass flux in the direction x. In a similar way, a momentum equation can be established, which is of the form

$$\frac{\partial \int_s \rho U}{\partial t} + \frac{\partial}{\partial x} \int_s \rho U^2 + \frac{\partial p}{\partial x} = 0 \quad . \tag{A.14}$$

The operation $\frac{\partial (A.13)}{\partial t} - \frac{\partial (A.14)}{\partial x}$ yields a one-dimensional wave equation:

$$\frac{\partial^2}{\partial t^2} \rho - a_o^2 \frac{\partial^2}{\partial x^2} \rho = \frac{\partial^2}{\partial x^2} \left\{ \int_s \rho U^2 + p - a_o^2 \rho \right\} \quad . \tag{A.15}$$

The right-hand side of this equation can be termed $(\partial^2/\partial x^2) \int T_{11}$ ds, and the equation can be recognized as the integral of Lighthill's wave equation across the pipe area:

$$\frac{\partial^2 \rho}{\partial r^2} - a_o^2 \frac{\partial^2 \rho}{\partial x^2} = \frac{\partial^2}{\partial x^2} \int_s T_{11} \, ds \quad . \tag{A.16}$$

This equation can be solved as follows.
The Green's function for the one-dimensional equation is the step function

$$\frac{1}{2a_o} H \left(t - \tau - \frac{|x-y|}{a_o} \right) \quad . \tag{A.17}$$

We consider steady-state conditions in an infinite pipe, so that the boundary value terms vanish. We then use the Green's function to integrate Eq. (A.16), so that

$$\rho(x,t) = \frac{1}{2a_o} \int_{-\infty}^{\infty} d\tau \int_{-\infty}^{\infty} dy\ H\left(t-\tau - \frac{|x-y|}{a_o}\right) \frac{\partial^2}{\partial y^2} \int_s T_{11}\, ds \quad . \tag{A.18}$$

Integration by parts with respect to y yields a delta function and, hence, a retarded-time integral. The space derivative at retarded time can be changed to a time derivative as the integrand vanishes at $\pm\infty$. Then, Eq. (A.18) becomes

$$\rho(x,t) = \frac{-1}{2a_o^2} \int_{-\infty}^{\infty} dy \left[\frac{\partial}{\partial y} \int_s T_{11} ds\right]_{t-\frac{|x-y|}{a_o}} \mathrm{Sgn}\,(x-y)$$

$$= \frac{1}{2a_o^3} \int_{-\infty}^{\infty} dg \int_s ds\, \frac{\partial}{\partial t}\left[T_{11}\right]_{t-\frac{|x-y|}{a_o}} \mathrm{Sgn}\,(x-y) \quad . \tag{A.19}$$

Equation (A.19) is analogous to a volume integral in three-dimensional space, but its form involves one less time derivative than is usual in aerodynamic noise theory. There is also no decay of the field with increasing separation of the observation point $\underset{\sim}{x}$ from the source point $\underset{\sim}{y}$. In fact, Eq. (A.19) is seen to be identical to Eq. (A.9) so that, again, dimensional

analysis predicts the mean square radiation density of a volume distribution of quadrupoles within a pipe to vary in proportion to

$$\rho_o^2 \frac{U^6}{a_o^6} \quad . \tag{A.20}$$

Again we stress the difference with the three-dimensional case, which predicts a much less intense sound. This new result must surely apply to turbulence sufficiently deeply immersed within the pipe. Precisely how far it must be immersed is a matter to be resolved by experiment.

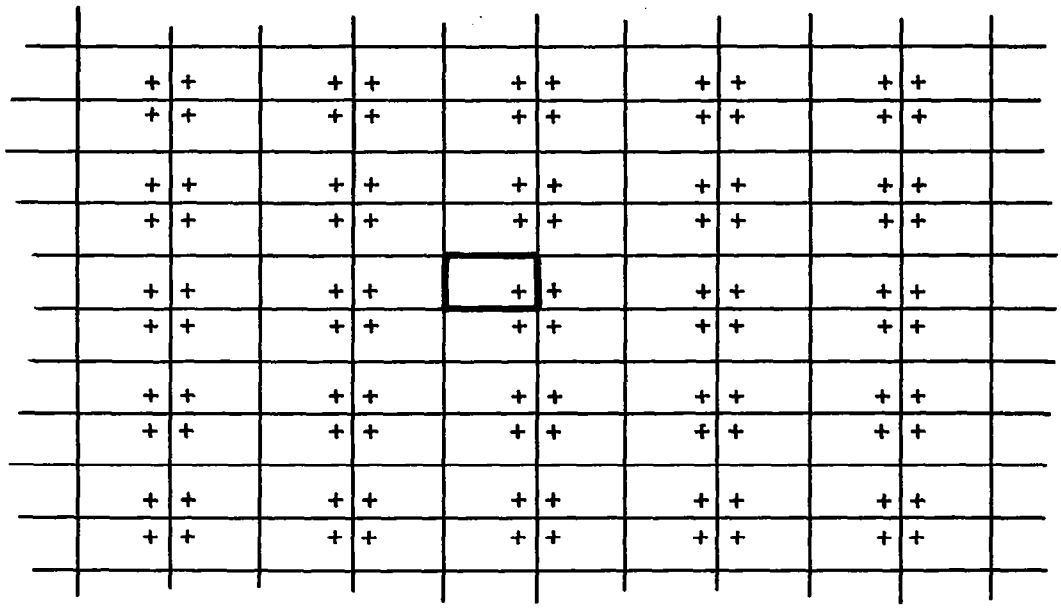

FIG. A-1 DIAGRAM OF IMAGE ARRAY FOR A THREE-DIMENSIONAL ANALOGY TO THE PROBLEM OF A SIMPLE SOURCE IN A SQUARE-SECTIONED HARD WALLED STRAIGHT TUBE. THE ACTUAL TUBE CROSS SECTION IS INDICATED BY A HEAVY LINE.

REFERENCES

1. Lighthill, M. J.: On Sound Generated Aerodynamically: I, General Theory. Proc. Roy. Soc. (London), vol. 211A, 1952, pp. 564-587.

2. Mawardi, O. K.; and Dyer, I.: On Noise of Aerodynamic Origin. J. Acoust. Soc. Am., vol. 25, 1952, pp. 389-395.

3. Lassiter, W. L.; and Hubbard, H. H.: Experimental Studies of Noise from Subsonic Jets in Still Air. NACA TN 2757, 1952.

4. Fitzpatrick, H. M.; and Lee, R.: Measurements of Noise Radiated by Subsonic Air Jets. David Taylor Model Basin, Rept. 835, 1952.

5. Ffowcs Williams, J. E.; and Gordon, C. G.: Noise of Highly Turbulent Jets at Low Exhaust Speeds. A.I.A.A.J., vol. 3, 1965, pp. 791-793.

6. Curle, N.: The Influence of Solid Boundaries upon Aerodynamic Sound. Proc. Roy. Soc. (London), vol. 231A, 1955, pp. 505-514.

7. Taylor, G. I.: The Singing of Wires in a Wind. Nature, vol. 113, 1924, p. 536(L).

8. Lighthill, M. J.: Jet Noise. A.I.A.A.J., vol. 1, 1963, pp. 1507-1517.

9. Lighthill, M. J.: On Sound Generated Aerodynamically: II, Turbulence as a Source of Sound. Proc. Roy. Soc. (London), vol. 222A, 1954, pp. 1-32.

10. Powell, A.: Theory of Vortex Sound. J. Acoust. Soc. Am., vol. 36, 1964, pp. 177-195.

11. Ribner, H. S.: The Generation of Sound by Turbulent Jets. Advan. Appl. Mech., vol. 8, 1964, pp. 182-184.

REFERENCES (continued)

12. Morse, P. M.; and Feshbach, H.: Methods of Theoretical Physics (Parts I and II). McGraw-Hill Book Co., Inc., 1953.

13. An account of sound radiation from a point source in a pipe of nonrectangular cross section is given in ref. 12, p. 1515. The radiation from multipoles can be obtained by spatial differentiation of the field of the point source.

14. Yudin, E. Ya.: The Acoustic Power of the Noise Created by Airduct Elements. Soviet Phys.-Acoust., vol. 1, 1955, pp. 383-398.

15. Waterhouse. R. V.; and Berendt, R. D.: Reverberation Chamber Study of the Sound Power Output of Subsonic Air Jets. J. Acoust. Soc. Am., vol. 30, 1958, pp. 114-121.

16. Atvars, J.; Schubert, L. K.; Grande, E.; and Ribner, H. S.: Refraction of Sound by Jet Flow or Jet Temperature. Univ. Toronto Inst. Aerospace Sci., NASA CR 494, May 1966.

17. Plumblee, H. E.; Gibson, J. S.; and Lassiter, L. W.: A Theoretical and Experimental Investigation of the Acoustic Response of Cavities in an Aerodynamic Flow. WPAFB, Ohio, Rept. No. WADD-TR-61-75, 1962.

18. Hubbard, H. H.; and Maglieri, D. J.: Noise Characteristics of Helicopter Rotors at Tip Speeds up to 900 Feet per Second. J. Acoust. Soc. Am., vol. 32, 1960, pp. 1105-1107.